DEPARTMENT OF THE ARMY
U.S. Army Corps of Engineers
Washington, DC 20314-1000

EP 1110-2-12

CECW-ED

Pamphlet
No. 1110-2-12

30 September 1995

Engineering and Design
SEISMIC DESIGN PROVISIONS FOR ROLLER COMPACTED CONCRETE DAMS

1. Purpose

The purpose of this engineer pamphlet (EP) is to provide preliminary guidance and direction for the earthquake-resistant design of new roller compacted concrete (RCC) dams, and for the evaluation of safety and serviceability of existing RCC dams subjected to earthquake loading.

2. Applicability

This EP applies to all HQUSACE elements and USACE commands having responsibilities for the design of civil works projects.

3. Discussion

a. This EP presents preliminary guidance concerning the design of new RCC dams and the evaluation of existing RCC dams located in zones of high seismic activity. References are included in Appendix A.

b. Appendices B-D present examples of applying this guidance to the design of a new RCC dam.

c. Both the preliminary guidance contained herein and the example problems are based on EM 1110-2-2200 and ER 1110-2-1806. Both of these documents are under revision and the final guidance contained in these documents may vary somewhat from the provisions of this EP. Draft copies of these documents may be obtained from CECW-ED for use in the design of RCC structures.

d. A dynamic stress analysis shall be performed as part of the design procedure for all new RCC dams, or the evaluation of existing RCC dams, located in areas of strong seismicity. Dams shall be shown capable of satisfying general performance requirements for design earthquake seismic events described herein. Linear-elastic analysis methods shall be used in performing dynamic stress analysis.

e. Consultation and approval of CECW-ED are required prior to performing a nonlinear dynamic stress analysis based upon the theory of fracture mechanics to qualify a new design or to evaluate an existing RCC dam with regard to dam safety.

FOR THE COMMANDER:

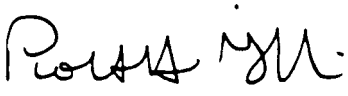

ROBERT H. GRIFFIN
Colonel, Corps of Engineers
Chief of Staff

CECW-ED

DEPARTMENT OF THE ARMY
U.S. Army Corps of Engineers
Washington, DC 20314-1000

EP 1110-2-12

Pamphlet
No. 1110-2-12

30 September 1995

Engineering and Design
SEISMIC DESIGN PROVISIONS FOR ROLLER COMPACTED CONCRETE DAMS

Table of Contents

Chapter 1
Introduction

1-1. General

Roller compacted concrete (RCC) dams are designed in accordance with EM 1110-2-2200. The proportions of the RCC dam are derived by stability analysis in a manner identical to that for a conventional concrete gravity dam and are governed by the static forces to be resisted and not by the dynamic forces generated during seismic activity. After the geometric proportions are determined based on the static loads a dynamic analysis is conducted. Zones requiring superior RCC mixes are established, and vibratory compaction methods and joint preparation methods which affect the RCC tensile strength are also established based on the criteria provided in this engineer pamphlet (EP).

1-2. References

Required and related publications are listed in Appendix A.

1-3. Explanation of Terms

Abbreviations, symbols, and notations used throughout this EP are explained in the glossary.

1-4. Background

Basic criteria and guidance for the design of RCC dams are provided in EM 1110-2-2200. ER 1110-2-1806 provides guidance on analysis methods and procedures for new designs and an investigative program for existing dams. ETL 1110-2-301 gives additional information on specifying earthquake ground motions for a particular site. ETL 1110-2-303 provides guidance on finite element dynamic analysis methods and on evaluating the severity of cracking based on tensile stresses from the linear analysis. EM 1110-2-2006 provides guidance concerning RCC usage and mix design.

1-5. Design Philosophy

a. Response spectrum analysis. The nonlinearities associated with concrete behavior under seismic loading are difficult to assess and beyond practical analyzing capabilities of most design offices. Procedures which permit the use of a linear-elastic type of dynamic analysis adjusted to provide a reasonable but conservative approximation of the nonlinear behavior are adequate in almost all design situations. The philosophy of design followed in this EP will be to establish the procedures applicable to the majority of design situations. This consists of providing in some detail the requirements for performing the linear-elastic response spectrum analysis and the criteria for evaluating the results.

b. Refined analyses. For the few occasions where this approach does not produce a satisfactory design or where an existing dam does not satisfy criteria, the designer is then advised to pursue the more refined analysis methods. Should the even more complex nonlinear analysis become necessary, it should be performed under the guidance of a recognized expert in this specialized field and should only be undertaken with approval of CECW-ED.

1-6. Design Earthquakes

The linear-elastic response spectrum method of analysis is the simplest dynamic analysis method and provides adequate results for most designs. The ground motion is usually defined by design response spectra scaled to peak ground accelerations (PGA) for the two design earthquakes described below.

a. Operating basis earthquake. The operating basis earthquake (OBE) is defined as the earthquake producing the greatest level of ground motion that is likely to occur at the site during the economic life of the dam.

b. Maximum credible earthquake. The maximum credible earthquake (MCE) is defined as the earthquake which produces the greatest level of ground motion at the site as a result of the largest magnitude earthquake that could reasonably occur along the recognized faults or within a particular seismic source.

c. Types of design spectra. Design response spectra for the OBE are usually developed using a probabilistic approach, and design response spectra for the MCE are developed using a deterministic approach. Design response spectra are further classified into two types: (1) site-specific or (2) standard. The seismic zone location of the site, the height of the dam, and the proximity to active faults are the factors used to determine if it is necessary to develop a site-specific design response spectra or if the standard spectra may be used in the dynamic analysis. When standard design response spectra are acceptable, Chapter 5 provides the appropriate spectra along with the PGA values to be used for scaling. These standard design spectra are based on the mean level of the ground motion parameters for the records selected in the development of the standard spectra.

d. Ground motion time histories. The more refined analysis methods require a ground motion time history representation of the design earthquakes. These may be developed using actual past earthquake ground motion records, synthetically, or by modifying an actual record. Ground motion time histories are developed so their response spectrum closely matches the site-specific design response spectrum.

1-7. Acceptance Criteria

a. Cracking of RCC. The ground motion that is produced during a seismic event can cause cracks to occur in an RCC dam. As cracking progresses, serviceability is eventually impaired. If ground shaking is extremely severe, or if strong ground shaking combines with a foundation fault displacement, it is conceivable that continued propagation of the system of cracks could eventually lead to a failure mechanism where the dam is no longer capable of containing the pool. This EP establishes acceptance criteria which maintain serviceability during an OBE, and provide a reasonable safety factor against developing a failure mechanism during a MCE. Because of the complexity and the great number of variables involved in seismic design, the EP criteria should be supplemented with the judgment of structural engineers experienced in seismic design.

b. Direct tensile strength. The direct tensile strength of the RCC is the design parameter used for establishing the acceptance criteria. Unlike conventional concrete, tensile strength of RCC depends on mix consistency and placement and compaction methods as well as mix proportions. Tensile strength of both the lift joint and the parent concrete shall be determined from cores taken from test fill placements for new dam design and from the in-place RCC for existing dams. Although splitting tensile tests may be used, the test results shall be adjusted to reflect direct tensile strength. From the direct tensile strength, the allowable design tensile stresses shall be established for both lift joints and parent concrete by applying adjustment factors to account for high strain rate associated with dynamic loading and certain nonlinear characteristics of the stress/strain curve. Adjustment factors shall be selected to maintain serviceability during an OBE and to produce a reasonable safety factor for a MCE.

1-8. Important Factors

Discussed below are recommendations regarding factors which are important because they have a significant impact on the dynamic response. Recommendations that differ from those contained in ETL 1110-2-303 and ER 1110-2-1806 are identified.

a. Effective damping. The material and radiation damping of the foundation contribute significantly to the damping of the combined dam-foundation system, and must be considered in the analysis. This requires calculating an effective viscous damping ratio to reflect the damping contribution of both the dam and the foundation. This will result in a considerably higher damping ratio for a foundation having a very low modulus than the damping ratio used previously.

b. Hydrodynamic effect. Added mass shall be calculated using standard hydrodynamic pressure function curves which consider compressibility of the water, stiffness characteristics of the dam, and reservoir bottom absorption (Fenves and Chopra 1986). Appendix D provides an example showing the required procedure.

c. Mode combination methods. The complete quadratic combination method (CQC) of combining modes shall be used for final design of dams under critical seismic design conditions and for evaluation of existing dams. Critical conditions are considered to exist when site-specific design response spectra are required by this EP. Either the square root of the sum of the squares method (SRSS) or the CQC

method is acceptable for all preliminary designs and for final designs under noncritical seismic conditions. Since the modal frequencies are fairly well separated in gravity dams, the simpler SRSS method produces adequate results which are in balance with the general level of precision required for preliminary or noncritical analyses.

d. Seismic zone map. The seismic zone map, Figure 5-1, shall be used in the dynamic stress analysis phase of the seismic design. The peak ground accelerations for use in scaling standard design response spectra are contained in Table 5-2 and are based on the zone map. The seismic zone maps and the seismic coefficients contained in ER 1110-2-1806 shall be used only in the stability analysis phase of seismic design.

1-9. Analysis Methods and Procedure

In general a dynamic stress analysis shall be performed, and the results shall be evaluated to determine if the response of the RCC dam to the design earthquakes is acceptable. If the response is not acceptable, the design of a new dam may be modified and reanalyzed using the same analysis method, or a more refined analysis method may be employed. For an existing dam, progressively more refined methods of analysis are employed.

a. Method attributes. There are four attributes that characterize a particular dynamic analysis method.

(1) Material behavior. Options are (a) linear-elastic or (b) nonlinear behavior.

(2) Design earthquake definition. Options are (a) design response spectrum or (b) time history ground motion record input.

(3) Dimensional representation. Options are (a) two-dimensional representation or (b) three-dimensional representation.

(4) Model configuration. Options are (a) Chopra's "standardized" model, (b) composite finite element-equivalent mass system model, or (c) finite element-substructure model.

b. Computer programs. Various computer programs are available which are identified with certain analysis methods. Also, Chopra's Simplified Method may be either hand-calculated or done by a computer program. Some computer programs, such as the general purpose finite element programs, allow the attribute options to be changed so that one of several possible methods may be employed for the dynamic analysis. This often allows a transition to a more refined method without necessarily abandoning all the previous computer model input effort. Other computer programs, such as the EAGD-84 program, and Chopra's Simplified Method are single method programs since they have fixed attributes. Chapter 8 discusses dynamic analysis methods in more detail.

c. Preliminary and final design. The two-dimensional, linear-elastic, response spectrum method shall be used for the preliminary design analysis. Either Chopra's Simplified Method or a general-purpose finite element program shall be employed depending on the design conditions. The simplest final design analysis utilizes a composite finite element-equivalent mass system model and general-purpose finite element program.

1-10. Coordination

A fully coordinated team of structural engineers, geotechnical and materials engineers, geologists, and seismologists should ensure that all factors relevant to the dynamic analysis are correct and that the results of the analysis are properly evaluated. Some of the critical analysis and design aspects requiring coordination are discussed below.

a. Design response spectra. Developing site-specific design response spectra when required.

b. Tensile strength of RCC. Obtaining representative cores from test-fill placements for new dams or from the in-place concrete for existing dams for use in determining the direct tensile strength and dynamic tensile strength of both the lift joints and the parent RCC.

c. Foundation properties. Obtaining exploratory corings and evaluating tests to determine the foundation deformation modulus and other foundation properties.

d. Foundation fault displacement. Evaluating geoseismic conditions at the site to determine if foundation fault displacement is possible, and to map the location, strike, and dip of the potential faults.

Chapter 2
Seismic Design Criteria

2-1. Stability

a. Resultant location and sliding. RCC dams shall satisfy the overturning and sliding stability requirements for gravity dams using inertia forces calculated by the seismic coefficient method as set forth in EM 1110-2-2200 and ETL 1110-2-256. The seismic coefficients shall be as shown on the seismic zone maps provided in ER 1110-2-1806.

b. Extreme stability conditions. When intense ground shaking causes serious tensile cracking at the dam-foundation interface, a nonlinear time history analysis shall be performed to evaluate cracking, potential permanent displacements, and the effect these have on sliding stability. Certain stipulations regarding nonlinear analyses are covered in paragraph 2-2*g*.

2-2. Response to Ground Shaking

RCC dams shall be capable of resisting the strong motion ground shaking associated with design earthquakes within the allowable tensile stress design criteria specified in Chapter 4. Dynamic stress analysis methods and procedures are described in Chapter 8. The dynamic analyses shall incorporate the dynamic characteristics of the dam, foundation, reservoir, and backfill or silt deposition when applicable.

a. Defining ground motion. The free field ground motions are used to define the ground motion that would be felt at the site due to two design earthquakes. Free field ground motion associated with each shall be represented by design response spectra and, when required, design acceleration time histories. The design earthquakes are operating basis earthquake (OBE), and maximum credible earthquake (MCE). Both are discussed in detail in Chapter 4.

b. Propagation of cracks in RCC. Most dams with earthquake resistant provisions will probably survive the most severe earthquake shaking possible at the site with little or no damage, although high dams located near major faults have experienced extensive cracking during major earthquakes (Chopra and Chakrabarti 1973). Concrete cracking due to ground shaking combined with cracking due to foundation fault displacement could propagate to an extent where a failure mechanism is formed thus impairing the ability of the dam to contain the pool. Criteria defining an acceptable response of the dam to design earthquakes are based on initiation and propagation of tensile cracking within the RCC.

c. Analyzing response to ground shaking. The process of cracking and the propagation of the cracks result in nonlinear behavior of the dam. There are also nonlinearities associated with dam-foundation interaction and dam-reservoir interaction which are difficult to assess. Approximate linear relationships account for some of the nonlinear dynamic behavior and allow the response of the dam to the design earthquake ground motion to be determined using a linear-elastic analysis method. Tensile stresses can then be evaluated based on tensile strength parameters adjusted to be compatible with linear-elastic analysis methods.

d. Analysis methods. The simplest of the linear-elastic methods uses a response spectrum to define the ground motion as outlined in Chapter 5. Most RCC dams will be found adequate using this method. For the few exceptions, the next level of refinement in determining the dynamic response is the linear-elastic time history method, and in rare cases a nonlinear time history finite element analysis may be required.

e. Allowable tensile stress. The tensile strength of the RCC is the single concrete material property used to evaluate cracking, and to establish acceptable response. Allowable tensile stresses are defined in paragraph 4-2*c* and paragraph 4-3*c* for the OBE and MCE, respectively.

f. Evaluating time-history response. When dynamic response is determined by the linear-elastic time-history method, the allowable tensile stress is the principal criterion for evaluating acceptable response, but additional criteria are also required to qualify other response characteristics such as the number of stress cycles approaching or exceeding the allowable stress, and the magnitude and pattern of these excursions beyond the specified limits.

g. Evaluating nonlinear analyses. When dynamic response is determined by the nonlinear time-history method, criteria for evaluating acceptable response are based on the theory of fracture

mechanics. This type of analysis should only be undertaken in consultation with and as approved by CECW-ED.

2-3. Foundation Fault Displacement

a. General. Most RCC dam sites are not subject to any significant differential displacement of the ground surface at the dam-foundation interface during a seismic event. Dam sites should always be avoided when located near a major active fault system with the potential to trigger sympathetic foundation displacements at the site. Occasionally it is not possible to avoid these sites, and it becomes necessary to evaluate the response of the dam should such a foundation fault displacement occur.

(1) Considerable judgment is required in the evaluation process. At best, analysis methods for foundation fault displacement are approximate and are generally unsupported by past observations of the response of existing dams to fault displacements occurring at the dam foundation. Furthermore, considerable judgment is required in the prediction of future fault movement and in the magnitude of the fault displacement. For example, the estimate of the magnitude of potential fault displacement provided by different experts for a specific site could vary from a few inches to several feet. This necessitates consulting several geotechnical firms to provide site-specific fault displacement estimates, and then carefully scrutinizing these estimates before finally establishing the design fault displacement.

(2) Experts in plate tectonics, geology, seismology, and finite element analysis techniques should be consulted to provide guidance for any dam located on a site subject to foundation fault displacement. Because of the many uncertainties and the risk involved, approval by CECW-ED is required for any RCC dam which is located on a site subject to foundation fault displacement.

b. Types of faults. Fault slip is the relative displacement of two adjacent tectonic plates with respect to each other. This refers to large active fault systems such as the San Andreas or Hayward faults in California. On a smaller scale, the foundation rock mass beneath a dam contains various discontinuities, joint sets, and shear and fault zones. Normally this is a system of historically inactive discontinuities; however, there is a potential for fault slippage particularly when triggered by a great earthquake on a nearby large active fault. The three general types of fault slips are strike-slip, normal-slip (dip-slip), and reverse-slip (thrust-slip). Refer to Figure 2-1 for illustrations of the various types of faults and how the magnitude of slip is measured. The strike of the fault is the trace the fault makes with respect to the ground surface, and it may be at any orientation with respect to the dam axis.

c. Design fault displacement. The design fault displacement (DFD) is defined as the maximum possible free field fault slip movement that could reasonably occur in the dam foundation as measured at the ground surface. The return period that would be associated with the DFD is similar to that of the MCE. Therefore, the DFD and the free field ground motion together specify the site-specific seismic activity associated with the MCE. To fully describe the DFD, three factors must be specified: magnitude, type of slip, and strike of the fault.

(1) The geology of the dam foundation is complex, and the foundation may be crossed by a number of discontinuities with fault displacement potential. Experts in the fields of geology and seismology should be consulted to study the foundation fault system, determine which faults are capable of surface displacement, and finally recommend which faults are critical and specify the DFD for each critical fault.

(2) Normally, foundation fault displacements are not considered to occur concurrently with strong motion shaking associated with the OBE. The active fault near the dam site that produces a seismic event of OBE magnitude is not likely to trigger sympathetic slippage in the fault system in the dam foundation. The probability of sympathetic foundation fault displacement is normally several orders of magnitude less than the recurrence rate for the strong motion shaking associated with the OBE; therefore, the probability of the OBE being accompanied by significant foundation displacement is usually considered negligible.

(3) On rare occasions, the probability logic discussed above may not apply when considering if it is appropriate to combine foundation fault displacement with ground shaking in specifying the OBE. For example, unusual geology of the foundation could make it susceptible to a reservoir-induced foundation fault displacement or to other

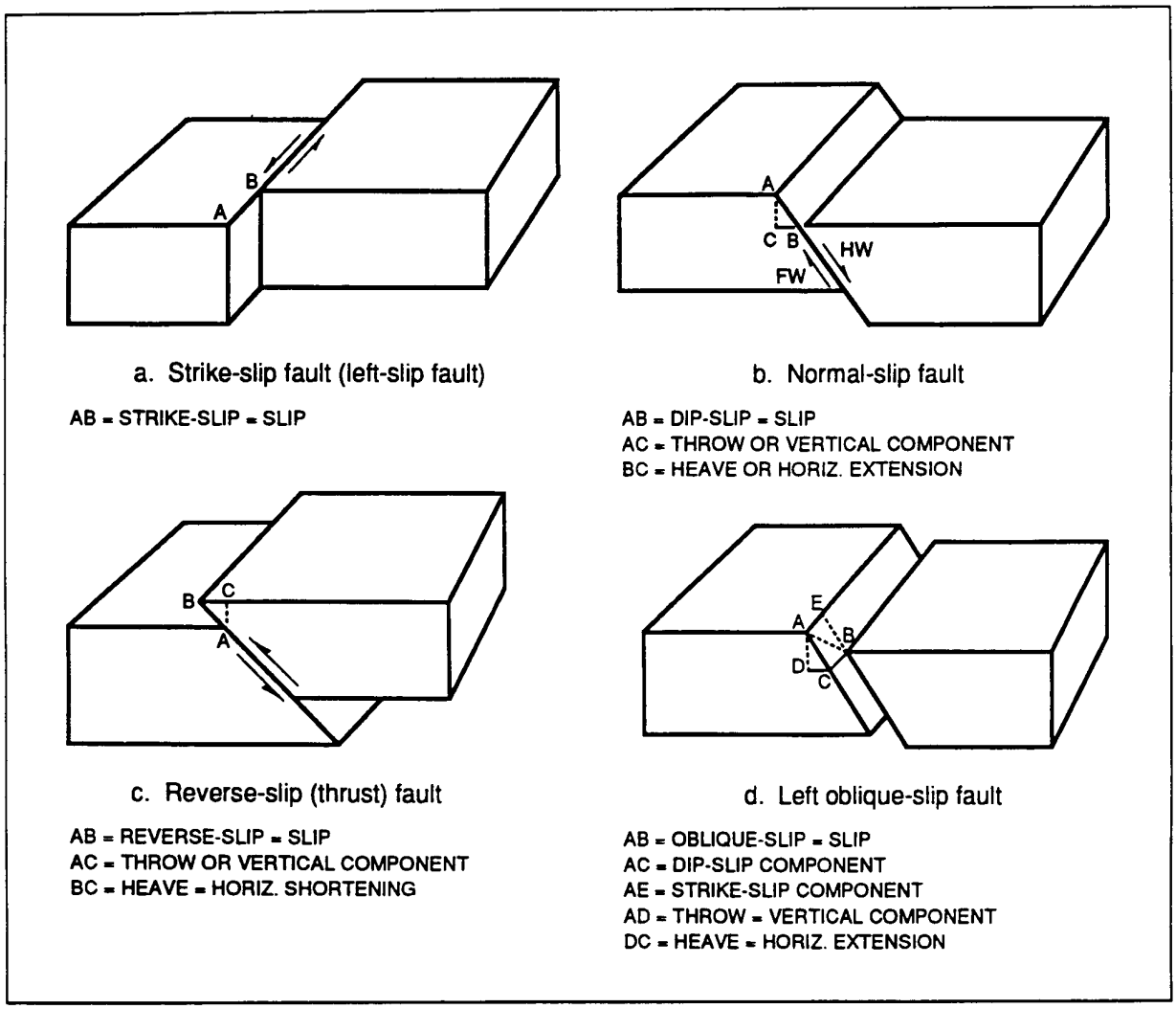

Figure 2-1. Types of fault slips

unusual causes of foundation fault displacement discussed later in this chapter. In these situations the strong motion shaking accompanying the local fault slip may be nearly as intense or even more intense than the gound motion shaking associated with an OBE produced by a major active fault slip occurring some distance from the site. When this is the case, a reduced value of the DFD would be included with free field ground motion to describe the OBE.

d. Combined DFD and ground shaking. Stresses associated with the DFD result from highly complex nonlinear behavior; however, simplified fault displacement analysis procedures, such as the one described below, are normally used to investigate concrete stresses that may occur due to fault displacement. Stresses due to ground shaking are determined by methods discussed earlier in this chapter. Thus, stresses due to fault displacement and stresses due to ground shaking are obtained from two separate, independent, and approximate analyses. The response to the design earthquake is then obtained by direct addition of the two sets of stresses without accounting for any interaction. Actually, the fault displacement may cause inelastic behavior at the dam-foundation interface, cracking within the RCC, or other inelastic response which changes the dynamic characteristics of the dam, which in turn interacts with and effects the ground shaking response. Because these simplified and approximate procedures have not been supported by nonlinear finite element analyses that properly combine the effects of fault displacement

and ground shaking, they should be used with caution.

e. Simplified DFD analysis procedure. The simplified procedure described below was used to investigate concrete stresses due to fault displacement in the Auburn Dam in California (U.S. Department of the Interior, Bureau of Reclamation 1980). The dam and foundation are modeled with finite elements with the mesh geometry adjusted to allow the fault to be properly oriented. Refer to Figure 2-2. The foundation model consists of a fixed block with conventional boundary supports, and a movable block with special boundary conditions that allow forces to be applied at the boundary parallel to the fault to produce the DFD. The fixed and movable block are separated by elastic orthotropic elements which allow the sharp displacement discontinuity to take place as the movable block displaces upward.

(1) The finite element model is first loaded with the gravity loads followed by the hydrostatic loads, and finally the movable block is forced to undergo the DFD. Each loading is applied incrementally. After each loading increment, tensile stresses are evaluated and elements are softened in areas where the tensile strength is exceeded. Elements are softened by reducing their elastic modulus until the tensile stress is eliminated. Most elements requiring softening are located in the foundation because jointing and discontinuities in the rock prevent it from sustaining high tensile stress. When the DFD is reached, the extent of the tensile failure areas is evaluated. The dam tends to bridge over the fracture zone in the foundation. Resulting stresses induced in the RCC are obtained from the finite element analysis for the final increment of loading which produced the DFD.

(2) The method of incremental loading and softening of element properties allows the use of a simplified static, linear-elastic finite element analysis approach. Disadvantages of the procedure are that it gives only an approximation of the complex nonlinear behavior associated with fault displacement, it is time consuming, and it requires considerable judgment.

(3) The example shown in Figure 2-2 is typical for a normal or reverse fault where the fault strike is approximately parallel to the dam axis so a two-dimensional analysis is adequate. If the fault strike is not close to parallel to the dam axis, or for a strike-slip fault, a three-dimensional analysis is required. The three-dimensional analysis is even more time consuming and complex, but the principles and general procedure are similar to the two-dimensional analysis described.

f. Acceptable response to DFD. When the seismic activity associated with the design earthquake consists of both fault displacement and ground shaking, stresses for the combined response described in paragraph 2-3*d* must satisfy the allowable tensile stress criteria of paragraph 2-2*e*. Beyond these tensile stress requirements, additional consideration is required regarding general performance requirements of Chapter 4 related to dam safety and operations in the event of foundation fault displacement. The potential fault displacement and the effect it has on the dam must be evaluated on a case-by-case basis. The analysis procedures described above for evaluating the effect of fault displacement are rough approximations, but they do provide an indication of the extent of the fracture zones that could occur in the foundation or lower portions of the RCC dam. The analysis results must be coupled with considerable judgment to determine if this damage could lead to the erosion of the foundation or RCC materials to the extent that finally causes an uncontrolled release of the reservoir.

g. Dam failures caused by fault displacements. To help identify some of the judgment factors involved in evaluating sites with fault displacement potential, the following is a brief review of historical information on dams that failed directly or indirectly as a result of fault displacement. Differential displacements across a fault have been recorded due to: triggering of the fault by a seismic event; a difference in consolidation of materials on either side of the fault; a reduction in resistance to fault movement created by the lubricating effects of water, or the erosion of fault materials by flowing water; and increase in hydrostatic pressures along the fault.

(1) Earth-fill dams, concrete gravity dams, and concrete arch dams have failed due to fault movements. Failures of the Baldwin Hills earth-fill dam, the Malpasset concrete arch dam, and the St. Francis concrete gravity dam (James et al. 1988) can all be attributed in part to forces and movements occurring along fault surfaces. Although these forces and movements were not triggered by seismic activity, it can be surmised that if a seismic event had occurred, it would have likely triggered similar failures. These examples show that fault movement can cause a

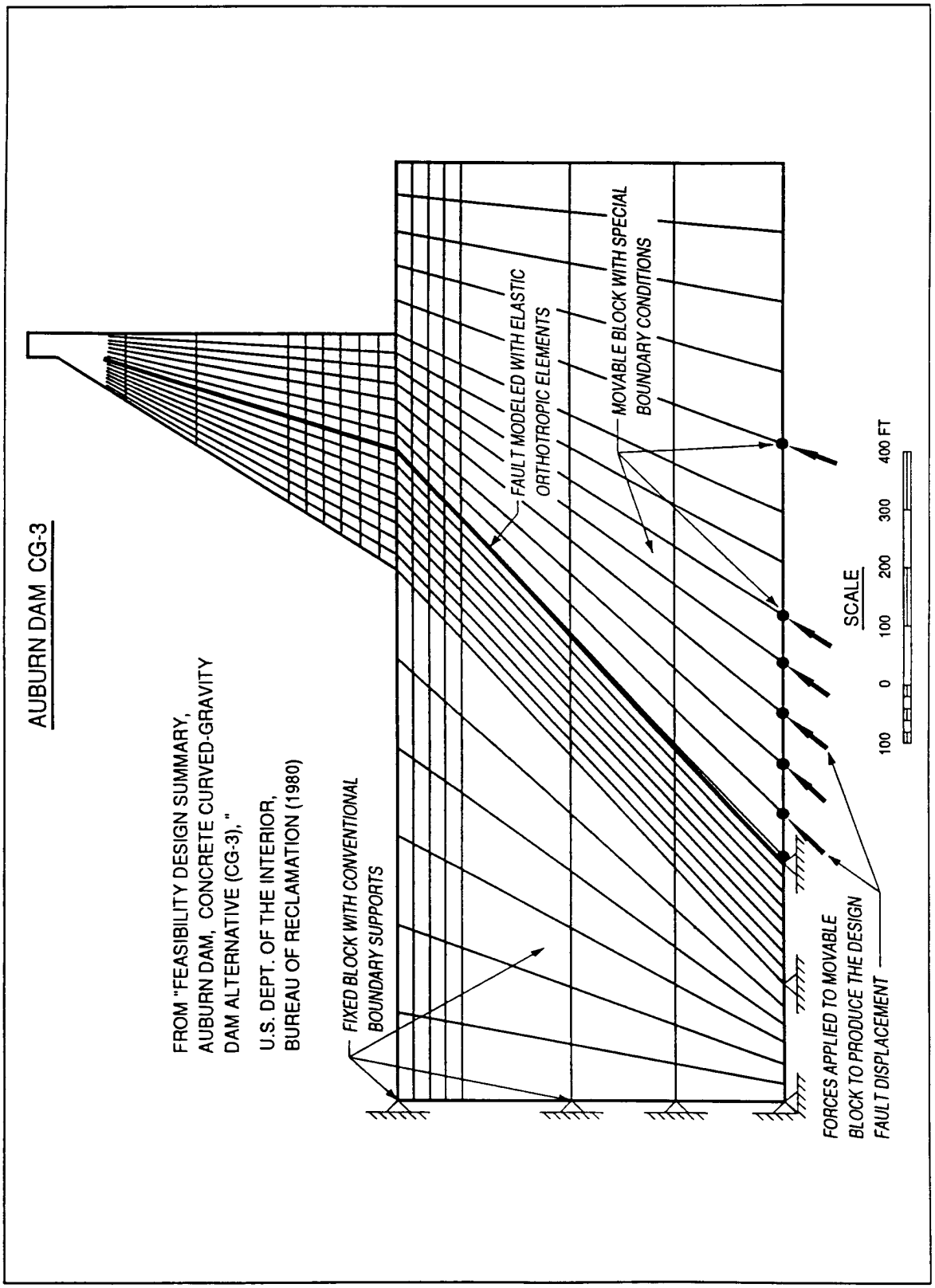

Figure 2-2. Finite element model for fault displacement analysis

failure mechanism to form in the dam structure which results in dam failure; however, it is more likely that the fault movement would create flow paths that could lead to a release of the impounded reservoir. Seepage can erode dam or foundation materials which eventually results in failure because capability for controlled release of the pool is lost.

(2) An earth-fill dam with a flexible core is normally considered less susceptible to failure due to foundation fault displacement because it would tend to conform to the displaced shape of the foundation. Although this flexibility of the dam material will reduce voids and flow paths in the dam and foundation it will not completely eliminate them. Thus, an earth-fill dam is susceptible to erosion of core or foundation material from water flowing through faults or through voids in the dam or foundation created by fault movements. For this reason, an earth-fill dam is not necessarily superior to a concrete gravity dam in resisting the effects of fault movement.

h. Defensive design features. Defensive design features which can be employed in the design of an RCC dam susceptible to foundation displacement are discussed below.

(1) The arching action provided by laying out the dam axis on a curve may better distribute the forces on a gravity dam due to foundation fault displacement, and reduce the tensile stresses and cracking of the RCC. This defensive feature is only effective if the heave of the foundation block is generally in a downstream direction, and providing the fault movement does not occur at either abutment.

(2) Special sliding joints may also be used to reduce cracking of the RCC due to fault displacement. For example, vertical joints may be located in the RCC to accommodate potential strike-slip fault displacements where the strike is generally in the upstream-downstream direction.

(3) A design feature for controlling the reservoir release is to provide a buttress fill against the upstream face of the dam. This requires the reservoir water to pass through a succession of filters and crack stoppers in a manner analogous to the behavior of the transitions and filters in a zoned embankment dam. This defensive measure would be effective for flood-control projects where the reservoir pool elevation is low enough that the required height of the buttress fill is economically feasible, and does not impair the stability of the dam.

2-4. Refined Dynamic Analyses Methods

a. Need for refinement. When the simplified linear-elastic analysis methods described above for an existing RCC dam produce tensile stresses in excess of the allowables discussed in paragraph 2-2*e*, more refined analyses methods shall be pursued before the dam is judged unsafe. Also, if all practical and economical adjustments to the design of a new dam have been exhausted in the attempt to satisfy the allowables based on simplified linear-elastic methods, the more refined analyses methods may be pursued to better evaluate nonlinear structural behavior. Refined analyses consist of linear or nonlinear time history analyses as discussed in paragraph 2-2*d*, with some additional details of the nonlinear analysis provided below. The response produced by refined analyses shall be evaluated in accordance with the stipulations of paragraphs 2-2*f* and 2-2*g*.

b. Fracture mechanics. Nonlinear dynamic analysis is based on fracture mechanics theory which is presently in the research phase. It is also difficult to determine just what level of structural damage can be sustained safely by the dam and still consider it to satisfy the performance requirements. The nonlinear attribute requires this type of dynamic analysis be performed in a time domain (time history analysis) rather than a frequency domain (response spectrum analysis), and use a direct integration solution. The analysis accounts for: energy dissipation by cracking, strength of cracked concrete, changes in vibration characteristics caused by cracking, changes in damping, and changes in strength due to strain rate and loading history.

c. Nonlinear analysis requirements. Because it is very complex, costly, and requires a considerable amount of judgment to interpret the results, an expert in fracture mechanics and nonlinear analysis techniques should be consulted to provide guidance when pursuing a nonlinear analysis.

Chapter 3
Material Properties of RCC

3-1. Similarities of RCC and Conventional Concrete

The strength and elastic properties of RCC vary depending on the mix components and mix proportions in much the same manner as that for conventional mass concrete. Aggregate quality and water-cement ratio are the principal factors affecting strength and elastic properties. Properties important to the seismic analysis of RCC dams include compressive strength, tensile strength, shear strength, modulus of elasticity, Poisson's ratio, and unit weight. Except for unit weight, all these properties are strain rate sensitive, and the strain rates that occur during major earthquakes are in the order of 1,000 times greater than those used in standard laboratory testing. Guidance concerning the determination of RCC material properties is given in EM 1110-2-2006 and ETL 1110-2-343.

3-2. Compressive Strength

The relationship between water-cement ratio and compressive strength is the same for RCC as for conventional mass concrete. Normally, for durability reasons, the RCC mix will be designed to provide a minimum strength of 2,000 psi; however, for seismic reasons higher compressive strengths are often required to achieve the desired tensile and shear strength. The compressive strength at seismic strain rates will be 15 to 20 percent greater than that at the quasi-static rates used during laboratory testing (ACI Committee-439 1969); however, compressive strength is never the governing factor in seismic design.

3-3. Tensile Strength

The tensile strength of RCC shall be based on the direct tensile strength tests of core samples. For the final design of new dams, cores shall be taken from test-fill placements made with the proposed design mixes, and placed with the proposed consolidation and joint treatment methods. When an existing dam is evaluated for compliance with the requirements of this EP, cores shall be taken directly from the structure. Cores should be taken vertically so that tests can be made which reflect weaknesses inherent at lift joint surfaces in addition to the tests to determine the tensile strength of the parent concrete.

a. Location of critical tensile stress. Critical tensile stresses are located at the upstream and downstream faces of the dam. The tensile stress distribution within the dam mass is of interest to help establish zone boundaries for superior, higher strength RCC mixes that may be required to control cracking near the faces.

(1) Usually the tensile stress in the lift joints in the direction normal to the joint surface is critical near the upstream face of the dam. This is because the direction of the principal tensile stress near the upstream face is very nearly normal to the joint surface, thus there is little difference between the joint stress and the maximum principal stress in the parent concrete. Since tensile strength of the lift joint is notably less than the parent RCC, it will control the design near the upstream face.

(2) Near the downstream face, the direction of the principal tensile stress is nearly parallel to the face which results in significantly higher principal tensile stresses in the parent concrete compared to the tensile stresses in the lift joints normal to the joint surface. The ratio of the tensile strength of parent concrete to the tensile strength of the lift joints varies according to several parameters including workability of the mix, joint preparation, and maximum size aggregate. Thus, it usually becomes necessary to investigate both the principal tensile stress and the component tensile stress normal to the lift joints to determine which is critical near the downstream face.

b. Preliminary design. For preliminary design, the tensile strength of the RCC may be obtained from Figures 3-1 through 3-6 for the proposed concrete compressive strength (f'_c). These figures show both the tensile strength of the parent material and the tensile strength of the lift joint based on the proposed consolidation and joint treatment method. These figures were developed from Tables E2 and E3, Appendix E.

c. Tensile strength tests. Splitting tensile tests are easier to perform and provide more consistent results than direct tensile tests. However, splitting tensile test results tends to overpredict actual tensile strengths, and should be adjusted by a strength reduction factor to reflect results that would be obtained from direct tensile tests. When splitting tensile tests

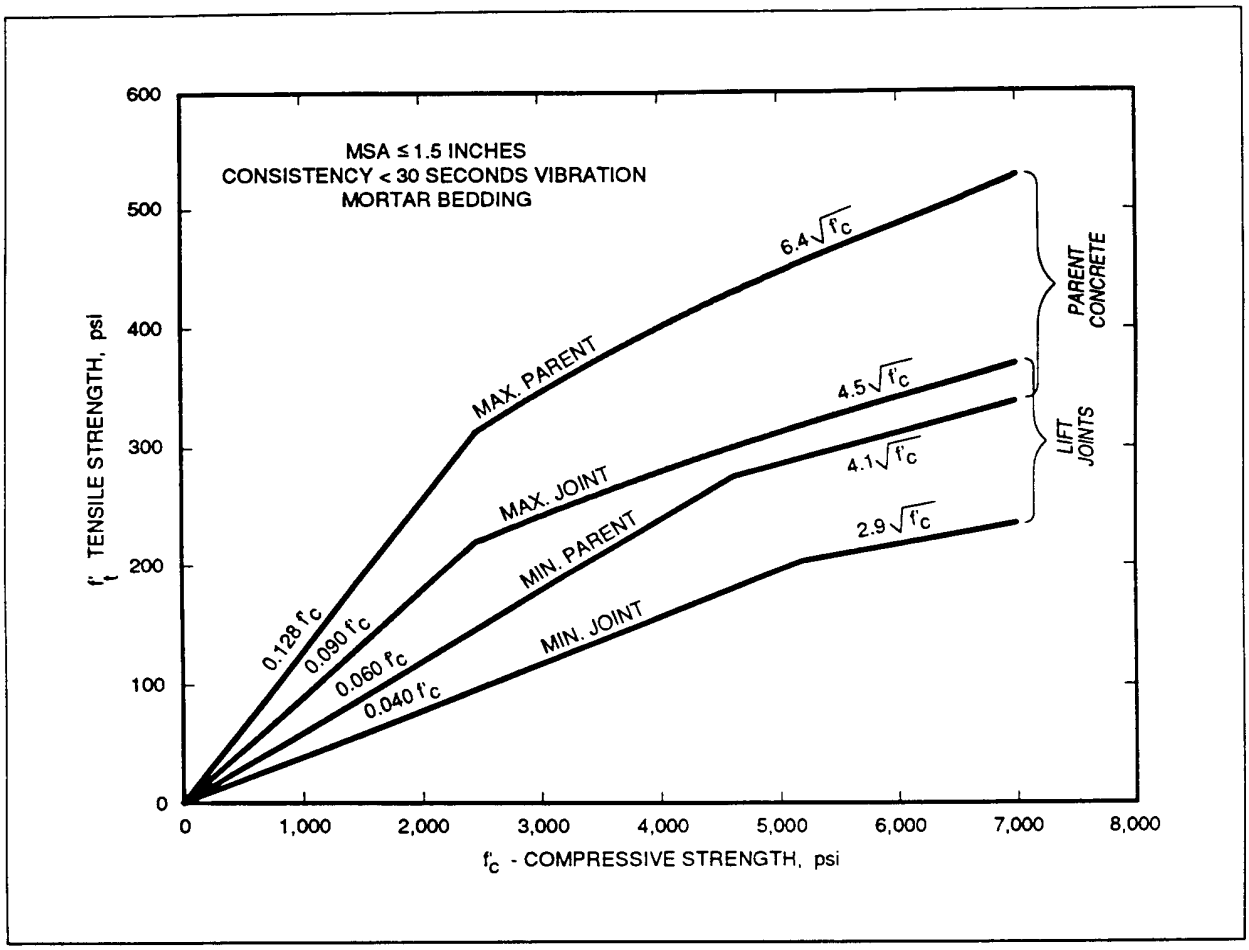

Figure 3-1. Tensile strength range, RCC, MSA ≤ 1.5 inches, consistency < 30 seconds vibration, mortar bedding

are used as the basis for determining the tensile strength of RCC, the test results shall be reduced by a strength reduction factor of 75 percent as recommended in Appendix E.

d. Factors affecting tensile strength. The tensile strength of RCC, as well as of conventionally placed mass concrete, is dependent on many variables including paste and aggregate strength, aggregate size, loading history, and load deformation rates. See paragraph 3-9 concerning strain rate sensitivity and dynamic tensile strength.

(1) RCC differs from conventionally placed mass concrete due to the many horizontal planes of weakness (construction joints) created during placement. RCC is placed and compacted in layers ranging from 6 to 24 inches with each layer creating a joint with tensile strength less than that of the parent concrete. The joint strength can be improved by placing a layer of high slump bedding mortar on each lift; however, the resulting joint strength is always somewhat less than the parent concrete. The consistency of RCC can also affect tensile strength with lower strength values for harsh mixes with low paste contents. Refer to Chapter 2 for additional discussion of these factors.

(2) Inherent in some RCC mixes are certain anisotropic material properties. In the RCC compaction process, the flatter coarse aggregate particles in these mixes have a tendency to align themselves in the horizontal direction. When this occurs, the strength of vertical cores will be less, and the strength of horizontal cores greater than the average tensile strength. The variance from average could be as high as 20 percent, although in general these effects will

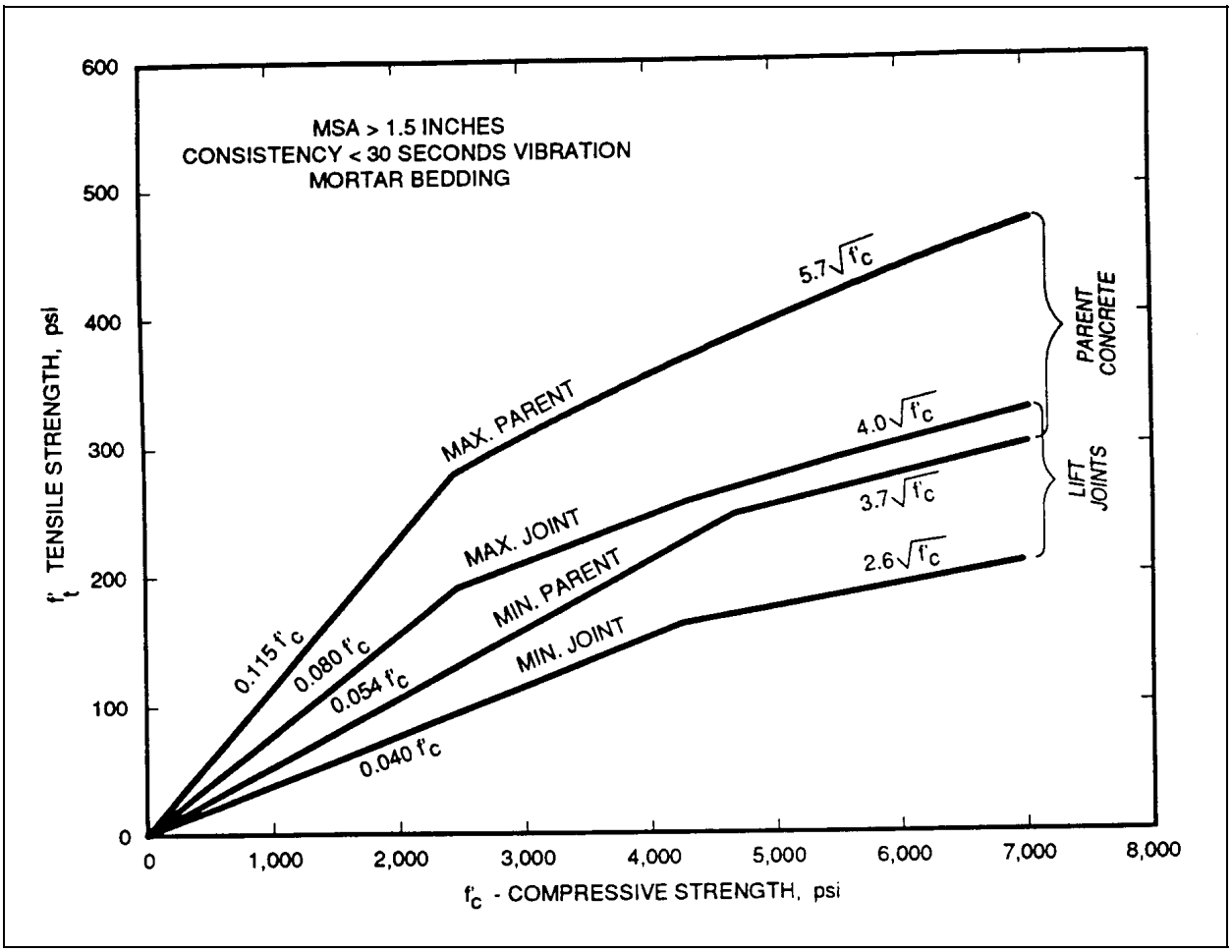

Figure 3-2. Tensile strength range, RCC, MSA > 1.5 inches, consistency < 30 seconds vibration, mortar bedding

be small. If the coarse aggregate particle shape indicates the possibility of significant anisotropy, both vertical and horizontal cores obtained from the laboratory test placement should be tested.

3-4. Shear Strength

The shear strength along lift joint surfaces is always less than the parent concrete; therefore, final shear strength determination should be based on tests of representative samples from the dam or test fill. Both the bond strength and the tangent of the angle of internal friction can be increased by 10 percent to account for the apparent higher strengths associated with seismic strain rates.

3-5. Modulus of Elasticity

RCC will usually provide a modulus of elasticity equal to, or greater than, that of conventional mass concrete of equal compressive strength. The modulus of RCC in tension is equal to that in compression. The static modulus of elasticity, in the absence of testing, can be assumed equal to (ACI Committee-207 1973):

$$E = 57{,}000\sqrt{f'_c}$$

where E = static modulus of elasticity

f'_c = static compressive strength of RCC

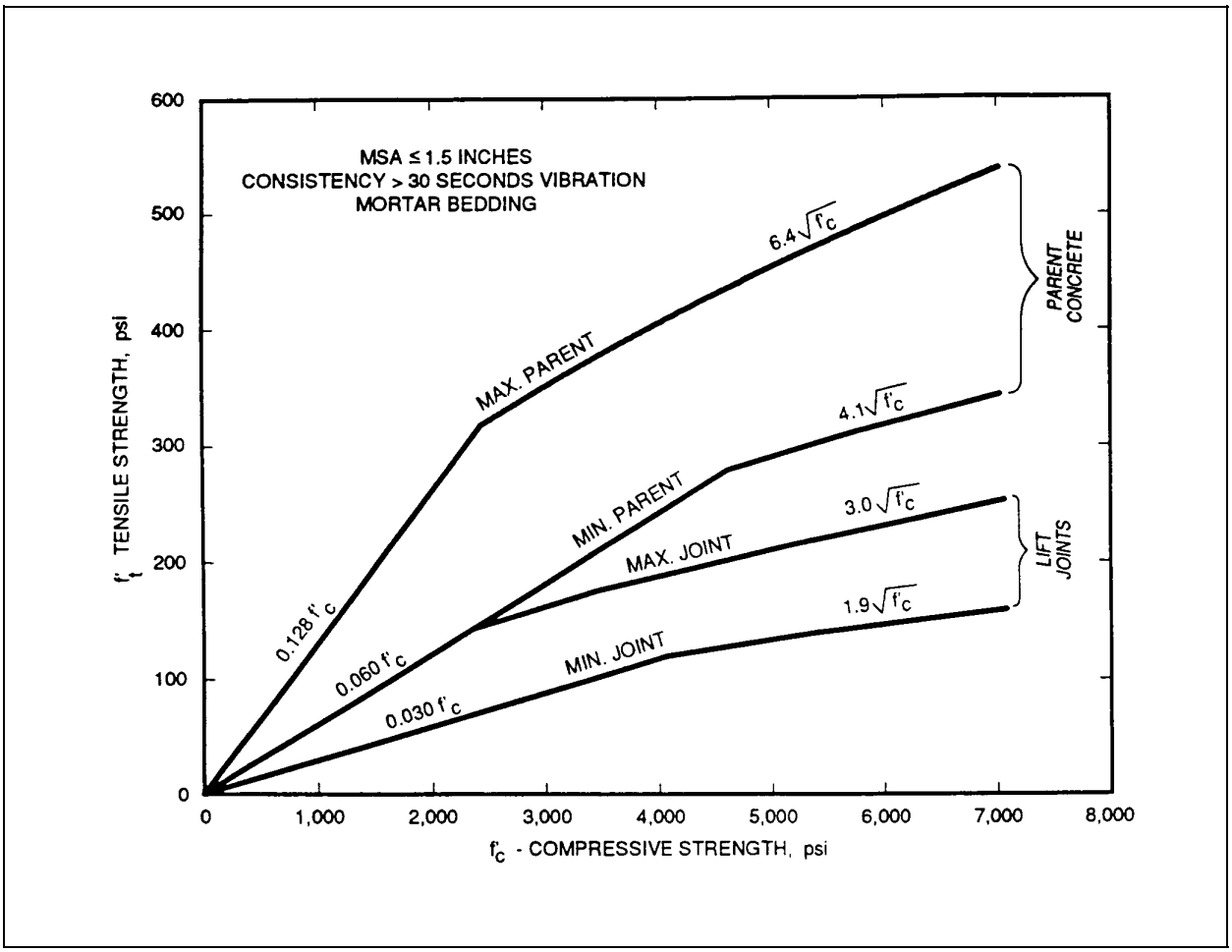

Figure 3-3. Tensile strength range, RCC, MSA ≤ 1.5 inches, consistency > 30 seconds vibration, mortar bedding

The relationship between strain rate and modulus of elasticity is as follows (Bruhwieler 1990):

$$E' = E(E_r)^{0.020}$$

where E = static modulus of elasticity

E' = seismic modulus of elasticity at the quasi-static rate

$$E_r = \frac{\text{high seismic strain rate}}{\text{quasi-static rate}}$$

For a seismic strain rate equal to 1,000 times the quasi-static rate the seismic modulus of elasticity is 1.15 times the static modulus. For long-term loadings where creep effects are important, the effective modulus of elasticity may be only 2/3 the static modulus of elasticity calculated by the above formula (Dunstan 1978). The modulus of elasticity may exhibit some anisotropic behavior due to the coarse aggregate particle alignment as discussed in paragraph 3-3*d*(2); however, the effects on the modulus will be small and can be disregarded when performing a dynamic stress analysis.

3-6. Poisson's Ratio

Poisson's ratio for RCC is the same as for conventional mass concrete. For static loads, values range between 0.17 and 0.22, with 0.20 recommended when testing has not been performed. Poisson's ratio is also strain rate sensitive, and the static value should be reduced by 30 percent when evaluating stresses due to seismic loads (Bruhwieler 1990).

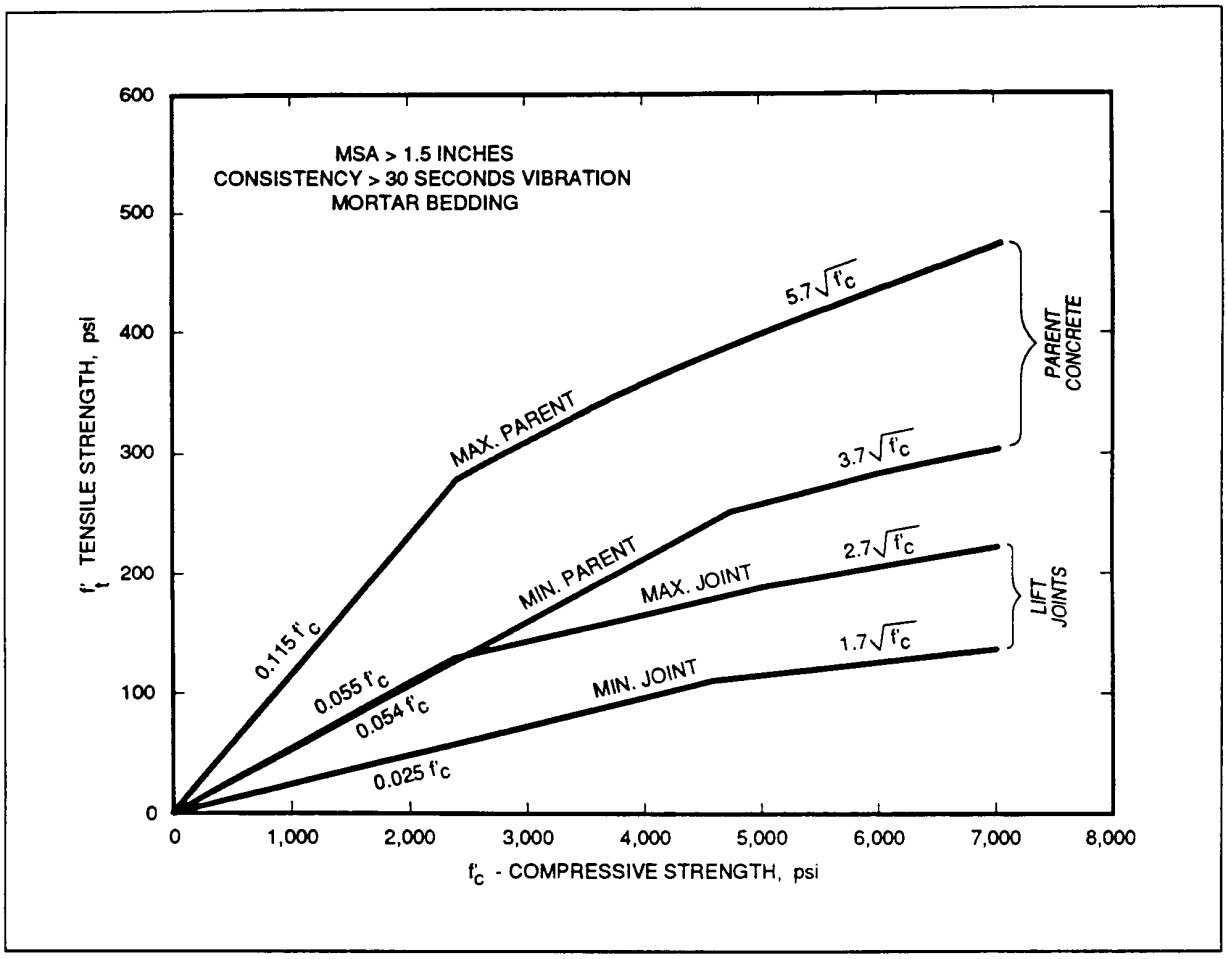

Figure 3-4. Tensile strength range, RCC, MSA > 1.5 inches, consistency > 30 seconds vibration, mortar bedding

3-7. Tensile Stress/Strain Relationship

As mentioned in paragraph 2-2*b*, concrete cracking, crack propagation, and the energy dissipated in the process are complex and nonlinear in nature. For a simplified linear-elastic analysis, a constant modulus of elasticity is required. Thus, a linear stress/strain relationship is used for the analysis with a tensile modulus equal to the modulus of elasticity for concrete in compression.

a. Compression and tension differences. Although a linear relationship is assumed for the analysis, in actuality the stress/strain relationship becomes nonlinear after concrete stresses reach approximately 60 percent of the peak stress (Raphael 1984). In compression this does not cause a problem because, in general, concrete compressive stresses even during a major earthquake are quite low with respect to the peak stress or ultimate capacity. In tension, it is a different matter since tensile stress can approach and exceed the peak tensile stress capacity of the concrete and in some cases cracking will occur.

b. Tensile stress/strain curve. The actual nonlinear stress/strain relationship for RCC concrete is shown in Figure 3-7. The assumed linear relationship used for finite element analysis was developed from the work done by Raphael (1984). The actual nonlinear performance of concrete in tension consists of a linear region from zero stress up to 60 percent of the peak stress, a nonlinear ascending region from 60 percent of peak stress to peak stress (this point on the curve corresponds to the direct tensile strength test value described in paragraph 3-3*c*), and a nonlinear descending region from peak stress back to zero

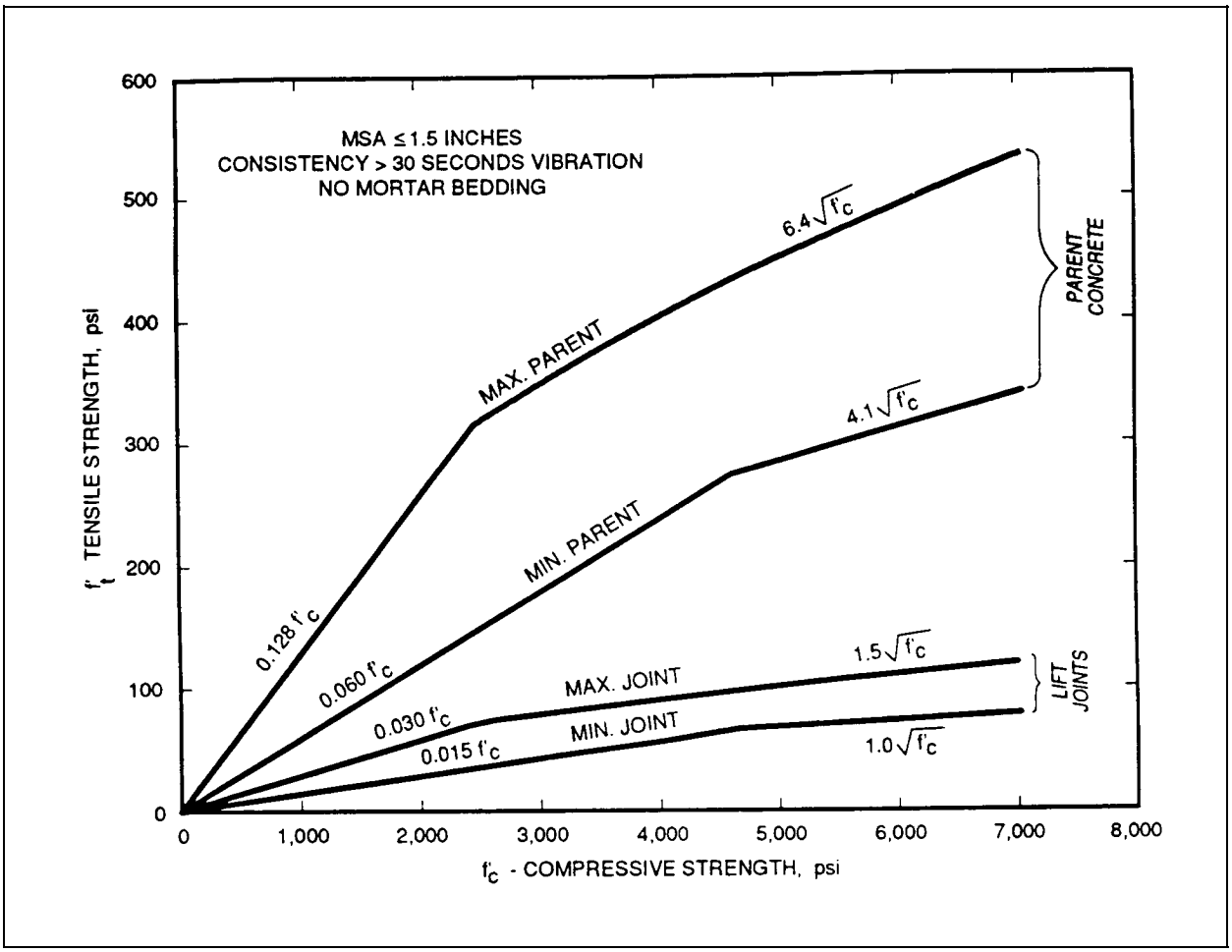

Figure 3-5. Tensile strength range, RCC, MSA ≤ 1.5 inches, consistency > 30 seconds vibration, no mortar bedding

stress. The last region is termed the "tensile softening zone." In this region, where deformation increases with decreasing stress, deformation controlled stable test procedures are required to capture the stress/strain behavior (Bruhwieler 1990), where conventional test procedures will cause the strain to fall off abruptly to zero strain at a point on the curve just beyond the peak stress point. The area under the tensile softening region of the stress/strain curve represents additional energy absorbed by the RCC structure during the crack formation process. As such, this region is quite instrumental in dissipating the energy imparted to the dam through seismic ground motion. The transition from linear to nonlinear in the ascending region of the stress/strain curve represents the development of microcracking within the concrete. These microcracks eventually coalesce into macrocracks as the tensile softening zone is reached.

3-8. Dynamic Tensile Strength (DTS)

The tensile strength of concrete is strain rate sensitive. During seismic events strain rates are related to the fundamental period of vibration of the dam with the peak stress reached during a quarter cycle of vibration. The high strain rates associated with dam response to ground motion produce tensile strengths 50 to 80 percent higher than those produced during direct tensile strength testing where the strain rate is very slow. For this reason, the dynamic tensile strength (DTS) of RCC shall be equivalent to the direct tensile strength multiplied by a factor of 1.50 (Cannon 1991, Raphael 1984). This adjustment factor applies to both the tensile strength of the parent material and to the tensile strength at the lift joints.

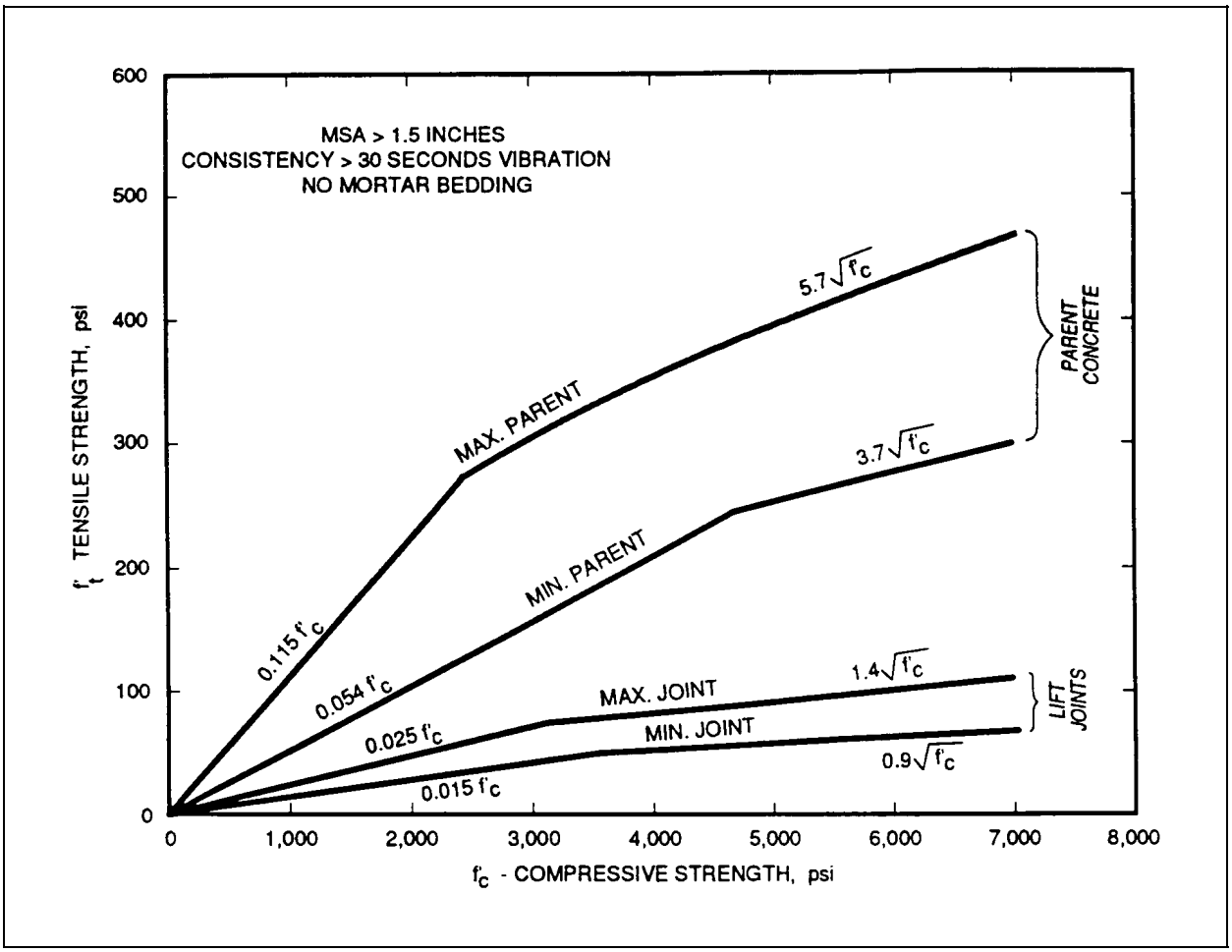

Figure 3-6. Tensile strength range, RCC, MSA > 1.5 inches, consistency > 30 seconds vibration, no mortar bedding

3-9. Allowable Tensile Stresses

When the response to ground motion increases beyond the elastic limit, energy is dissipated through crack development and crack propagation in accordance with the stress/strain relationship shown in Figure 3-7. To account for all nonlinear response including that in the tensile softening zone of the stress/strain curve requires a complex nonlinear analysis. The simpler linear-elastic analysis may be utilized in a manner which accounts for response in the linear region, and the nonlinear pre-peak region.

a. Comparing linear and nonlinear curves. Since a linear-elastic analysis converts strains to stress using a constant modulus of elasticity, the stresses from the analysis will be higher than actual stresses when in the nonlinear pre-peak and post-peak strain regions. This may be compensated for by establishing an allowable tensile stress which is greater than the actual peak tensile stress as shown in Figure 3-7. In this figure, the dashed line represents the tensile stress/strain relationship assuming linear-elastic behavior as opposed to the actual nonlinear stress/strain relationship which is shown as a heavy solid line. The amount the peak tensile stress is increased in establishing the allowable stress depends on the extent of tensile cracking that can be tolerated, which in turn is based on the performance requirements for the design earthquake under consideration. The economics of the design also becomes a factor in the higher seismic zones. In these zones, a somewhat greater amount of cracking can be justified economically because there is a point where the cost of producing RCC mixes with high tensile strengths to resist cracking will exceed the cost of repairing the cracks as long as the cracking is not too extensive.

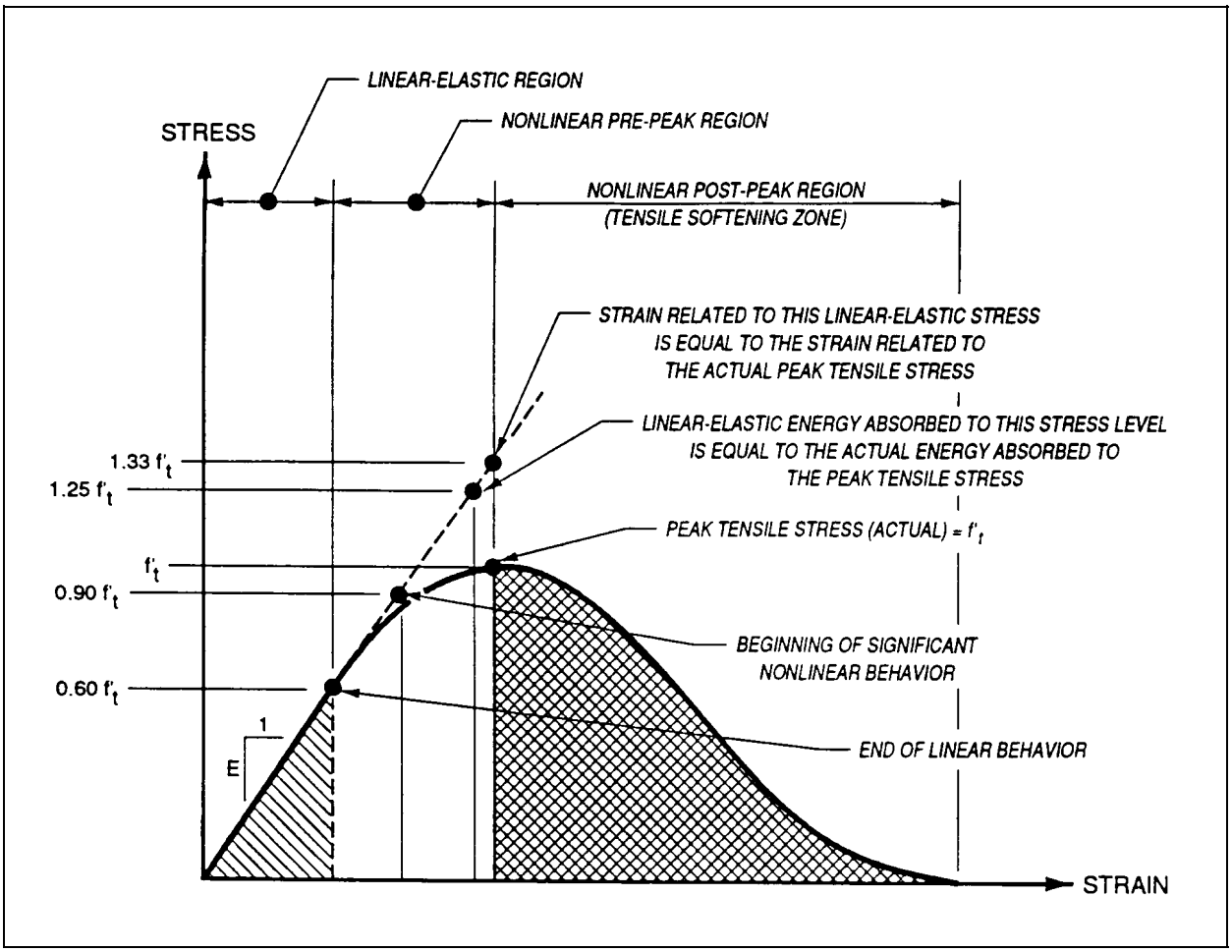

Figure 3-7. Tensile stress/strain diagram for RCC

b. Key points on stress/strain curve. Several points on the stress/strain curve are of interest when establishing the allowable tensile stresses that are used in linear-elastic analyses (refer to paragraphs 4-2*c* and 4-3*c*). Based on f'_t = actual peak tensile stress (tensile stress that corresponds to that which would be attained by a direct tensile strength test), and f_t = the stress level based on linear-elastic behavior (refer to the dashed line in Figure 3-7), the following key values of f_t are of interest:

(1) $f_t = 0.60\ f'_t$ -- the end of the elastic range and the beginning of microcracking.

(2) $f_t = 0.90\ f'_t$ -- this point was selected because the stress/strain dashed line for linear-elastic behavior is just beginning to significantly separate from the actual stress/strain curve. If the tensile stresses for a linear-elastic analysis stay within the stress level for this point, the response can still be judged as primarily linear.

(3) $f_t = 1.25\ f'_t$ -- the area under the dashed line for linear-elastic behavior up to this stress level is approximately equal to the area under the solid line for the actual stress/strain curve up to the peak tensile stress point (this point is the end of microcracking and the beginning of macrocracking). Thus, the energy absorbed in a linear-elastic analysis to this point of stress is equal to the actual energy absorbed through the microcracking pre-peak region.

(4) $f_t = 1.33\ f'_t$ -- the strain corresponding to this point of stress based on linear-elastic behavior is equal to the strain corresponding to the actual peak tensile stress. This strain point signifies the end of microcracking and the beginning of macrocracking. This point also represents a practical limit for the

linear-elastic response spectrum analysis described in paragraph 2-2*c*. Beyond this point in the tensile softening zone, the stress/strain relationship based on linear-elastic behavior diverges so rapidly from the actual stress/strain curve that a linear-elastic analysis will no longer provide an acceptable approximation of either the energy absorbed by the dam-foundation system, or the strain deformation of the system. Cracking could be extensive enough to change the dynamic properties of the dam structure.

Chapter 4
Design Earthquakes

4-1. Definition

The term "design earthquake" refers to the specification of the free field ground motion that would be felt at the dam site due to a particular seismic event that is used as the basis for earthquake resistant design of new RCC dams, or to evaluate the response of existing RCC dams.

4-2. Operating Basis Earthquake (OBE)

The OBE is defined as the earthquake producing the greatest level of ground motion that is likely to occur at the site during the service life of the dam. The service life shall be taken as 100 years for both new dams and existing dams. The seismic risk or adverse consequences of failure of an existing dam is not reduced as long as the dam is in operation; therefore, the "remaining service life" of an existing dam shall not be substituted for the 100-year service life specified above. The OBE is determined using probabilistic methods and, as such, is defined as the earthquake with a 50 percent chance of exceedance in the service life of the dam.

a. General performance requirements. All structural, mechanical, and control equipment used to regulate the reservoir shall be capable of remaining fully operational during and after an OBE. New RCC dams located in low seismic regions shall be designed to prevent the initiation of cracking in the concrete structure. Tensile cracking in new RCC dams located in high seismic regions and in existing dams in all seismic regions is allowed; however, it shall be limited to only "minor cracking" that requires little or no repair.

b. Structural criteria. The following general structural criteria shall be the basis for satisfying the concrete cracking performance requirements stated above.

(1) Initiation of cracking is prevented when the tensile stresses are less than $0.60\ f'_t$ as shown in Figure 3-7.

(2) The level of cracking is considered to be "minor cracking" when the tensile stresses are less than $1.25\ f'_t$ as shown in Figure 3-7.

c. Allowable tensile stress. The allowable tensile stresses $f_{t\ (allowable)}$ for the OBE are established below. The formulae apply to the calculation of both allowable tensile stress of the parent material and allowable tensile stress of the lift joints. DTS = Dynamic Tensile Strength, and f'_t = direct tensile strength.

(1) Existing dams:

$$f_{t\ (allowable)} = 1.25 \times \text{DTS} = 1.875 \times f'_t$$

(2) New dams in seismic zones 0, 1, 2A, and 2B:

$$f_{t\ (allowable)} = 0.60 \times \text{DTS} = 0.90 \times f'_t$$

(3) New dams in seismic zones 3 and 4:

$$f_{t\ (allowable)} = 0.90 \times \text{DTS} = 1.35 \times f'_t$$

d. Damping. Studies on dams under severe ground motion which cause stresses in the upper reaches of the elastic range indicate a dampened response which corresponds to a damping factor of about 5 percent of critical. On this basis the OBE shall be analyzed using a damping ratio equal to 5.0 percent of critical damping for the concrete dam structure only. This factor must be modified as outlined in paragraph 7-3 to account for foundation damping.

4-3. Maximum Credible Earthquake (MCE)

The MCE is defined as the largest possible earthquake that could reasonably occur along the recognized faults or within a particular seismic source. Often several fault sources must be investigated to determine which will produce the critical site ground motion. By definition the MCE has a very low probability of occurence. Ground motion associated with the MCE is established using the deterministic approach.

a. General performance requirements. Both new RCC dams and existing dams shall be capable of surviving the MCE without a failure of a type that would result in the loss of life or significant damage to downstream property caused by an uncontrolled release of the reservoir pool. Nonlinear behavior with associated damage is permissible, but the post earthquake damaged condition of the dam shall allow for controlled lowering of the pool to facilitate repair.

b. Structural criteria. The upper limit of linear elastic analysis is considered to be that point on the straight stress/strain line corresponding to a linear stress level of 1.33 f'_t (see Figure 4-7). When tensile strains exceed the strain associated with this linear stress limit, macrocracking occurs and the RCC will be subject to some degree of structural damage. As the strain level increases well into the tensile softening zone, response becomes markedly nonlinear and it is clear that a linear-elastic analysis no longer approximates the response. Although crack damage increases in this zone, performance requirements may still be satisfied. Thus, the structural criteria for the MCE, when using linear-elastic analysis, are set by limitations of the method of analysis rather than on criteria that relate to an acceptable level of structural concrete damage.

c. Allowable tensile stresses. The allowable tensile stress $f_{t\ (allowable)}$ for the MCE is established below. DTS = Dynamic Tensile Strength, and f'_t = the direct tensile strength.

$$f_{t\ (allowable)} = 1.33 \times \text{DTS} = 2.000 \times f'_t$$

d. Damping. The linear-elastic analysis for the MCE shall utilize a damping ratio equal to 7.0 percent of critical damping for the concrete dam structure only. The increase in the damping ratio from 5 percent for the OBE to 7 percent for the MCE helps account for some additional nonlinear behavior while using a linear-elastic approach.

Chapter 5
Design Response Spectra and Acceleration Time Histories

5-1. Defining the Design Earthquake

In a linear-elastic response spectrum analysis, response spectra define the free field ground motion for the design earthquake. A response spectrum gives the maximum damped response (expressed as displacement, velocity, or acceleration) of all possible linear single degree-of-freedom systems using the natural frequency (or period) to describe the system. Viscous damping expressed as a percentage of critical damping is used to develop a response spectra. A design earthquake is often defined by a set of response spectra for various damping ratios. The response spectra produced by recorded earthquake events are characterized by a jagged shape made up of peaks and valleys of varying magnitude; however, design response spectra are smoothed so that they are not frequency sensitive.

5-2. Developing Design Response Spectra

a. Deterministic and probabilistic approaches. Design response spectra are developed by using either a "deterministic approach" or a "probabilistic approach." The probabilistic approach is based on probabilistic seismic hazard analysis methodology which in essence uses the same elements as the deterministic approach, but adds an assessment of the likelihood that ground motion will occur during a specified time period.

b. Procedures. There are two basic procedures for developing design response spectra using either the deterministic or probabilistic approach. They are: (1) anchoring the spectral shape to the peak ground acceleration; and (2) estimating the spectrum directly. Although procedure (1) is more often used, the use of procedure (2) is increasing, and for some situations is preferred because it incorporates factors besides just the local site conditions.

c. Obtaining design response spectra. It is beyond the scope of this EP to present the detailed procedures for developing design response spectra, or for forecasting PGA's for design earthquakes. Refer to ETL 1110-2-301, ETL 1110-2-303, and "Tentative Provisions for the Development of Seismic Regulations for Buildings" (Applied Technology Council 1984) for further information on developing design response spectra to define the design earthquakes.

5-3. Developing Acceleration Time Histories

a. Matching design response spectrum. The more refined methods of analysis discussed in paragraph 2-2*d* are of the time-history type. Time histories usually express the ground motion as a record of acceleration with respect to time. Acceleration time histories should be developed so their response spectrum is consistent with the previously established site-specific design response spectrum described in paragraph 5-5*c*. The time histories should also have a strong motion duration appropriate to the particular design earthquake.

b. Procedures. There are two basic procedures for developing acceleration time histories: (1) selecting a suite of past recorded earthquake ground motions, and (2) synthetically developing or modifying one or more ground motions.

(1) When selecting a suite of time-history records for the first procedure, the intent is to cover the valleys of the spectrum produced by one record, which fall significantly below the site-specific design response spectrum, with better matching spectral values at these frequencies as produced by the other records in the suite. It is also necessary that the spectra produced by the suite of records not significantly exceed the site-specific design response spectrum. Primary advantage of this procedure is that the structure is analyzed by real, natural ground motions that are representative of what the structure could experience.

(2) When using the second procedure, it is possible to either completely synthesize an accelerogram, or modify an actual recorded earthquake accelerogram so that the response spectrum of the resultant accelerogram closely fits or matches the site-specific design response spectrum. The primary advantage of this procedure is that a good fit to the design response spectrum can be achieved with a single accelerogram, thus only a single dynamic analysis is required.

5-4. Dynamic Analysis by Modal Superposition

a. Frequencies and mode shapes. The linear-elastic response spectrum method utilizes modal superposition dynamic analysis to determine the structural response.

b. Time-history analysis. Once the modes are derived, the response of the complex multiple degree-of-freedom system is reduced to the solution of the simple, single basic equation of motion for a single degree-of-freedom (SDOF) system. For time-history analysis, the response is easily obtained using step-by-step integration of the equation of motion for the SDOF system for each significant mode based on the frequency (eigenvalue) of the mode. In essence the response contribution of each mode is determined for a series of time steps using a prescribed time-step interval, and the response at each time step is simply the superposition, or addition, of characteristic mode shapes adjusted by coefficients obtained from the integration procedure. Normally, only a few mode shapes are found to contribute significantly to the response, so that the modal superposition method produces a precise response with minimum computational effort.

c. Response spectrum analysis. In a response spectrum analysis, the step-by-step integration part of the dynamic analysis, described above for time-history analysis, is performed in the process of developing the response spectrum. The response spectrum may be envisioned as a display of the results of this part of the modal analysis, and it is presented in the form of "maximum" response versus frequency (or period). In the response spectrum modal analysis, eigenvalues, eigenvectors, and modal participation factors are computed and used in the analysis procedure just as they are in a time-history modal analysis. Precise "maximum" modal responses are easily calculated from a simple equation that relates these parameters and the appropriate spectral value that corresponds to the modal frequency.

d. Combining modal responses. The final step in a response spectrum analysis consists of correct superpositioning of the "maximum" modal responses; however, there is not a unique solution to this final step in the response spectrum method. This is because the exact mode contributions at the critical point in time when the response peaks are not available from a response spectrum representation of a particular ground motion. One advantage of a smooth design response spectrum is that it is a statistical representation, or an envelope, of the many possible ground motions that could occur at the site rather than only a single ground motion. The superposition of the maximum modal responses is accomplished by use of one of several statistical methods described in Chapter 7.

5-5. Types of Design Response Spectra

a. Probability level. Design response spectra are usually based statistically either on the mean, median (50th percentile probability level), or the median plus one standard deviation (84th percentile probability level), of the ground motion parameters for the records chosen. Design response spectra used for design of new RCC dams or for evaluation of the safety and serviceability of existing dams shall be based on the mean level of the ground motion parameters.

b. Type of spectrum required. Either a "site-specific" or a "standard" design response spectra shall be used to describe the design earthquakes. The type required shall be based on the seismic zone, the proximity of the seismic source, and the maximum height of the dam.

c. Site-specific design response spectra. The site-specific design response spectra should be developed based on earthquake source conditions, propagation path properties, and local foundation characteristics associated with the specific site. This type of design spectra may be established by anchoring a selected response spectral shape for the site to the estimated peak ground acceleration, or by estimating the design spectra directly using response spectral attenuation relationships, performing statistical analysis of strong-motion records, or applying theoretical (numerical) ground motion modeling. In the requirements that follow, a site is classified as a "high seismic risk site" when it is located within 20 kilometers of an active fault or area source in the western United States (WUS), or within a tectonic province in the eastern United States (EUS) where the source or province has a maximum local magnitude of 6.0 or greater. The boundary between the WUS and the EUS is defined as the eastern boundary of the Rocky Mountains. Site-specific design response spectra are required for:

(1) Dams greater than 100 feet in height located at a site classified as a "high seismic risk site."

(2) Dams greater than 100 feet in height located in Seismic Zone 2B, 3, or 4 even though the site is not classified as a "high seismic risk site."

(3) Dams not greater than 100 feet in height located in Seismic Zone 2B, 3, or 4 when the site is classified as a "high seismic risk site."

d. Standard design response spectra. Standard design response spectra are based on fixed spectral shapes established for very general site classifications such as rock or soil site. They ignore the effects of earthquake magnitude and distance, and the specific foundation characteristics at the site. The standard design spectra are usually "anchored" to the estimated peak ground acceleration (PGA) established for the design earthquake. The fixed spectral shape is usually presented such that it is normalized to a 1.0 g value of maximum ground acceleration. This normalized value can be easily checked by observing the spectral acceleration value from the spectrum plot for frequencies above about 50 cps where the response and the maximum ground acceleration coincide. Standard design response spectra are adapted to the severity of ground motion associated with the OBE or MCE by using the PGA as a scaling factor. The standard design response spectra can be used for:

(1) Dams greater than 100 feet in height located in Seismic Zone 0, 1, or 2A when the site is not classified as a "high seismic risk site."

(2) Dams not greater than 100 feet in height located in Seismic Zone 0, 1, or 2A.

(3) Dams not greater than 100 feet in height located in Seismic Zone 2B, 3, or 4 when the site is not classified as a "high seismic risk site."

e. Required design spectrum. When it is acceptable to use a standard design response spectrum to define the design earthquakes, the standard design spectrum shown in Figure 5-2 shall be used (Applied Technology Council 1984). This spectrum is considered conservative but reasonable for essential structures such as dams. It is fully described by only five control points on a tripartite plot. Table 5-1 presents the spectrum in equation format so it is easily developed for any damping value. The standard design spectrum shown in Figure 5-2 and defined in equation format in Table 5-1 is normalized to 1.0 g PGA. The standard spectrum shall be anchored to the PGA for the OBE and the MCE by using the appropriate scaling factors provided in Table 5-2. The correct scaling factors are selected based on the seismic zone location of the site using the seismic zone map shown in Figure 5-1.

5-6. Horizontal and Vertical Design Response Spectra

a. Site-specific design response spectra. When site-specific design response spectra are required in accordance with paragraph 5-5*c*, two independent design response spectra shall be developed, one to define the horizontal component of ground motion, and the second to define the vertical component. The vertical component of ground motion usually contains much higher frequency content than the horizontal component, therefore the spectral shape is quite different than that of the horizontal component. The PGA associated with the vertical component will also be different than the PGA of the horizontal component. Both values of PGA are dependent on the distance from the source, but for short distances, the PGA of the vertical component may actually exceed the PGA of the horizontal component.

b. Standard design response spectra. When it is acceptable to use standard design response spectra to define the design earthquakes, the horizontal component of ground motion shall be defined by anchoring the standard design response spectra for the appropriate damping factor developed from Table 5-1 with the scaling factor provided in Table 5-2. The vertical component of ground motion shall utilize the same standard design response spectrum used for the horizontal component, but it shall be scaled using the appropriate ratio of the PGA for the vertical component to the PGA for the horizontal component as provided in Figure 5-3. This ratio is based on the site to source distance (R) and the fundamental natural period of vibration of the structure.

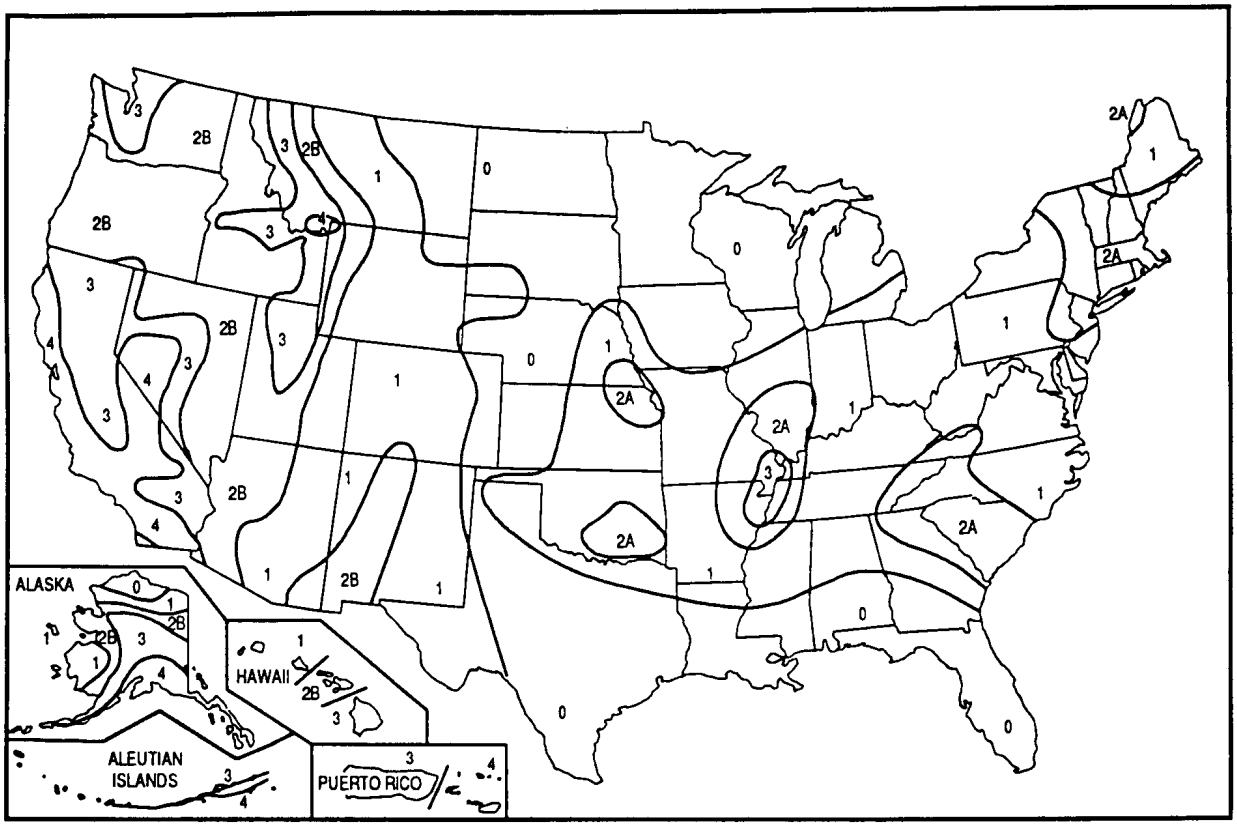

Figure 5-1. Seismic zone map of the United States. (Uniform Building Code, 1988 Edition)

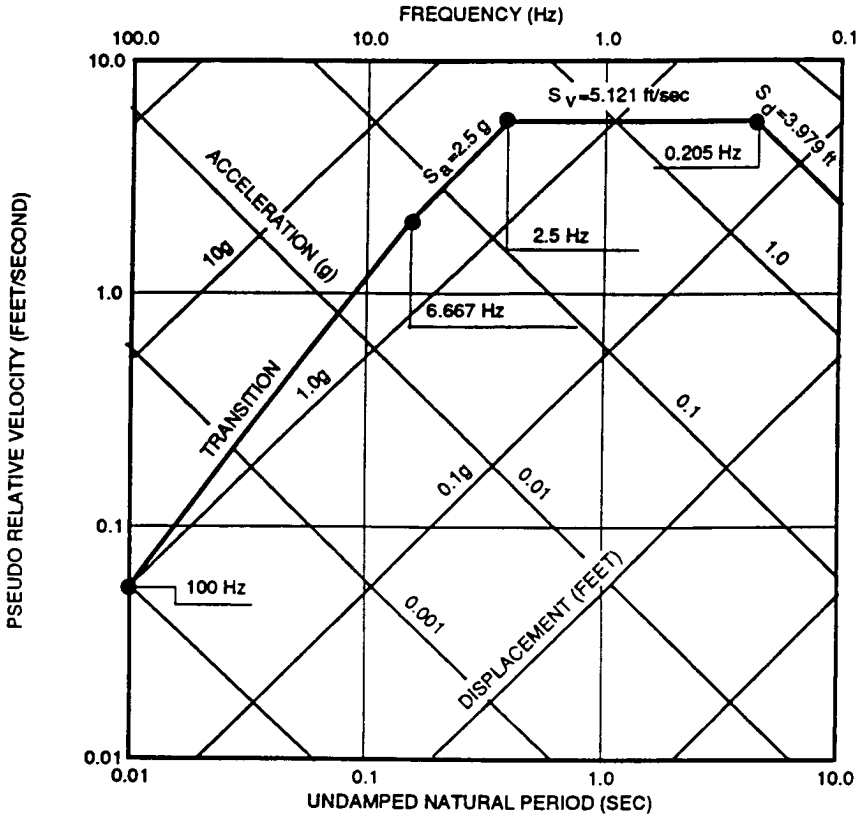

Tripartite Logarithmic Representation (5% damped)

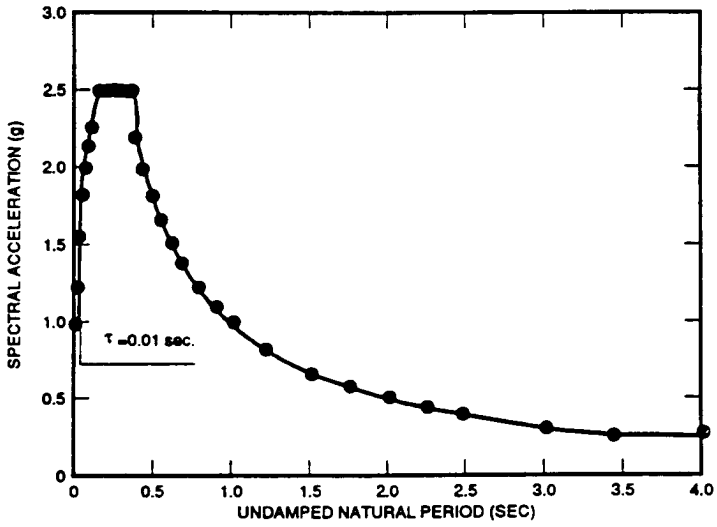

Arithmetic Plot of Spectral Acceleration versus Period (5% damped)

Figure 5-2. Standard design response spectra for horizontal component of ground motion - normalized to PGA = 1.0 g. (Applied Technology Council ATC-3-06 Tentative Provisions, 1984)

Table 5-1
Determining the Standard Design Response Spectrum for Horizontal Component of Ground Motion - Normalized to PGA = 1.0 g, for Any Value of β (Percent of Critical Damping)

	T (sec)	f (Hz)	$S_{a(5\%)}$(g's)	K_1	
*	0.002	500.000	1.0000	0.00000	EQUATION 1
	0.005	200.000	1.0000	0.00000	
	0.008	125.000	1.0000	0.00000	
*	0.010	100.000	1.0000	0.00000	
	0.020	50.000	1.2643	0.25596	
	0.040	25.000	1.5985	0.51192	
	0.060	16.667	1.8335	0.66164	
	0.080	12.500	2.0210	0.76787	
	0.100	10.000	2.1795	0.85028	
	0.120	8.333	2.3182	0.97160	
*	0.150	6.667	2.5000	1.00000	
	0.200	5.000	2.5000	1.00000	
	0.250	4.000	2.5000	1.00000	
	0.300	3.333	2.5000	1.00000	
	0.350	2.857	2.5000	1.00000	
*	0.400	2.500	2.5000	1.00000	
	0.450	2.222	2.2222		EQUATION 2
	0.500	2.000	2.0000		
	0.550	1.818	1.8182		
	0.600	1.667	1.6667		
	0.650	1.538	1.5385		
	0.700	1.429	1.4286		
	0.800	1.250	1.2500		
	0.900	1.111	1.1111		
	1.000	1.000	1.0000		
	1.250	0.800	0.8000		
	1.500	0.667	0.6667		
	1.750	0.571	0.5714		
	2.000	0.500	0.5000		
	2.250	0.444	0.4444		
	2.500	0.400	0.4000		
	3.000	0.333	0.3333		
	3.500	0.286	0.2857		
	4.000	0.250	0.2500		
*	4.882	0.205	0.2048		
	5.000	0.200	0.1953		
	6.000	0.167	0.1356		
	7.000	0.143	0.0996		
	8.000	0.125	0.0763		
	9.000	0.111	0.0603		
*	10.000	0.100	0.0488		

* INDICATES THE ONLY POINTS NEEDED TO SPECIFY THE RESPONSE SPECTRUM FOR COMPUTER PROGRAMS WITH LOGARITHMIC INTERPOLATION CAPABILITY.

DEFINITION OF TERMS

S_a = SPECTRAL ACCELERATION IN g's FOR β PERCENT OF CRITICAL DAMPING

$S_{a(5\%)}$ = SPECTRAL ACCELERATION IN g's FOR 5 PERCENT OF CRITICAL DAMPING

T = UNDAMPED NATURAL PERIOD, SECONDS

f = FREQUENCY, Hz

β = PERCENT OF CRITICAL DAMPING

K_1, K_2, K_3 = CORRECTION FACTORS USED TO DEVELOP A DESIGN RESPONSE SPECTRUM FOR β PERCENT OF CRITICAL DAMPING

CORRECTION FACTORS

K_1 = FACTOR SHOWN IN TABLE FOR VALUES OF THE NATURAL PERIOD T BETWEEN 0.000 AND 0.400

$K_2 = 1.466 - 0.2895 \text{ LN } (\beta)$

$K_3 = \text{LOG}(2.5 \times K_2)$

EQUATIONS FOR S_a

WHEN $T \leq 0.400$ $S_a = 10.0^{K_1 K_3}$ (EQUATION 1)

$T > 0.400$ $S_a = K_2 S_{a(5\%)}$ (EQUATION 2)

NOTE: THE VALUES OF SPECTRAL VELOCITY S_v AND SPECTRAL DISPLACEMENT S_d CAN BE CALCULATED ONCE S_a IS KNOWN:

$S_v = 5.1207 (S_a T)$

$S_d = 0.81498 (S_a T^2)$

Table 5-2
Peak Ground Accelerations (PGA's) for Use in Scaling the Standard Design Response Spectra

Seismic Zone	PGA	
	Operating Basis Earthquake (OBE)	Maximum Credible Earthquake (MCE)
0	0.030	0.130
1	0.050	0.210
2A	0.095	0.360
2B	0.115	0.430
3	0.210	0.550
4	0.270	0.610

NOTES:

1. Refer to Figure 5-1 for the seismic zone maps.
2. PGA's are expressed as the decimal ratio of the acceleration due to gravity (g).
3. PGA's are obtained from curves of "Annual Risk of Exceedance vs. PGA" in Figure C1-7 of ATC-3 Tentative Provisions, April 1984.
4. The PGA for the OBE is based on a 50 percent chance of exceedance in 100 years.
5. The MCE is considered to be the event with a 5,000-year return period (annual risk of exceedance = 0.0002 chance/year).

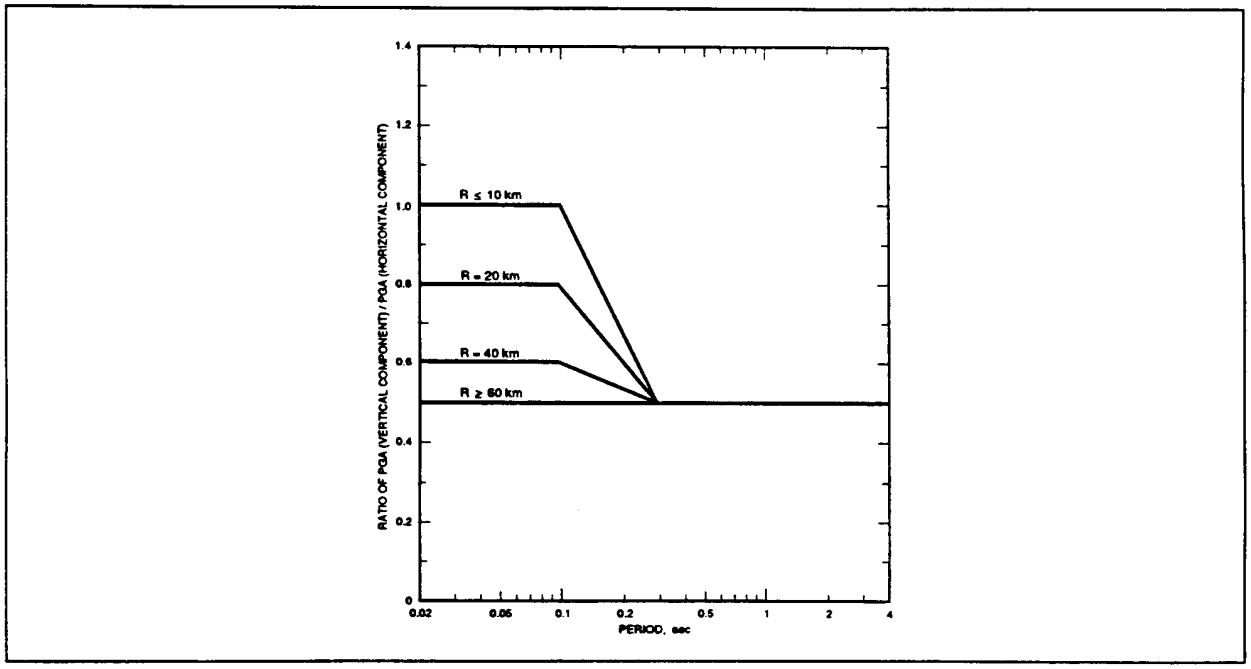

Figure 5-3. Ratio of PGA for the horizontal component to the PGA for the vertical component as a function of source to site distance (R) and the fundamental period of vibration of the structure

Chapter 6
Earthquake Load Cases

6-1. Load Combinations

The cyclic and oscillatory nature of vibratory response can cause critical tensile stresses to occur in either the upstream or the downstream face of the dam. Therefore, the earthquake load cases must consider combinations of the design earthquake loading with other loads which lead to critical tension in both the upstream and downstream faces. Usually two or more OBE load cases and two or more MCE load cases must be evaluated. The discussion of earthquake load cases that follows refers to seismic criteria regarding ground shaking and foundation fault displacement as discussed in paragraphs 2-2 and 2-3, respectively, and not stability criteria described in paragraph 2-1. Load case requirements for stability are covered in EM 1110-2-2200.

6-2. Dynamic Loads To Be Considered

The design earthquake imposes several types of dynamic loads on the dam. The greatest dynamic load is the inertia load caused by the response of the concrete mass to ground motion accelerations. Next is the hydrodynamic load created by a high reservoir and tailwater condition. Hydrodynamic forces are imposed on the dam due to motions of the dam reacting with the surrounding water, and motions of the reservoir bottom. Finally, backfill or silt deposits against the faces of the dam will interact with the structural mass of the dam in a manner similar to the hydrodynamic load.

6-3. Static Loads To Be Considered

The effects on the dam structure due to static loads, as discussed below, are determined by conventional static analysis methods. The results of the dynamic and static analyses are combined by superposition to determine the total stresses for the earthquake load case.

a. Reservoir and tailwater loads. Load cases shall be included to cover both the highest and the lowest reservoir pool elevations that can be judged on a statistical basis to have a reasonable chance of occurrence at the time of the design earthquake.

(1) Flood frequency data from project flood flow and flood routing studies provide a basis for establishing reasonable high pool elevations. Each dam must be evaluated based on its own set of unique conditions.

(2) The conservation pool elevation for the project shall be used for earthquake load cases involving low pool conditions. If there is no established conservation pool, use the lowest average pool elevation that can best be judged to exist for a 30-day period in a normal yearly flow cycle.

(3) Where tailwater is applicable for an earthquake load case, the elevation shall be selected which increases the response while being consistent with the reservoir conditions.

b. Backfill load. Earth or rock fill placed against either face of the dam has both a static and dynamic load effect during an earthquake. These loads shall be included in all earthquake load cases. Static loading shall be based on at-rest pressures. Dynamic loading may be approximated by the Mononobe and Okabe method utilizing the inertia force acting on the Coulomb sliding wedge in the appropriate direction as discussed in EM 1110-2-2502. For finite element analyses the dynamic effect may be approximated by added mass based on the Coulomb sliding wedge.

c. Siltation load. During the life of the dam, silt may build up against the upstream face to a depth which may cause a moderate increase in the tensile stresses in load cases where tension in the upstream face is critical. For these load cases, siltation loading shall be considered based on the full depth expected during the life of the dam. In load cases where tension in the downstream face is critical, the siltation load will decrease the tensile stresses. For these load cases a zero depth of silt shall be assumed. When silt is included, both static and dynamic loading effects should be incorporated using the same methods as discussed for backfill loads.

d. Gravity loads. Gravity loads shall include the weight of the RCC, weight of backfill or silt on battered faces of the dam, and weight of equipment if significant.

6-4. Static Loads Not To Be Considered

There are several types of loads where the magnitude of the load and the load pattern that would exist at the time of the design earthquake event cannot be defined on a logical basis or to any degree of accuracy. However, based on the general nature and range of magnitude normally associated with loads of this type, and in comparing these loads with the dynamic and static loads already discussed, these loads normally do not contribute significantly to the results of the analyses for earthquake load cases. However, the designer should at least make a cursory evaluation of these loads to be sure that no unusual site conditions exist that would warrant including one or more of them in the earthquake load cases. For this reason, a brief discussion of these loads is included.

a. Pore pressure. When evaluating dam stability using the seismic coefficient method described in paragraph 2-1, uplift is considered to act over the entire interface area. Under the MCE, any cracking in the concrete would only extend just beyond the microcracking level. These fine cracks are open and subject to buildup of internal water pressure for a short period of time due to the oscillatory nature of the dynamic response. Therefore, uplift or internal water pressure within concrete cracks would be quite small and may be ignored in the dynamic analysis phase of design.

b. Temperature stresses. Except under extreme climatic conditions, temperature stresses need not be included as part of the earthquake load cases.

c. Wind load. Wind load on an RCC dam is so small it can be considered insignificant.

d. Ice load. Ice loading need not be included as part of an earthquake load case except for unusual climatic conditions which would cause a great depth of ice to exist over an extended period of time.

Chapter 7
Factors Significantly Affecting Dynamic Response

7-1. Evaluation Procedure and Objectives

There are many important factors in a dynamic stress analysis that can greatly affect the response of a dam. The influence which the various material and strength parameters and loads have on the final results must be evaluated. This can be done by executing the model using a typical dam cross-section and typical material properties, then modifying the loads and parameters one-by-one to give an indication of the influence each factor has on the dynamic response. Once the important factors have been identified, the design effort should concentrate on the more critical factors that form the input to the dynamic analysis. Following is a discussion of the impact some of the parameters have on the response of a dam.

7-2. Design Response Spectra

a. Spectral shape. Both the shape of the spectrum and the PGA used to anchor the spectrum affect the dam response and should be established carefully. The dynamic response in a linear-elastic analysis is directly proportional to the PGA, but minor changes in the shape of the spectra may not result in proportional changes in the response.

b. Comparison of standard spectra. For comparison purposes, three widely accepted standard design response spectra will be considered, each representing the same site conditions. The design spectra are: (1) Applied Technology Council spectrum for rock of any characteristic whether shalelike or crystalline in nature (ATC 1984), (2) H. B. Seed spectrum for rock based on 28 records (Seed 1974), and (3) Newmark-Hall spectrum using recommended values for maximum ground velocity and displacement for competent crystalline rock (Newmark and Hall 1987). Figure 7-1 shows all three spectra normalized to 1.0 g PGA for the same rock foundation site conditions. The Newmark-Hall spectrum is based on the median or 50th percentile cumulative probability, where the other two spectra are based on the mean of the records used in their development. This difference in probability level is reflected in the spectral shape. The primary cause for the difference in shape of these three spectra can be attributed to the assumptions and techniques used in smoothing the jagged spectra produced from the statistical combination of real earthquake records.

c. Spectral accelerations. Referring to Figure 7-1, the range of interest of natural period would be for periods of less than 1.0 second. This range would cover the mode shapes that produce significant response. In this range the spectral acceleration values for a given period vary between spectra up to as much as 65 percent. The ATC spectrum envelopes the other two design spectra, and is recommended for use as the standard design response spectrum. In linear-elastic response spectrum analyses, dynamic response of a particular system evaluated by two different response spectra is directly proportional to the spectral ordinates taken from the two spectra at the natural period of the system. Thus the shape of the design response spectrum greatly influences the results of the dynamic analysis.

7-3. Dam-Foundation Interaction, Damping Effect

a. Properties of the foundation. The two properties of the foundation rock that have a significant influence on the dynamic response are the damping ratio and the deformation modulus. The damping characteristics of the foundation contribute significantly to the damping of the combined dam-foundation system and must be considered in the analysis. When the foundation deformation modulus is low, the damping ratio of the combined system is considerably higher than the damping ratio of the RCC dam structure alone.

b. Effective damping ratio. There are two sources of damping for the foundation rock: (1) material (hysteretic) and (2) radiation. In contrast to this type of damping is the viscous type of damping (directly proportional to velocity) used in producing design response spectra. Therefore, it is necessary to develop an effective viscous damping ratio to represent the combined dam-foundation system in a response spectrum analysis. This is accomplished by using the curves provided in Figure D-6 of Appendix D, and the following equation is for an empty reservoir condition which allows the effects of foundation damping to be isolated. This method, developed by A. K. Chopra, is based on the

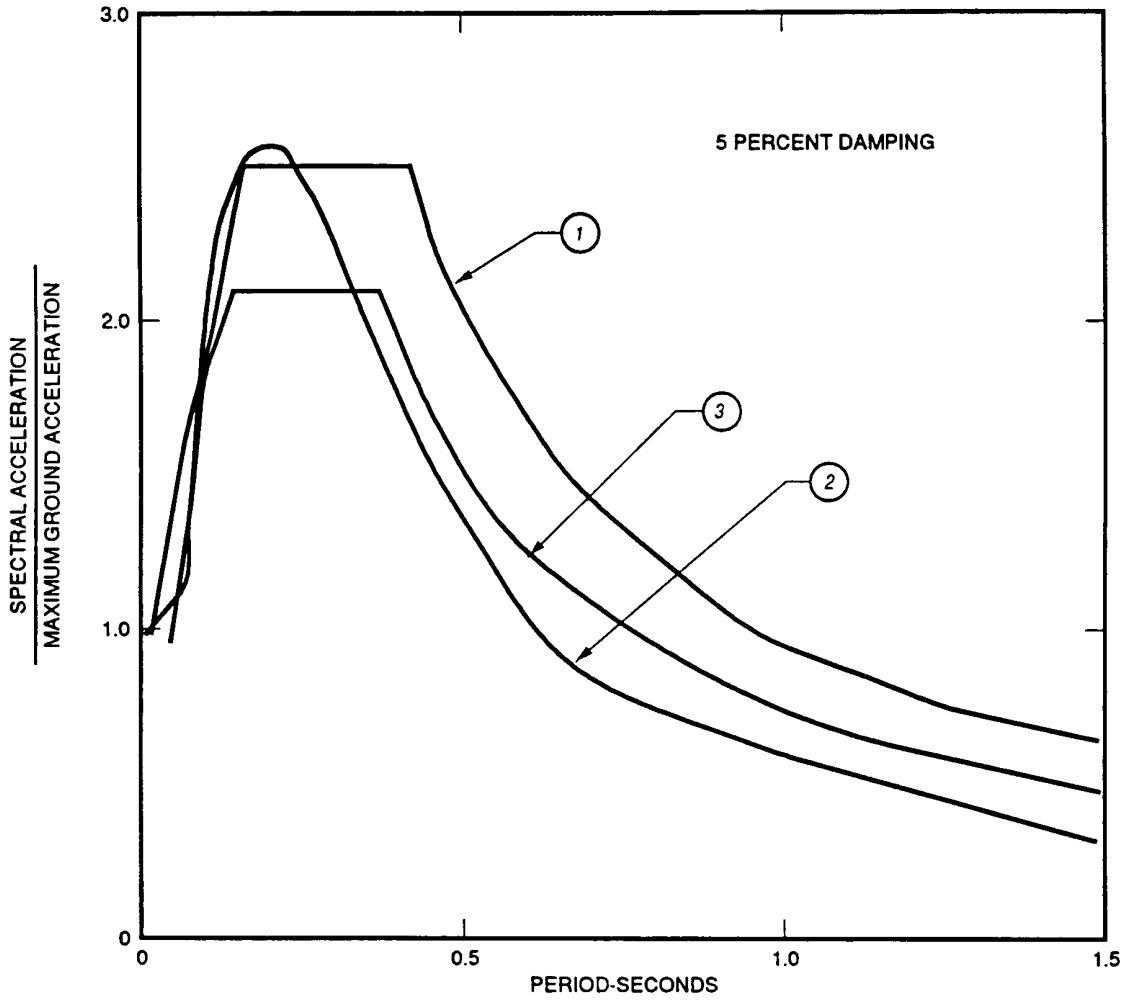

(1) APPLIED TECHNOLOGY COUNCIL (1984) DESIGN RESPONSE SPECTRUM, SOIL TYPE S_1=ROCK OF ANY CHARACTERISTIC.

(2) SEED (1974) DESIGN RESPONSE SPECTRUM FOR ROCK, 28 RECORDS ON ROCK

(3) NEWMARK-HALL (1987) DESIGN RESPONSE SPECTRUM FOR COMPETENT ROCK, 28 HORIZONTAL RECORDS

Figure 7-1. Comparison of design response spectra for rock foundations

fundamental mode of vibration, and has been shown to be reasonably close for the significant higher vibration modes (Fenves and Chopra 1986). In Figure D-6, damping for the foundation rock is expressed by the constant hysteretic damping factor.

$$\bar{\xi}_1 = \frac{1}{(R_f)^3}\xi_1 + \xi_f$$

where

$\bar{\xi}_1$ = the effective viscous damping ratio for the empty reservoir condition

ξ_1 = the viscous damping ratio for the RCC dam structure only

ξ_1 = 5.0 percent for the OBE
ξ_1 = 7.0 percent for the MCE

R_f = ratio of the fundamental period of the dam on a rigid foundation to the fundamental period of the dam on a foundation with a deformation modulus = E_f

ξ_f = added damping ratio due to dam-foundation rock interaction taken from Figure D-6

c. Effect of damping on response. To determine the effect that the damping ratio has on the response of a dam, the fundamental frequency of the composite finite element dam-foundation model must be determined. It is noted that for the response spectrum method, the effects of damping are contained only in the response spectrum itself. Thus, the ratio of the response of a dam/foundation system responding at one damping factor to the same system responding at a second damping factor is equal to the ratio of the spectral ordinates taken from the two spectra evaluated at the fundamental frequency of the system.

d. Conclusion. The damping characteristics of the foundation can have a great influence on the dynamic response. This indicates the need to carefully determine the value of the constant hysteretic damping factor for the foundation rock. This can be determined from experimental tests of appropriate rock samples subject to harmonically varying stress and strain. From such tests, the inelastic energy lost and the strain energy stored per cycle are determined and the hysteretic damping factor is calculated.

7-4. Dam-Foundation Interaction, Foundation Modulus Effect

a. Modulus of deformation. The flexibility of the jointed rock foundation is characterized by the modulus of deformation which represents the relationship between applied load and the resulting elastic plus inelastic deformation. It is best determined by in-situ testing, but may be estimated from the elastic modulus of the rock by applying an appropriate reduction factor. In a linear-elastic analysis, the modulus of deformation is synonymous with Young's modulus of elasticity (E_f).

b. Dynamic characteristics affected. The elastic modulus of the foundation influences the response because it directly affects the following dynamic characteristics of the dam-foundation system:

(1) Modal frequencies. As the modulus of deformation decreases, the modal frequencies of the composite dam/foundation system also decrease.

(2) Mode shapes. As the modulus of deformation decreases, the mode shapes are affected by increased rigid body translations and rotation of the dam on the elastic foundation.

(3) Effective damping ratio. As the modulus of deformation decreases, the effective damping ratio of the dam/foundation system increases.

c. Effect of foundation modulus on response. To determine the effect of the foundation modulus on dynamic response, a typical dam model was analyzed on foundations that bracket a wide range of foundation stiffness from infinitely stiff (E_s/E_f = 0.0), to relatively flexible (E_s/E_f = 2.5). The response was expressed as the distributed lateral inertia loading acting over the full height of the dam. Figure 7-2 shows the response graphically for three different values of E_s/E_f. It is noted that the total inertia load, or base shear, only varied by 15 percent, but a considerable variation occurred in the load pattern. As the foundation becomes more flexible, the greatest inertia load shifts from the upper portion of the dam to the lower portion. This would be accompanied by a considerable change in the concrete stresses.

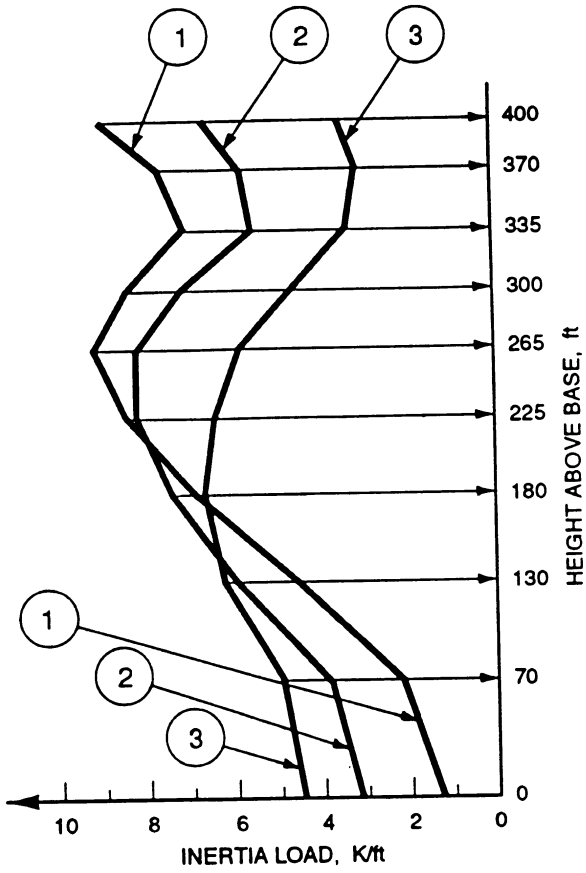

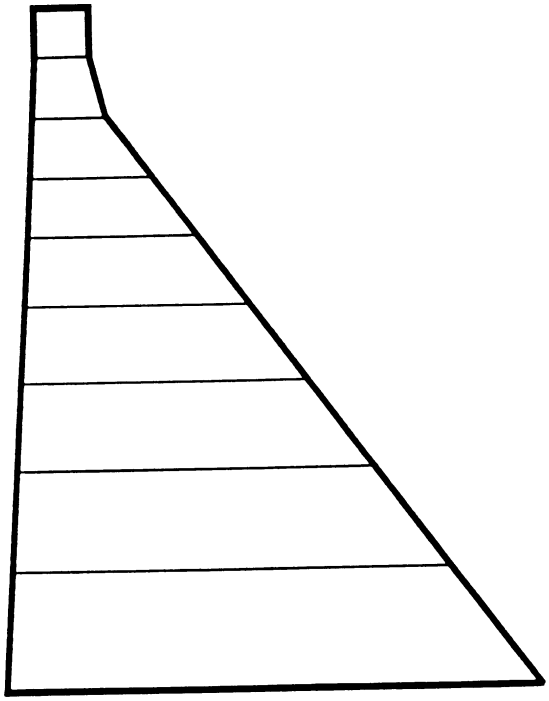

KEY PARAMETERS

	E_s / E_f	$\tilde{T}_1$	R_f	$\bar{\varepsilon}_t$	$\tilde{S}_a$	BASE SHEAR
1	0	0.295	1.000	5.0	25.12	2,450 K
2	0.5	0.333	1.127	7.08	18.23	2,489 K
3	2.5	0.462	1.565	15.6	11.16	2,171 K

Figure 7-2. Fundamental mode response expressed as the distributed lateral inertia load for various foundation stiffnesses

7-5. Hydrodynamic Effect

a. Dynamic characteristics affected. Hydrodynamic load results from the interaction of the reservoir and the structural mass of the dam in response to ground motion. The dam-reservoir interaction changes the water pressure acting on the face of the dam, and directly affects the following dynamic characteristics of the system:

(1) Modal frequencies. As the depth of the reservoir increases beyond a depth equal to about one half of the height of the dam, there begins to be a noted decrease in the modal frequencies.

(2) Mode shapes. The equivalent added mass to account for reservoir effects, as discussed in paragraph 7-5*c*, changes the relative distribution of mass in the system. Thus, the normalized mode shapes will be affected to some degree.

(3) Effective damping ratio. As the depth of the reservoir increases, dam-reservoir interaction tends to increase the effective damping ratio.

b. Added mass based on Westergaard's formula. Accounting for hydrodynamic effects when using a composite finite element model (refer to paragraph 8-1*d*(3)(a)) requires developing an equivalent mass system which strategically adds mass to the dam-foundation model. The amount and location of the added lumped masses must be such that they correctly alter the dynamic properties described above in a manner which will also produce the desired pressure changes. Often the added mass is calculated based on Westergaard's pressure diagram divided by the acceleration due to gravity to convert it from a distributed load to a distributed mass.

c. Added mass based on Chopra's method. A. K. Chopra's Simplified Analysis Procedure (Chopra 1978) uses an equivalent mass system to consider compressibility of water and the dynamic properties of the dam and reservoir bottom. Chopra suggests that the key parameter that determines the significance of water compressibility is

$$\Omega_r = \frac{\omega_1^r}{\omega_1}$$

where

Ω_r = water compressibility significance parameter

ω_1^r = fundamental frequency of the impounded water idealized by a fluid domain of constant depth and infinite length

ω_1 = fundamental frequency of the dam alone

and when

$\Omega_r \leq 0.5$, compressibility of water is significant and should be accounted for in determining the hydrodynamic effect

d. Standard pressure function curves. In Chopra's system, the hydrodynamic pressure distribution and equivalent mass system are derived using a set of standard hydrodynamic pressure function curves. The equivalent mass system for the composite finite element method may be developed using the same principles as those for the Simplified Procedure. The added mass is determined by using the appropriate pressure function curve, certain equations from Chopra's Simplified Procedure, and the fundamental mode shape and frequency obtained from the finite element analysis of the dam-foundation model. Some additional requirements applying to added mass are discussed in paragraph 7-8*c*, and complete details for deriving the equivalent mass system for the composite finite element method are provided in Appendix D of this EP.

e. Hydrodynamic pressure distribution. Figure 7-3 shows the hydrodynamic pressure distribution associated with the fundamental mode for a typical dam with a high reservoir condition. Plot 1 shows the distribution calculated by Chopra's Simplified Procedure, where Plot 2 and Plot 3 were obtained using the composite finite element method with equivalent mass systems as discussed above. The added mass for Plot 2 was based on Westergaard's formula, and the added mass for Plot 3 was based on the standard pressure function curves and the method described in Appendix D. To extract the hydrodynamic pressure distribution using the composite finite element method, the dynamic analysis was

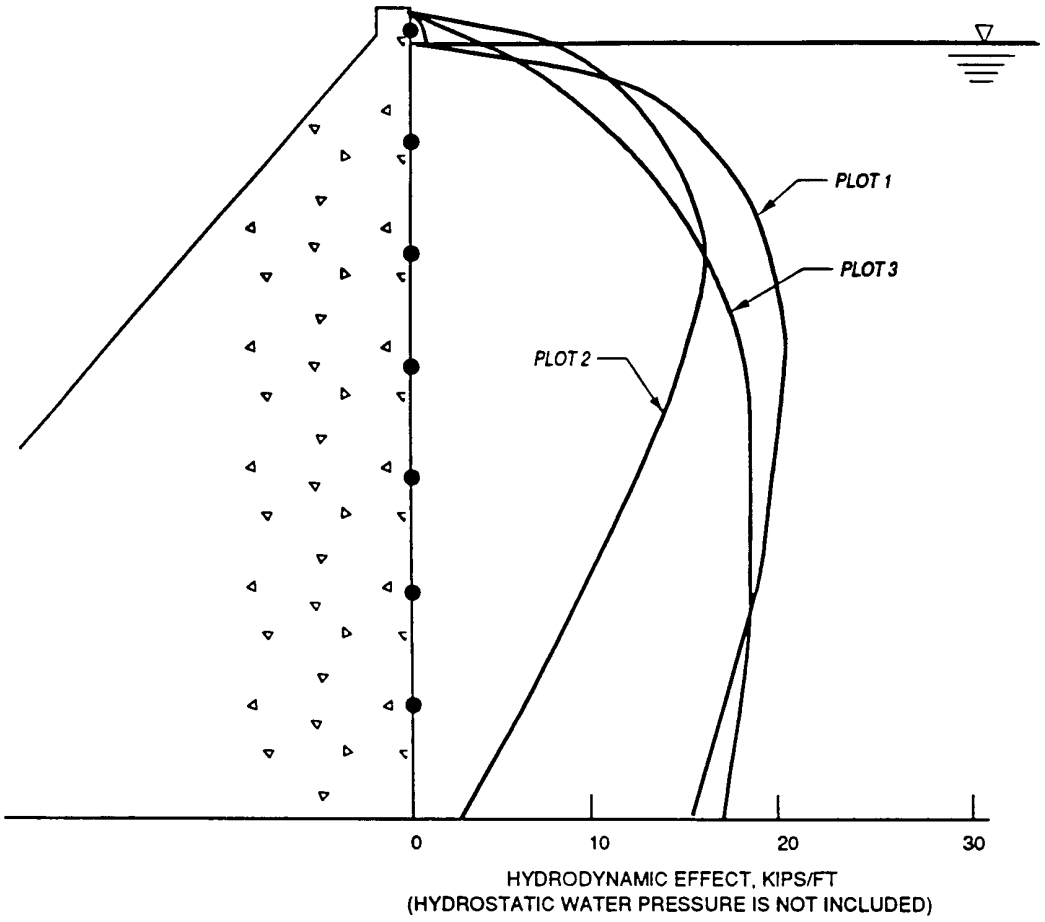

LEGEND

PLOT 1 CALCULATED USING CHOPRA'S SIMPLIFIED ANALYSIS PROCEDURE FOR THE FUNDAMENTAL MODE RESPONSE WHICH INCORPORATES THE ELASTIC STIFFNESS CHARACTERISTICS OF THE DAM AND THE FOUNDATION, AND COMPRESSIBILITY OF WATER.

PLOT 2 RESULTS FROM FINITE ELEMENT ANALYSIS WHICH MODELS THE HYDRODYNAMIC EFFECT AS ADDED MASS CALCULATED BY WESTERGAARD FORMULA.

PLOT 3 RESULTS FROM FINITE ELEMENT ANALYSIS WHICH MODELS THE HYDRODYNAMIC EFFECT USING THE "EQUIVALENT MASS SYSTEM" WITH THE ADDED MASS CALCULATED USING CHOPRA'S STANDARD HYDRODYNAMIC PRESSURE FUNCTION CURVES AND EQUATIONS FROM THE SIMPLIFIED ANALYSIS PROCEDURE.

Figure 7-3. The hydrodynamic effect expressed as an "equivalent applied static pressure"

first performed on the dam-foundation model without added mass (which represents the empty reservoir condition), and then a second dynamic analysis was performed on the model with added mass. The difference in the unbalanced nodal forces between these two analyses represented the hydrodynamic forces exerted on the nodes. From these nodal forces the pressure distribution was readily determined.

f. Comparison of hydrodynamic methods. Although Chopra's Simplified Procedure is only an approximate procedure based on the standard fundamental mode shape and simplified methods for determining the required periods of vibration, it is assumed that the procedure provides hydrodynamic loading that is at least within the general order of accuracy expected in dynamic analyses. On this basis, the equivalent mass system based on Westergaard's formula (Plot 2), underestimated the hydrodynamic loading on the typical dam section by about 40 percent. The equivalent mass system developed by the method described in Appendix D produced hydrodynamic loading (Plot 3) which correlated reasonably well with Chopra's Simplified Procedure. On this basis, the method described in Appendix D, which uses the standard pressure function curves, is recommended for developing the equivalent mass system.

g. Hydrodynamic contribution to response. For high pool conditions, a large portion of the dynamic response is attributable to the hydrodynamic effect. In the example that produced Plot 3 in Figure 7-3, 47 percent of the total equivalent mass system consisted of the added mass representing the hydrodynamic effects. Therefore, the equivalent mass system will significantly affect the response for pool depths greater than about half of the height of the dam.

7-6. Reservoir Bottom Absorption

a. Wave reflection coefficient. The nonrigid reservoir bottom partially absorbs incident hydrodynamic pressure waves. This moderates the increase in response of the dam due to the dam's interaction with the impounded water. This is readily apparent by comparing the standard hydrodynamic pressure function curves for two different reservoir bottom absorption conditions. Reservoir bottom absorption is expressed by a wave reflection coefficient which varies from zero for a fully absorptive condition to 1.0 for a fully reflective condition. Figure D-4 in Appendix D shows the pressure function curves for reservoir bottom conditions with wave reflection coefficients of 0.50 and 0.75. As apparent from these curves, the hydrodynamic pressure increases with an increase in the reflection coefficient.

b. Effects of R_w. When the fundamental vibration period of impounded water and the fundamental period of the dam are approximately equal, R_w approaches 1.0. This condition indicates the approach of a state of resonance, and the pressure function then becomes quite large for a nonabsorptive reservoir bottom. In contrast, the pressure function for an absorptive bottom is much less affected by the approach of resonance, because the effect of reservoir bottom absorption is to reduce the large resonant displacement peaks.

c. Estimating reservoir bottom absorption. Assuming a nonabsorptive reservoir bottom may lead to an overly conservative hydrodynamic response for dams when the earthquake load condition includes a high forebay pool. The degree of adsorptiveness characterized by the wave reflection coefficient is usually difficult to determine reliably. The value of the wave reflection coefficient will likely increase during the life of the dam as sediments are continuously deposited. Therefore, it is recommended that the effects of reservoir bottom absorption be included in the dynamic analysis by using a wave reflection coefficient based on the properties of the impounded water and the foundation rock, and neglect the additional adsorptiveness due to sediments that will eventually be deposited (Fenves and Chopra 1984). The wave reflection coefficient is determined by the following equation:

$$\alpha = \frac{1 - k}{1 + k}$$

where

α = wave reflection coefficient

$k = \rho C / \rho_r C_r$

ρ = mass density of water = 1.938 (lb-sec^2) /ft^4

C = velocity of pressure waves in water = 4,720 ft/sec

ρ_r = mass density of the foundation rock in (lb-sec^2) /ft^4

C_r = velocity of pressure waves in the foundation rock = $12\sqrt{E_f/\rho_r}$

E_f = deformation modulus of the foundation rock in lb/in.^{2}

7-7. Method of Combining Modes

a. Maximum modal responses. The maximum modal response in a response spectrum analysis is the maximum possible contribution that a particular mode can make to the dynamic response. However, all the modes do not arrive at their maximums at the same point of time during the period of ground motion. Thus, for a single ground motion record there is one point in time when the maximum dynamic response is reached, and this maximum response is made up of various fractional parts of the individual maximum modal responses. The "fractional parts" are unique for each ground motion record. If a response spectrum analysis is made for a single ground motion record, the maximum dynamic response can only be approximated because the exact makeup of the "fractional parts" of the maximum modal responses cannot be computed. A time-history analysis is required to determine the exact solution for a given ground motion record.

b. Statistical combination methods. A smooth design response spectrum may be considered as a convenient representation of many possible ground motion records that could make up the design earthquake. As discussed in paragraph 5-5*a*, design response spectra are often referred to as statistical representations of the ground motion records used in their development (such as mean, median, 84th percentile). On a similar basis, the maximum modal responses of a response spectrum analysis are combined by statistical methods to produce a reasonable dynamic response to the many possible ground motions that could make up the design earthquake.

c. Coupling coefficients. Tables 7-1 and 7-2 present four commonly used mode combination methods. The difference in the methods is in the calculation of the coupling coefficient between modes. The coupling coefficients may be simple discrete functions as is the case with the square root of the sum of the squares method (SRSS) which treats the modal responses as random variables. The functions may be more complex involving modal frequencies or both modal frequencies and damping factors as is the case with the complete quadratic combination method (CQC) and the double sum method (DSM). The more complex methods give additional accounting in the coefficient calculation when the frequencies of the two modes under consideration are close. Two closely spaced modes are coupled, and when one of the modes is excited, it tends to excite the other mode. However, the modal frequencies associated with gravity dams are normally fairly well separated.

d. Comparing methods. The base shear was the response parameter used for comparing the four combination methods. By using several load cases, foundation conditions, and damping ratios, eight sets of maximum modal base shear values were made available to test the combination methods. The more complex methods, CQC and DSM, increased the coupling coefficients for closely spaced mode which produced greater combined responses than the SRSS method. The spacing of the modal frequencies for the TPM was such that no two modes qualified for "additional accounting," so the combined response for the TPM is the same as SRSS. The two most often used methods are SRSS and CQC.

e. Conclusion. The mode combination method does not greatly affect the order of accuracy of the dynamic analysis. The factors discussed previously have far greater influence on the dynamic response. The preliminary design of new dams, and the final design of dams not considered to be under critical seismic conditions, may use either the SRSS or the CQC method. Final design of dams under critical seismic conditions and evaluation of existing dams shall use the more refined CQC method.

7-8. Vertical Component of Ground Motion

a. Factors that contribute to the response. It is very difficult to make a general assessment of the influence of the vertical component of ground motion on the total dynamic response because of the number of factors involved. The vertical component of ground motion can be significant under certain conditions. The most important factors that affect the contribution of the vertical component to the response are:

Table 7-1
Combining Modal Responses: Square Root of the Sum of the Squares Method (SRSS) and Ten Percent Method (TPM)

STATISTICAL METHODS consider the phasing of the modes by utilizing a "coupling coefficient" between the various modes as expressed by the basic equation:

$$R = \left[\sum_{i=1}^{N} \sum_{j=1}^{N} R_i \, P_{ij} \, R_j \right]^{1/2}$$

where: N = number of modes to be considered
R = total modal response
R_i = maximum modal response in the ith mode
R_j = maximum modal response in the jth mode
P_{ij} = coupling coefficient between modes i and j

There are several methods for determining the P_{ij} values. They are given below in the order of complexity:

Method 1: Square Root of the Sum of the Squares (SRSS)

$$P_{ij} = \begin{cases} 1.0 \ if \ i = j \\ 0.0 \ if \ i \neq j \end{cases}$$

The basic equation then reduces to

$$R = \sum_{i=1}^{N} \left[R_i^2 \right]^{1/2}$$

Method 2: Ten Percent Method (TPM)

$$P_{ij} = \begin{cases} 1.0 \ if \ \dfrac{\omega_j - \omega_i}{\omega_i} \leq 0.1 \\ 0.0 \ if \ \dfrac{\omega_j - \omega_i}{\omega_j} > 0.1 \end{cases}$$

where

ω_i = the natural frequency for the ith mode

ω_j = the natural frequency for the jth mode

This method gives additional accounting for modes with nearly the same frequency. If none exist, TPM reduces to SRSS.

Table 7-2
Combining Modal Responses: Complete Quadratic Combination Method (CQC) and Double Sum Method (DSM)

Method 3: Complete Quadratic Combination (CQC)

$$P_{ij} = \left[\frac{8\sqrt{\varepsilon_i \, \varepsilon_j} \; (\varepsilon_i + r\varepsilon_j) r^{3/2}}{(1 - r^2)^2 + 4\varepsilon_i \, \varepsilon_j \, r \, (1 + r^2) + 4 \left(\varepsilon_i^2 + \varepsilon_j^2\right) r^2} \right]$$

where

ε_i = modal damping ratio for the ith mode

ε_j = modal damping ratio for the jth mode

$$r = \frac{\omega_j}{\omega_i}$$

This method is based on both modal frequency and modal damping. However, for design of gravity dams, there is no procedure available to establish reasonable damping ratios for the higher modes. The effective viscous damping factor calculated according to the recommended procedure in this EP is used for all modes.

Method 4: Double Sum Method (DSM)

$$P_{ij} = \left[1 + \left\{ \frac{(\omega_i' - \omega_j')}{(\varepsilon_i' \, \omega_i + \varepsilon_j' \, \omega_j)} \right\}^2 \right]^{-1}$$

where

$$\omega_i' = \omega_i \, (1 - \varepsilon_i^2)^{1/2}$$
$$\omega_j' = \omega_j \, (1 - \varepsilon_j^2)^{1/2}$$
$$\varepsilon_i' = \varepsilon_i + \frac{2}{t_d \omega_i}$$
$$\varepsilon_j' = \varepsilon_j + \frac{2}{t_d \omega_j}$$
$$t_d = 10 \; seconds \; (earthquake \; duration)$$

This method is similar to CQC, but is slightly more conservative.

Note: Refer to Table 7-1 for the basic equation for obtaining the total modal response, and for definition of terms not provided on this table.

(1) The PGA associated with the vertical component. In some instances the vertical component PGA may be as great or greater than the horizontal component PGA. Refer to paragraph 5-6*a*.

(2) The shape of the vertical component design response spectrum. The frequency content of the vertical component of ground motion is usually higher than the frequency content of the horizontal component. This causes the vertical spectrum shape to be different than the horizontal spectrum shape. The vertical component will excite modes in the lower frequency range less than will the horizontal component.

(3) The depth of the reservoir. Vertical ground motion causes hydrodynamic pressure waves to be generated which exert a lateral load against the face of the dam (this hydrodynamic load is in addition to that discussed in paragraph 7-5). When considering stresses caused by the vertical component of ground motion, the stress induced by the hydrodynamic pressure waves can be larger than the stress caused by the inertia response associated with the mass of the dam. For a nonabsorptive reservoir bottom, the hydrodynamic load theoretically reaches infinity at the natural vibration frequencies of the reservoir. This is in contrast to stresses caused by the horizontal component of ground motion where the stress caused by the hydrodynamic load is small compared to the stress caused by the inertia response associated with the mass of the dam.

(4) Reservoir bottom absorption. Reservoir bottom absorption greatly reduces the added hydrodynamic load due to vertical ground motion and eliminates the unbounded peaks in the response, described above, at excitation frequencies equal to the natural vibration frequencies of the reservoir.

b. Method of analysis. Except for the hydrodynamic load contribution which is discussed later, determining the response due to the vertical component of ground motion follows the same general procedures and recommendations that apply in determining the horizontal component response. The vertical component design response spectrum, and the PGA associated with vertical excitation are used to define the design earthquake. It should be noted that for vertical direction excitation, the fundamental mode and some or all of the significant higher modes are often different than for horizontal excitation. The participation factor and the mode coefficient for a particular mode and direction of excitation may be used to judge the order of importance of the modes, and which modes will make a significant contribution to the dynamic response.

c. Equivalent added mass system. The added mass associated with the equivalent mass system discussed in paragraph 7-5*c* should be active in the horizontal direction, and inactive in the vertical direction. Added mass representing backfill or silt deposits against vertical or near vertical surfaces of the dam should also be active horizontally and inactive vertically. If the backfill is placed on the sloping face of the dam, the magnitude of the added mass acting vertically should be determined as described in paragraph 6-3*b*.

d. Hydrodynamic loading. The vertical component of ground motion causes hydrodynamic pressure waves to be generated from the reservoir bottom into the impounded water above. These pressure waves act horizontally against the vertical or near vertical face of the dam. In the composite finite element method, the equivalent mass system discussed in paragraph 7-5 accounts for the hydrodynamic reservoir effects caused by the horizontal component of ground motion, but it does not account for the effect of the hydrodynamic pressure waves generated by the vertical component of ground motion. To account for the effect of the pressure waves, a finite element-substructure model configuration is required as discussed in Chapter 8.

e. Combining component responses. The individual vertical and horizontal component dynamic responses are not in phase. They are independent maximum component responses that do not occur at the same point in time during the period of ground motion activity. Each pair of horizontal and vertical ground motion records representing a single earthquake event would have a unique phase relationship. Since the response spectrum method encompasses many possible ground motion events which make up the design earthquake, the maximum vertical and horizontal component responses are combined by a statistical method to produce a total dynamic response with reasonable probability of occurrence. It is recommended that the phasing of the two maximum component responses be treated as two unrelated random occurrences, and they be combined by the square root of the sum of the squares method (SRSS).

f. Conclusions. Under certain critical seismic conditions, the response to the vertical component of ground motion may be significant when compared to the response to the horizontal component; however the phase relationship will greatly moderate the vertical component contribution to the total response. On this basis, the vertical component of ground motion may be ignored in the preliminary design of new dams not subject to critical seismic conditions. The vertical component of ground motion shall be included for preliminary designs subject to critical seismic conditions, all final designs, and evaluation of existing dams.

Chapter 8
Dynamic Analysis Methods and Procedures

8-1. Attributes of Dynamic Analysis Methods

A dynamic analysis method is identified by four attributes: (1) material behavior, (2) design earthquake definition, (3) dimensional representation of project conditions, and (4) model configuration. The first two attributes have been discussed in preceding chapters. They are briefly summarized below, followed by a more detailed discussion of the latter two attributes.

a. Material behavior. This attribute defines material behavior as either (1) linear-elastic or (2) nonlinear. Associated with each of these two types of material behavior is a unique criterion for establishing acceptable response. Refer to paragraphs 2-2*d*, 2-2*e*, and 3-10.

b. Design earthquake definition. This attribute establishes which of two options will be used to specify the free field ground motion for the design earthquakes. The options are (1) design response spectra and (2) ground motion time-history records. Refer to Chapter 5 for details.

c. Dimensional representation of project conditions. This attribute defines whether project conditions will be represented in (1) two dimensions or (2) three dimensions. Project conditions refer to the geometry of the dam, the foundation, and the reservoir that have an affect on the seismic response. Examples of features governing which of these two options is appropriate include such things as layout of the dam axis, shape of the dam monoliths, foundation conditions, and orientation of potential fault slips if applicable.

(1) Two-dimensional (2-D) analysis. In the analysis of most gravity dams, it is assumed that the dam is composed of individual transverse vertical elements or cantilevers each of which carry loads to the foundation without transfer of load between adjacent elements. This assumption also applies to most RCC dams including dams with transverse joints that separate the dam into several monoliths, and dams with monolithic construction that contain no transverse joints. This assumption is usually valid, and stress analyses including the dynamic stress analysis phase can be based on 2-D representation of the dam cross-section. The design example provided in Appendix D presents a typical 2-D analysis. It demonstrates the most common procedure where a 2-D cross section of the structure is analyzed. However, most principles and procedures applying to the 2-D analysis also apply, or may be adapted to a 3-D analysis discussed below.

(2) Three-dimensional (3-D) analysis. Occasionally there are exceptions to the assumption justifying 2-D analysis. Dams in narrow canyons with a large enough ratio of height of the dam to distance between abutments may cause significant two-way distribution of stresses. Dams which are aligned on a curved axis may also allow significant transfer of stress into the abutments by arch action. Unusual shaped monoliths where there is substantial variation in the transverse cross section across the width of the monolith also may not be analyzed satisfactorily by 2-D methods. Another exception occurs when the trace of a potential fault slip is not parallel or nearly parallel to the dam axis. In this situation, a 2-D foundation fault displacement analysis will not adequately represent project conditions. All of these situations indicate the need for 3-D analysis if the response is to be determined to a reasonable degree of accuracy.

(a) Ground motion direction. The 3-D analysis introduces additional variables into the dynamic analysis. One important variable is determining the critical direction of the horizontal ground motion. This introduces a second horizontal component of ground motion into the dynamic analysis. The critical direction is defined by transforming the design earthquake ground motion into a pair of orthogonal components. Since no method exists to determine the critical direction directly, it usually becomes necessary to make some rough approximations.

(b) Simplified approach. This approach to determining the critical horizontal direction of ground motion is to select two orthogonal direction vectors (in the horizontal plane), and assume that the critical tensile stress at various locations on the dam will occur when the direction of ground motion is near one or the other vector. Since the accompanying orthogonal ground motion component is small, the stresses are assumed negligible and are neglected. Often the direction vectors are assumed to be the upstream-downstream direction, and the cross-stream

direction. This approach requires performing separate, independent dynamic analyses for the two orthogonal ground motion directions.

(c) Conservative approach. Another more conservative approach accounts for both orthogonal components of ground motion. It is necessary to perform the two dynamic analyses described above, but the first analysis includes the full magnitude design earthquake ground motion component acting in an assumed direction with a fraction of the design earthquake ground motion acting orthogonally. The second analysis includes the fractional part of the ground motion acting in the assumed direction and the full magnitude ground motion acting orthogonally. The fractional part of the design earthquake ground motion is usually assumed to be 30 percent of the design earthquake ground motion. In a response spectrum analysis, stresses produced by the two horizontal components of ground motion are added directly to produce the resultant stress component for horizontal ground motion. This resultant stress component is then combined with the stress component produced by the vertical component of ground motion using SRSS.

(d) Complexity of analysis. A 3-D analysis requires considerably greater effort to create the 3-D model as compared to a 2-D model, and may require a main frame computer and a substantial amount of computer time to perform the analysis. It also produces a large amount of output to evaluate and interpret. However, the general purpose structural finite element programs are continuously being improved and are much more user oriented than they were in the past. They have refined graphics capabilities which help greatly in checking for errors in the computer model input, and in displaying the stress output. Also, specialized post-processors are being developed so that results can be evaluated much more efficiently. These advances greatly enhance the practicality of the 3-D analysis.

d. Model configuration. This attribute of the dynamic analysis method is dependent on the type of model used to represent the dam-foundation-reservoir system. The three types of models used for dynamic analysis of gravity dams are (1) the “standardized” model developed by Chopra and used in his Simplified Method of Analysis, (2) the finite element-substructure model, and (3) the composite finite element-equivalent mass system model.

(1) Standardized model. This type of model is used in Chopra’s Simplified Method. It is based on standardizing certain parameters that define the dam-foundation-reservoir system. It recognizes the fact that these parameters have little variation within the range of geometry common to gravity dams. For example, the normalized fundamental mode shapes for six sample dam cross sections were studied and found to be almost identical. A standardized mode shape was then developed for use in the calculation procedure.

(a) Factors considered. In the latest version, the standardized model considers dam-foundation rock interaction, dam-reservoir effects, and reservoir bottom absorption. All of these factors are based on standard curves and formulae.

(b) Model limitations. The standardized model is the simplest of the three types of models. A computer is not required to formulate the model or even to perform the dynamic analysis. However, standardizing the mode shape, frequency, and other parameters makes this an approximate method limited strictly to the typical nonoverflow monolith shape.

(2) Finite element-substructure model. In this type of model, different techniques are used to represent the dam, foundation, and reservoir; however, by using common node points at the interfaces, a computer model is formulated that can be analyzed by conventional matrix methods.

(a) Dam. The dam is modeled as an assembly of discrete finite elements. Either solid quadrilateral plane stress or plane strain elements are used for a 2-D model.

(b) Foundation. The foundation is idealized as a viscoelastic half-plane. The elastic properties of the foundation are formulated into a substructure matrix using the theory of elasticity. This matrix is combined with the structural stiffness matrix developed from the finite element representation of the dam. The substructure matrix introduces the foundation stiffness to the equations associated with the degrees-of-freedom of the node points at the dam-foundation interface. There is no finite element model of the foundation. The dimensions of the structural stiffness matrix are set by the finite element model of the dam.

(c) Reservoir. The impounded water of the reservoir is idealized as a fluid domain of constant depth and infinite length. This can be interpreted as a series of subchannels of infinite length discretized to match the common upstream nodal points of the dam. The reservoir bottom absorption is modeled by adjusting the boundary condition at the reservoir bottom. This substructure representation of the reservoir produces more accurate hydrodynamic response to horizontal and vertical ground motion than does an equivalent mass system representation as described in paragraph 8-1*d*(3)(a).

(d) Specialized computer program. This type of model requires a specialized computer program to allow the foundation and the reservoir effects to be formulated in the manner described above. Also, the substructure method requires the foundation to be modeled as a uniform homogeneous material. Presently, a computer program is available which develops a 2-D finite element-substructure model for gravity dams. Refer to paragraph 8-2*b*.

(3) Composite finite element-equivalent mass system model. This method models both the dam and the foundation as an assembly of discrete finite elements. Either solid quadrilateral plane stress or plane strain elements are used for 2-D models or 3-D isoparametric solid elements are used for 3-D models. The foundation consists of a rectangular block with a width in the upstream-downstream direction about 3 times the base width of the dam at the foundation plane, and with a height about 1.5 times the height of the dam.

(a) Reservoir effects. The reservoir effects are modeled by developing an equivalent mass system which consists of adding mass to the finite element model to correctly alter the dynamic properties. The added mass is active in the direction normal to the vertical upstream face of the dam. This method also allows the reservoir bottom absorption characteristics to be incorporated into the analysis by using Chopra's standard hydrodynamic pressure function curves to determine the added mass. Although use of these curves in developing the equivalent mass system is only approximate, it has been shown to be reasonably accurate. Refer to paragraphs 7-5*c* and 7-5*d* and Appendix D for details.

(b) Boundary conditions. With this type of model, the earthquake ground motion is introduced at the rigid boundary. This boundary is along the sides and bottom of the rectangular foundation block rather than at the ground surface (dam-foundation interface) where the design earthquake ground motion is specified. To account for this, the foundation is assumed massless. Therefore, no wave propagation takes place in the massless foundation so the ground motion is transmitted to the dam-foundation interface without modification.

(c) Flexibility in modeling. The composite finite element model may be formulated to represent a variety of design conditions for both 2-D and 3-D models. For example, most any geometric shape may be accommodated, various zones of superior RCC mix may be incorporated in the dam model, and discontinuities such as fault zones or changes of deformation modulus in the foundation may also be included.

8-2. Comparison of Dynamic Analysis Methods

This section will describe the attributes associated with the most commonly used dynamic analysis methods, and the methods will be evaluated and compared.

a. Chopra's simplified method. This method uses the standardized model described in paragraph 8-1*d*(1). Other attributes include 2-D representation, linear-elastic material behavior, and response spectrum definition of the design earthquake. This method is not flexible because all of these attributes are fixed.

(1) Equivalent lateral force. The simplified method develops the maximum response to the first mode as a set of equivalent lateral forces. It also approximates the equivalent lateral forces associated with the higher vibration modes using a "static correction" method. The two sets of equivalent lateral forces are treated as statically applied distributed lateral loads. At present, response to a vertical component of ground motion is not possible with this type of model. Stresses may be hand calculated by beam theory treating the dam as a simple cantilever beam, or the static load may be applied to a finite element model of the dam to gain a more realistic stress distribution pattern.

(2) Advantages and limitations. The simplified method is easy to use and can be done without a

computer. However, it takes less time and effort to perform a simple 2-D analysis using a general purpose finite element program on a personal computer (PC) and the results of the finite element analysis will be more accurate. Also, comparative studies have indicated that as the flexibility of the foundation increases, the response calculated by the simplified method tends to diverge from the response determined by more refined methods, and the simplified method is not always conservative.

(3) Recommended use. Because of the limitations of the simplified method, it should be used only for preliminary design work as described in paragraph 8-4*a*. However, appropriate equations and design figures used in this method are helpful in checking the results from other more refined analyses and to prepare the computer input for these methods.

b. EAGD-84 Analysis Method. EAGD-84, A Computer Program for Earthquake Analysis of Concrete Gravity Dams (Fenves and Chopra 1984), is a specialized computer program that allows the foundation and the reservoir effects to be characterized by the substructure model described in paragraph 8-1*d*(2).

(1) Other attributes. Other attributes that define the EAGD-84 analysis method include 2-D representation, linear-elastic material behavior, and time-history ground motion definition of the design earthquake. All attributes of EAGD-84 are fixed and cannot be changed.

(2) Advantages and limitations. When compared to either a standardized model or a finite element-equivalent mass system model, the EAGD-84 substructure model is a better representation of the foundation and reservoir, as long as the project conditions properly fit the program requirements. Also, the time-history definition of ground motion is a level of refinement beyond response spectrum definition. Therefore, the EAGD-84 method is capable of producing the most accurate response, and the time-history response output provides additional information often needed to evaluate acceptable performance. The biggest disadvantage of EAGD-84 is the lack of attribute flexibility.

c. General purpose finite element program analysis methods. This comprises a number of methods each with a different combination of attributes, but all having the composite finite element-equivalent mass system model as a common attribute. These methods use any one of several proven general purpose finite element computer programs to perform the dynamic analysis. Examples are ANSYS, SAP6, GT-STRUDL, and STAAD III. The material behavior attribute for most of the general purpose programs is linear-elastic; however, some programs such as ANSYS and ADINA have nonlinear capability.

(1) Primary advantage. Attribute flexibility is the primary advantage of the general purpose finite element methods. Except for the common attribute mentioned above, design methods are possible which feature most of the other possible combinations of the remaining attributes. This allows the dynamic analysis phase to start with a simple method such as the 2-D, linear-elastic, response spectrum method. If the results of the simple analysis or the project conditions indicate the need of a more refined analysis, the procedure may transition conveniently into a more refined analysis by modifying or adding to the input to the same general purpose program.

(2) Other advantages. The general purpose finite element programs discussed above are large, comprehensive programs developed for main frame computers. In addition to these programs are several smaller general purpose finite element programs specifically developed for PC's. Since these desk-top PC's are now a standard item in most design offices, a considerable amount of the dynamic analysis phase may be completed without the need or expense of a large main frame computer.

8-3. Dynamic Analysis Procedure

The dynamic analysis procedure described hereafter is derived with the objective of arriving at a reasonable and economic design of a new dam, and evaluating the seismic resistance of existing dams using an analysis method with the simplest attributes possible. In general the procedure is to perform a dynamic stress analysis and evaluate the results to determine if the RCC dam response to the design earthquakes is acceptable. If not acceptable, the design of a new dam may be modified and reanalyzed, or a more refined analysis method may be employed when analyzing either new dams or existing dams.

a. Evaluating acceptable response. The response is judged acceptable for a linear-elastic analysis when the tensile stresses are within the

established allowables and the analysis method provides a reasonably accurate or conservative representation of project conditions. Should the analysis method utilize an extremely simplified representation of project conditions, the response may not necessarily be conservative and will likely be of relatively low order of accuracy. However, the response may still be judged acceptable without pursuing more refined analyses on the basis that the tensile stresses are far enough below the established allowables to clearly infer that the response satisfies the requirements and criteria described above. Refer to paragraphs 2-2*e*, 2-2*f*, and 2-2*g* for information on allowable tensile stress criteria for various methods of analysis.

b. Modifying the design of a new dam. When the response from a dynamic stress analysis for a new dam is judged not acceptable, consideration shall be given to modifying the design, adjusting the computer model to reflect the modifications, and reanalyzing. Modifications include:

(1) Modify geometric configuration.

(2) Superior mixes. Use richer, higher strength superior RCC mixes in overstressed areas.

(3) Reducing aggregate size. Increase tensile strength by reducing the maximum size aggregate.

(4) Mortar bedding. Provide mortar bedding to increase tensile strength at lift joints.

(5) Zone boundaries. Adjust the zone boundaries of the superior RCC mixes to better fit the tensile stress pattern.

c. Refining the dynamic analysis methods. When the response from a dynamic stress analysis of an existing dam is judged not acceptable, the next step in the procedure shall be to reanalyze using an analysis method with more refined attributes. In contrast to this, there is no clearly defined point in the design procedure for new dams that indicates when the analysis method should be refined. The design conditions and results of the design procedure already completed must be evaluated to determine when it is appropriate to suspend the design modification process, and pursue a more refined analysis of the latest modified design. When the attributes of the dynamic analysis method are to be refined, it is recommended that the refinements be considered in the following order:

(1) 3-D representation. Consider refining the analysis from two to three dimensions when the accuracy of the response from a 2-D analysis cannot lead to a confident judgment that the response is acceptable.

(2) Time-history analysis. Consider defining the design earthquakes with appropriate ground motion time-history records, and performing a time-history analysis when additional insight into the structural behavior beyond that provided by the response spectrum analysis is needed. A time-history analysis yields additional information regarding the excursions of tensile stress cycles beyond the allowables and provides a better understanding of the response. This applies both to existing dams or to the design of a new dam when all practical and economical modifications to the design of a new dam have been exhausted.

(3) Nonlinear analysis. The analysis based on nonlinear material behavior represents the greatest possible refinement and it produces the most accurate results. However, it is also the most complex and the most costly. It requires time-history ground motion input, direct integration solution, a large main frame computer, specialized computer programs, and a considerable amount of computer time. As such, it is the last recourse in the attribute refining process. The nonlinear analysis should only be undertaken under the guidance of an expert in the field of fracture mechanics and finite element methods.

8-4. Preliminary Design of New Dams

Preliminary design includes engineering and design through the Feasibility Phase, or through the General Design Memorandum (GDM) phase if a GDM is prepared for the project.

a. Initial dynamic analysis. The initial dynamic stress analysis shall use the simplest analysis method which is identified by the following attributes: (1) linear-elastic material behavior, (2) 2-D representation, and (3) design response spectrum definition of the design earthquake. The analysis shall be performed using the cross-section of the critical transverse element of the dam which usually consists of a

section of the nonoverflow monolith with the greatest height. The dam-foundation-reservoir system shall be represented by a composite finite element-equivalent mass system model for RCC dams subject to critical seismic design conditions. For other conditions, the dam-foundation-reservoir system may be characterized by either the standardized model using Chopra's simplified method or the composite finite element model described above.

b. Seismic and foundation investigations. Appropriate investigations of the regional tectonics and site seismicity shall be conducted at the preliminary design stage. When required, the site-specific design response spectra shall be developed in accordance with paragraph 5-5*c*. Preliminary dam site and reservoir geology investigations shall be conducted including exploratory corings and load testing to determine foundation conditions and deformation modulii.

c. Tensile strength. For preliminary design, the tensile strength may be taken from Figures 3-1 through 3-6 for the proposed basic RCC mix and for superior RCC mixes in the critical zones.

d. Satisfying criteria. The preliminary design procedure shall progress to the point where it becomes evident that the preliminary design will lead to a final design that fully satisfies established performance requirements and criteria.

8-5. Final Design of New Dams

The final design of an RCC dam shall result in a design that satisfies the provisions of this EP. The dynamic analysis phase for RCC dams under critical seismic design conditions shall be presented in an appropriate feature design memorandum.

a. Final design analysis method. The dynamic analysis method for the final design shall evolve from the simple initial method described in paragraph 8-4*a* to more refined methods of design conditions as warranted. RCC dams analyzed by Chopra's simplified method during the preliminary design phase shall be reanalyzed using a composite finite element-equivalent mass system model and general purpose finite element program in the final design.

b. Foundation and material investigations. The foundation conditions for the final design shall reflect the latest exploratory coring and other foundation and geology investigations. The final design shall be based on the RCC material properties obtained from tests on core samples taken from test fill placements made with the proposed design mixes.

8-6. Evaluating Existing Dams

The dynamic analysis procedure for evaluating existing dams is essentially the same as the combined preliminary design and final design procedures for a new dam, except modification of the design discussed in paragraph 8-3*b* does not apply to existing dams. As with the design of new dams, the dynamic analysis procedure shall utilize an analysis method with the simplest attributes possible to determine if the existing dam is capable of responding to the design earthquakes in an acceptable manner.

a. Material properties. Material properties of the RCC for an existing dam, including tensile strength, shall be obtained from tests on core samples taken directly from the dam.

b. Using available records. Exploratory coring logs, laboratory test data, and field geologic test results conducted during design and construction should be used for an existing dam and to provide information needed to model the foundation. Reservoir data should be used to determine the reservoir and tailwater elevations for earthquake load cases.

c. Special requirements and analysis methods. The regional tectonics and site geology and seismicity shall be investigated as required to develop a site-specific design response spectra in accordance with paragraph 5-5*c*. The initial analysis of an existing dam shall utilize a composite finite element-equivalent mass system model. Existing dams shall not be analyzed by Chopra's simplified method.

Appendix A
References

A-1. Required Publications

ER 1110-2-1806
Earthquake Design and Analysis for Corps of Engineers Projects

EM 1110-2-2006
Roller Compacted Concrete

EM 1110-2-2200
Gravity Dam Design

EM 1110-2-2502
Retaining and Flood Walls

ETL 1110-2-256
Sliding Stability for Concrete Structures

ETL 1110-2-301
Interim Procedure for Specifying Earthquake Motions

ETL 1110-2-303
Earthquake Analysis and Design of Concrete Gravity Dams

ETL 1110-2-343
Structural Design using the RCC Construction Process

A-2. Related Publications

ACI Committee 207 1973
ACI Committee 207. 1973. "Effect of restraint, volume change, and reinforcement on cracking of massive concrete," ACI Journal.

ACI Committee 439 1969
ACI Committee 439. 1969. "Effect of steel strength and of reinforcement ratio on the mode of failure and strain energy capacity of reinforced concrete beams," ACI Journal.

Applied Technology Council 1984
Applied Technology Council. 1984. *Tentative provisions for the development of seismic regulations for buildings*, second printing, 2471 E. Bayshore Road, Suite 512, Palo Alto, CA. 94303.

Bruhwieler 1990
Bruhwieler, E. 1990. "Fracture of mass concrete under simulated seismic action," *Dam Engineering*, I(3).

Cannon 1991
Cannon, R. W. 1991. "Tensile strength of roller compacted concrete," a preliminary submittal to U.S. Army Corps of Engineers, North Pacific Division.

Chopra 1978
Chopra, A. K. 1978. "Earthquake resistant design of concrete gravity dams," *Journal of the Structural Division, ASCE*, 104(ST6).

Chopra and Chakrabarti 1973
Chopra, A. K., and Chakrabarti, P. 1973. "The Koyna earthquake and the damage to Koyna Dam," *Bulletin of the Seismological Society of America*, 63(2), 381-97.

Dunstan 1978
Dunstan, M.R.H. 1978. *Rolled concrete*.

Fenves and Chopra 1984
Fenves, G., and Chopra, A. K. 1984. "EAGD-84: A computer program for earthquake analysis of concrete gravity dams," Report No. UCB/EERC-84/11, Earthquake Engineering Research Center, University of California, Berkeley.

Fenves and Chopra 1984
Fenves, G., and Chopra, A. K. 1984. "Earthquake analysis of concrete gravity dams including reservoir bottom absorption and dam-water-foundation rock interaction," *Earthquake Engineering and Structural Dynamics* 12(5), 663-80.

Fenves and Chopra 1986
Fenves, G., and Chopra, A. K. 1986. "Simplified analysis for earthquake resistant design of concrete gravity dams," Report No. UCB/EERC-85/10, Earthquake Engineering Research Center, University of California, Berkeley.

James, Jansen, Kiersch, and Leps 1988
James, L. B., Jansen, R. B., Kiersch, G. A., and Leps, T. M. 1988. "Lessons from notable events." *Advanced Dam Engineering for Design Construction and Rehabilitation*, Robert B. Jansen, ed., Van Nostrand Reinhold Publishers, New York.

Newmark and Hall 1969
Newmark, N. M., and Hall, W. J. 1969. "Seismic design criteria for nuclear reactor facilities," *Proceedings, 4th World Conference on Earthquake Engineering*, Santiago, Chile, B5-1 to B5-12.

Newmark and Hall 1987
Newmark, N. M., and Hall, W. J. 1987. "Earthquake spectra and design." *Engineering Monograph on Earthquake Criteria, Structural Design, and Strong Motion Records*, Earthquake Engineering Research Center.

Raphael 1984
Raphael, Jerome M. 1984. "Tensile strength of concrete," *ACI Journal*.

Seed 1974
Seed, H. B. 1974. "Site-dependent spectra for earthquake resistant design," Report No. EERC 74-12, Earthquake Engineering Research Center, University of California, Berkeley.

U.S. Department of the Interior, Bureau of Reclamation 1980
U.S. Department of the Interior, Bureau of Reclamation. 1980. "Feasibility design summary, Auburn Dam, concrete curved - gravity dam alternative (CG-3), Central Valley Project, California," Water and Power Resources Service, Denver, CO.

Westergaard 1933
Westergaard, H. M. 1933. "Water pressure on dams during earthquakes." *Transactions, ASCE*, 98.

Appendix B
Design Example Problem

B-1. General Layout of Dam

a. This design example is for a new RCC dam with a straight axis located in a relatively wide canyon site. The highest nonoverflow section of the dam has a cross section which is constant over a considerable length of the dam and is considered critical for design. The dam is to be constructed with no vertical monolith joints.

b. Because of the wide canyon and straight axis, the dam can be adequately represented two-dimensionally. A transverse cross-sectional element will be used to model the dam.

B-2. Site Location

a. The dam is located in northern California, in seismic Zone 3. The proposed dam will be well over 100 ft in height; therefore, the design earthquakes must be described by site-specific design response spectra.

b. The nearest potential seismic source is a fault located approximately 35 km from the site. Fault displacement in the proposed dam foundation is not considered a reasonable possibility for this site.

B-3. Design Work Completed

For this example the design procedure will be assumed to have progressed as follows:

a. The stability analysis and stress analysis phase of design is complete for the non-earthquake load conditions and a proposed dam cross section has been developed which satisfies the overturning, sliding, and stress criteria in accordance with EM 1110-2-2200.

b. The proposed dam cross section for the critical monoliths is as shown in Figure B-1. H_s = 600 ft, and other key dimensions are shown in the figure.

c. A stability analysis was conducted using the seismic coefficients and the seismic zone maps provided in ER 1110-2-1806. The proposed dam cross section satisfies the stability requirements of EM 1110-2-2200 for these load conditions.

B-4. Factors Influencing Seismic Design

Due to the seismic zone and height of the dam, a dynamic stress analysis is required. Factors that influence the design are:

a. The low pool and normal pool elevations (el) used for the OBE and MCE design load conditions have been selected as follows:

Low pool (conservation pool el)
= el 2220.0 H=270 ft

Normal pool
= el 2445.0 H=495 ft

b. Tailwater, siltation, or static earth (backfill against the dam face) are not applicable to the OBE or MCE design load condition for this section of the dam.

c. The deformation modulus of the foundation rock expressed as Young's modulus of elasticity is

E_f = 3,500,000 psi = 504,000 ksf

d. The density of the foundation rock is 160 lb/ft^3.

e. Poisson's ratio u = 0.20 is assumed for the rock foundation.

f. The material characteristics and layering distribution of the reservoir bottom sediment deposits have not been estimated. Therefore, the wave reflection coefficient for the reservoir bottom will be based only on the water and the foundation rock. The wave reflection coefficient is calculated as follows:

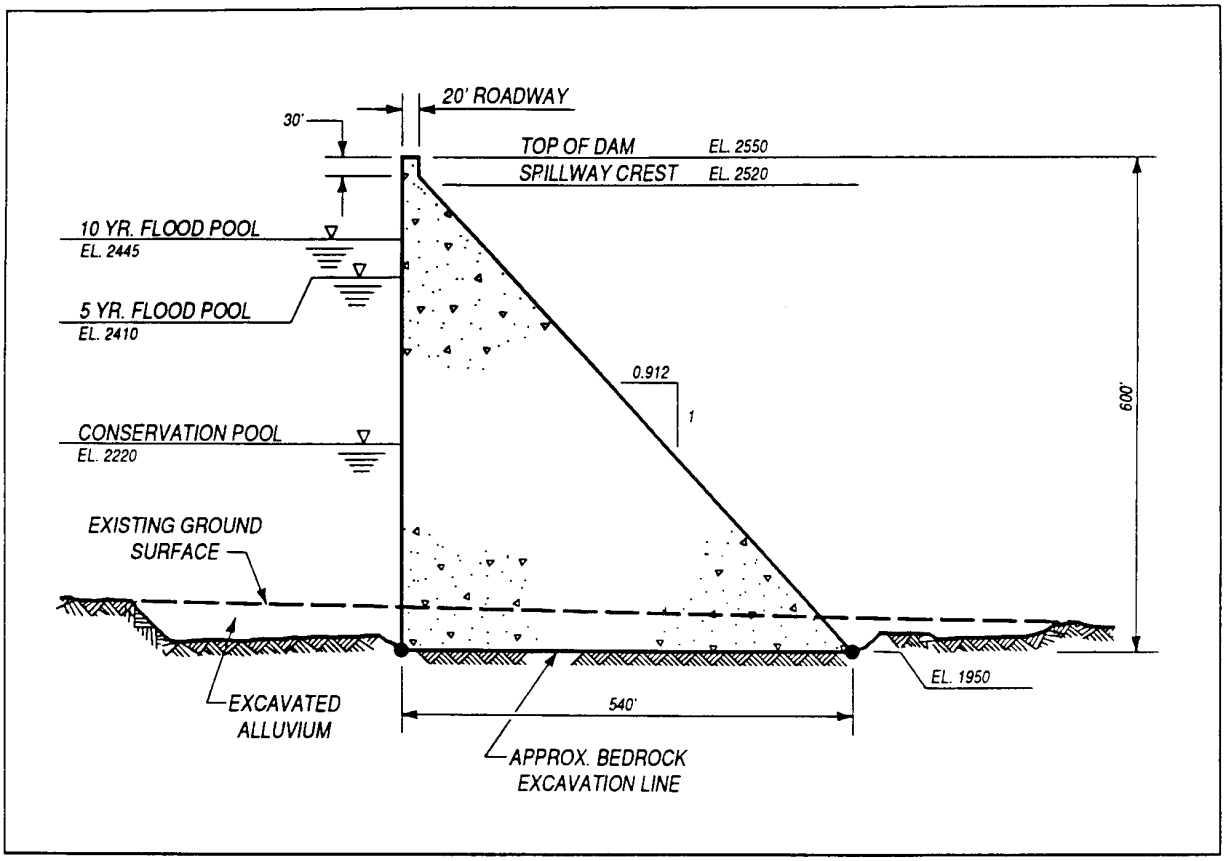

Figure B-1. Design example problem: Proposed dam cross section for the critical non-overflow monolith

$$\alpha = \frac{1 - k}{1 + k}$$

where $k = \rho C/\rho_r C_r$

$$\rho_r = \frac{160}{32.174} = 4.973 \ (lb\text{-sec}^2)/ft^4$$

$$C_r = 12 \times \sqrt{\frac{3{,}500{,}000}{4.973}} = 10{,}067 \ ft/\text{sec}$$

thus $k = \frac{1.938(4{,}720)}{4.973(10{,}067)} = 0.1827$

$$\alpha = \frac{1 - 0.1827}{1 + 0.1827} = 0.69$$

B-5. Basic RCC Mix Design

A typical basic RCC mix design will be used for the example problem. Characteristics of the basic RCC mix are as follows:

a. MSA > 1.5 in.

b. Consistency < 30 sec vibration.

c. Lift joints will have mortar bedding.

d. f'_c = 3,000 psi.

e. Unit weight = 155 pcf.

f. The seismic modulus of elasticity of the RCC is calculated as follows:

E = static modulus = $57{,}000 \sqrt{3{,}000}$
= 3,122 ksi

E_r = ratio of seismic strain rate to quasi-static rate is assumed to be 1,000

E_s = seismic modulus = E' = $E(E_r)^{0.020}$
= $3{,}122(1{,}000)^{0.020}$

E_s = 3,590 ksi = 517,000 ksf

g. Poisson's ratio for high seismic strain rate is calculated as follows:

$u' = 0.7u = 0.7 \times 0.20 = 0.14$

h. Direct tensile strength has been determined from cores taken from test-fill placements and is

f'_t = 290 psi (for the parent concrete)

f'_t = 205 psi (for the lift joints)

B-6. Superior RCC Mixes

The design for this example problem will not be considered to have progressed to the stage where zones of superior RCC concrete will be included in the computer models for analyses. However, the analyses will indicate if superior zones are needed, and, if so, where the zone boundaries might be located.

B-7. Horizontal Design Response Spectra

Since the site is in Seismic Zone 3, site dependent design response spectra are required to establish the design earthquakes. The standard design response spectrum for the horizontal component of ground motion shown in Figure 5-1 and Table 5-1 will be considered to be the site dependent design response spectrum. The design response spectrum will be anchored using the peak ground accelerations (PGA's) provided in Table 5-2, which for seismic Zone 3 are:

OBE: 0.210 g

MCE: 0.550 g

B-8. Vertical Design Response Spectra

For this example, the vertical design response spectrum will be considered equal to the horizontal design response spectrum described above; however, it will be anchored on the basis of the ratio of the vertical component PGA to the horizontal component PGA as shown in Figure 5-3.

B-9. Dynamic Analysis Procedure

a. This example problem represents an RCC dam subject to critical seismic design conditions as defined in Chapter 8. Under these critical seismic conditions, the simplest method of dynamic analysis to utilize a dam-foundation-reservoir model composed of a composite finite element-equivalent mass system shall be used for either preliminary or final design. Appendix D will show the analysis of the example problem by this method. To reduce the amount of data and to make the procedure easier to follow, only the MCE load cases will be analyzed. Analysis for the OBE load cases would follow the identical procedure.

b. Although an RCC dam subject to critical seismic conditions would not normally be analyzed by Chopra's simplified method, Appendix C shows an analysis of the example problem by this method for demonstration purposes and to allow a comparison of the results by the two different methods.

Appendix C
Design Example-Chopra's Simplified Method

C-1. General

a. The design example problem described in Appendix B will be analyzed using Chopra's simplified design response spectrum method. All hand calculations are included.

b. Definitions of symbols and notations used in this appendix can be found in the Glossary. Refer to Appendix B where the values of several parameters required for the analysis were derived.

C-2. Fundamental Natural Period (Empty Reservoir/Rigid Foundation)

$T_1 = 1.4\ H_s/\sqrt{E_s} = 1.4\ (600)/\sqrt{3.59\times10^6}$

$T_1 = 0.443$ sec

C-3. Reservoir Effect on Natural Period

$\tilde{T}_r = R_r T_1$

$H_s = 600$ ft $\qquad R_r$ from Figure C-1

	POOL ELEVATION	
	NORMAL	LOW
H	495 ft	270 ft
H/H_s	0.825	0.450
R_r	1.110	1.000
$\tilde{T}_r$	0.492 sec	0.443 sec

C-4. Ratio of Resonant Period of Dam To Fundamental Period of the Reservoir

$R_w = T_1^r/\tilde{T}_r$

$T_1^r = 4H/C$

$C = 4720$ ft/sec

	POOL ELEVATION	
	NORMAL	LOW
H	495 ft	270 ft
T_1^r	0.420 sec	0.229 sec
R_w	0.85	0.52

C-5. Foundation Effect On Natural Period

$E_s/E_f = 3.59 \times 10^6/3.50 \times 10^6 = 1.025$

$R_f = 1.190$ from Figure C-2

$\tilde{T}_1 = R_r R_f T_1$

	POOL ELEVATION	
	NORMAL	LOW
R_r	1.110	1.000
R_f	1.190	1.190
T_1	0.443 sec	0.443 sec
$\tilde{T}_1$	0.585 sec	0.527 sec

C-6. Effective Damping Factor

$\tilde{\varepsilon}_1 = \frac{1}{R_r}\ \frac{1}{(R_f)^3}\ \varepsilon_1 + \varepsilon_r + \varepsilon_f$

$\varepsilon_f = 0.0701$ from Figure C-3

$\varepsilon_r =$ values from Figure C-4

	POOL ELEVATION	
	NORMAL	LOW
R_r	1.110	1.000
R_f	1.190	1.190
ε_1	7.00 %	7.00 %
H/H_s	0.825	0.450
ε_r	0.0158	0
$\tilde{\varepsilon}_1$	12.33 %	11.16 %

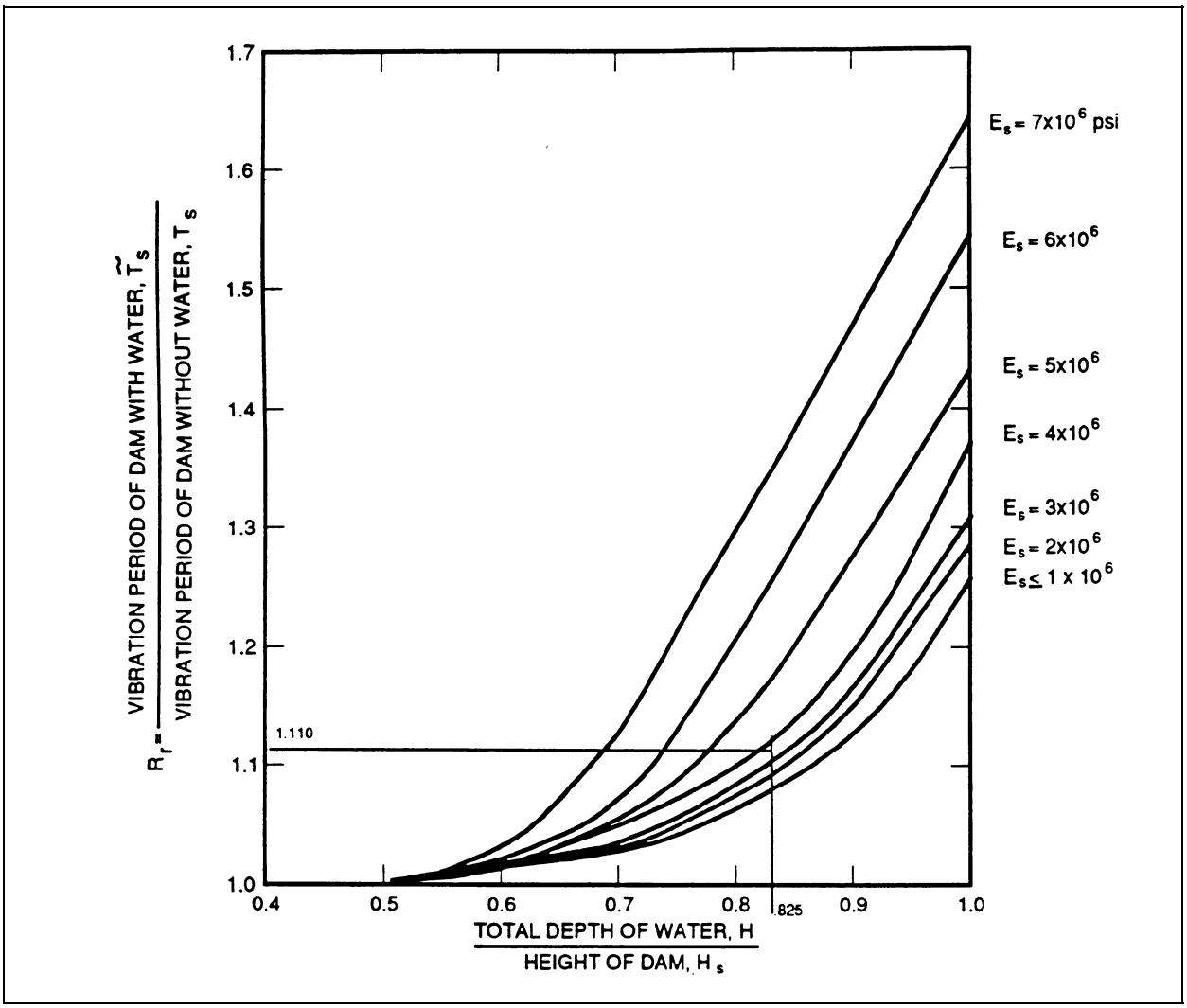

Figure C-1. Standard values for R_f, the ratio of fundamental vibration periods of the dam with and without water. Chopra (1978)

7. Key Dimensions

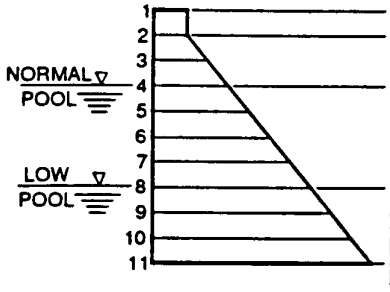

y	y/H_s	Section Width
600	1.000	20.0
570	0.950	20.0
533	0.888	53.8
495	0.825	88.4
460	0.767	120.4
420	0.700	156.8
345	0.575	225.3
270	0.450	293.7
180	0.300	375.8
90	0.150	457.9
0	0.000	540.0

8. Properties of Concrete Mass

For sections y distance above the foundation,

w_s = (section width) × 0.155 k/ft^3

ϕ = value from Figure C-5 (based on y/H_s)

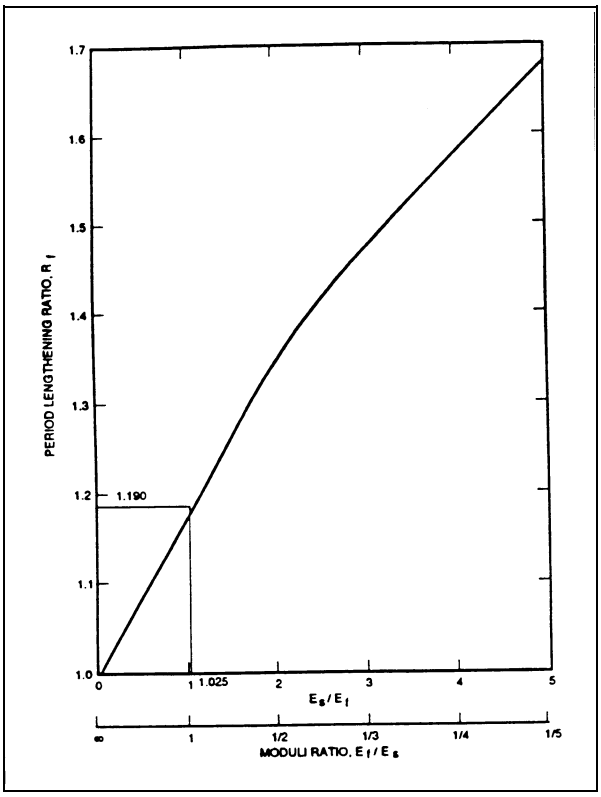

Figure C-2. Standard values for R_f , the period lengthening ratio due to dam-foundation rock interaction. Fenves and Chopra (1986)

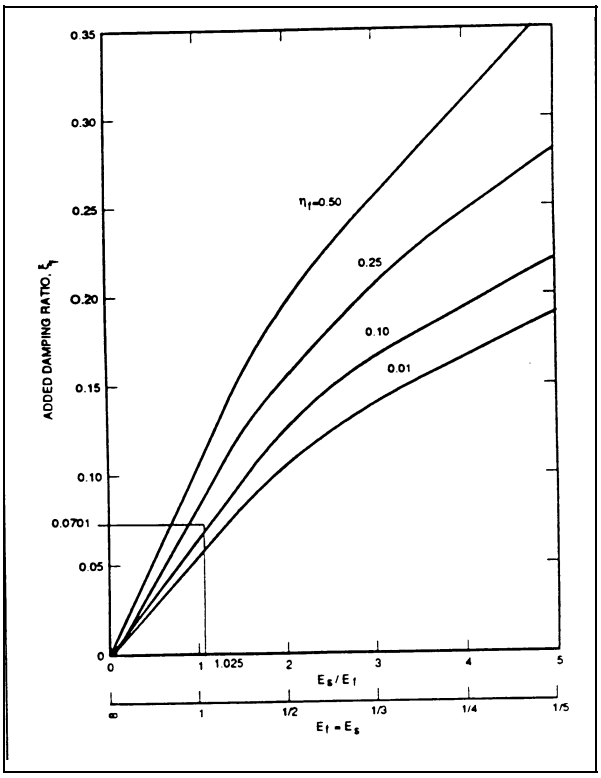

Figure C-3. Standard values for ε_f , the added damping due to dam-foundation rock interaction. Fenves and Chopra (1986)

y	w_s (k/ft)	ϕ	$w_s\phi$	$w_s\phi^2$	dy (Segment Height)	$w_s\phi dy$	$w_s\phi^2 dy$
600	3.10	1.000	3.10	3.10	30	84.9	78.5
570	3.10	0.829	2.56	2.13	37	151.9	110.3
533	8.34	0.678	5.65	3.83	38	251.0	152.0
495	13.70	0.552	7.56	4.17	35	282.1	141.8
460	18.66	0.459	8.56	3.93	40	350.6	144.8
420	24.30	0.369	8.97	3.31	75	666.4	207.4
345	34.92	0.252	8.80	2.22	75	606.4	127.9
270	45.52	0.162	7.37	1.19	90	538.6	69.8
180	58.25	0.079	4.60	0.36	90	299.7	18.9
90	70.97	0.029	2.06	0.06	90	92.7	2.7
0	83.70	0	0	0			
					600 ft	3,324.3	1,054.1

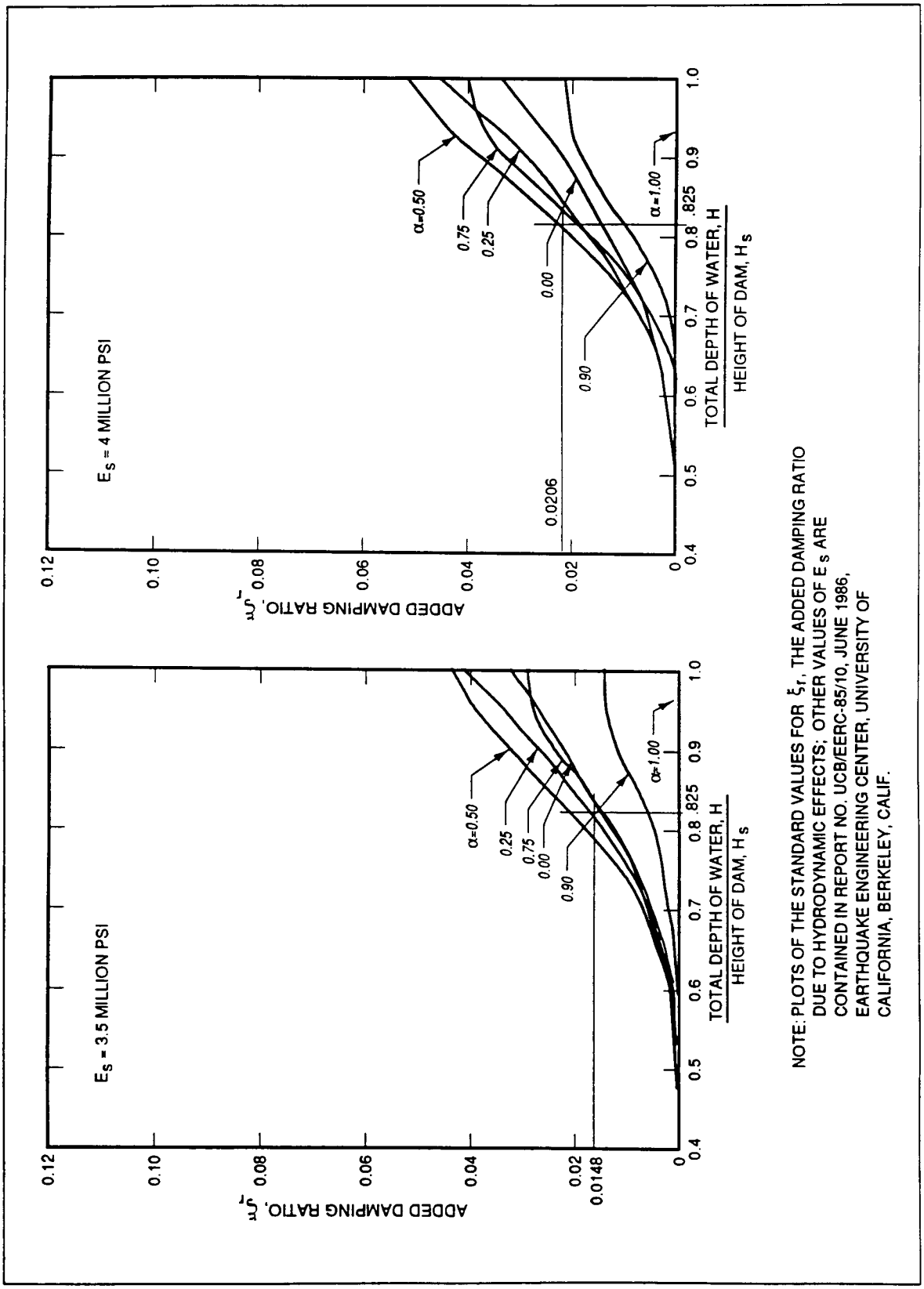

Figure C-4. Values for ε_r, the added damping ratio due to hydrodynamic effects; E_s = 3.5 and 4.0 million psi

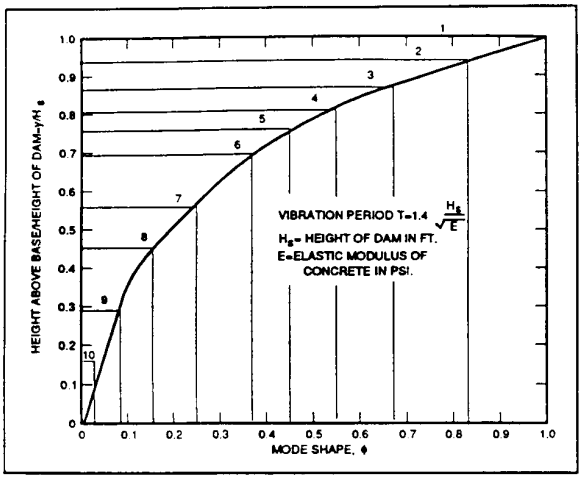

Figure C-5. Standard mode shape and fundamental period for the dam on a rigid foundation and empty reservoir. Chopra (1978)

C-9. Hydrodynamic Influence

For sections y distance above the foundation,

$g\bar{p}/wH$ = value from Figure C-6 (based on y/H and R_w) interpolate Figure C-6 plots for α = 0.75 and α = 0.50 for the required α = 0.69 as calculated in Appendix B

w = 0.0624 k/ft^3

H_s = 600 ft

gp = $[wH(H/H_s)^2]$ $(g\bar{p}/wH)$ = CONSTANT × $(g\bar{p}/wH)$

	POOL ELEVATION	
	NORMAL	LOW
H	495	270
R_w	0.85	0.52
CONSTANT	21.02	3.41

NORMAL POOL						LOW POOL			
y	dy (Seg Ht)	$\frac{y}{H}$	$\frac{g\bar{p}}{wH}$	gp	$\frac{g\bar{p}}{wH}\,dy$	$\frac{y}{H}$	$\frac{g\bar{p}}{wH}$	gp	$\frac{g\bar{p}}{wH}\,dy$
495		1.000	0	0					
	35				1.75				
460		0.929	0.100	2.10					
	40				4.88				
420		0.848	0.144	3.03					
	75				11.89				
345		0.697	0.173	3.64					
	75				13.24				
270		0.545	0.180	3.78		1.000	0	0	
	90				16.06				6.39
180		0.364	0.177	3.72		0.667	0.142	0.48	
	90				15.57				11.66
90		0.182	0.169	3.55		0.333	0.117	0.40	
	90				14.90				9.77
0		0	0.162	3.41		0	0.100	0.34	
					78.29				27.82

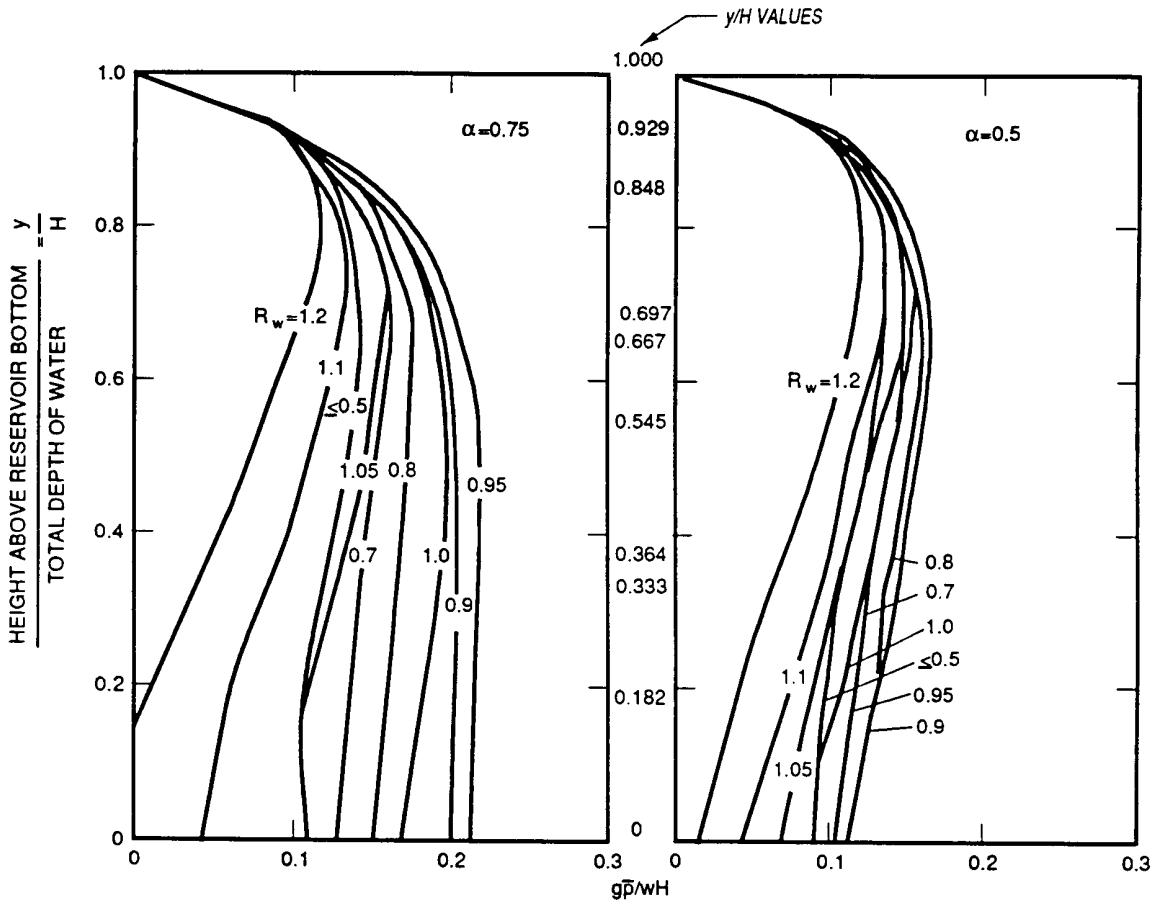

NOTE: PLOTS OF THE STANDARD VALUES FOR THE HYDRODYNAMIC PRESSURE FUNCTION $\bar{p}$: OTHER VALUES OF α ARE CONTAINED IN REPORT NO. UCB/EERC-85/10, JUNE 1986, EARTHQUAKE ENGINEERING RESEARCH CENTER, UNIVERSITY OF CALIFORNIA, BERKELEY, CALIF.

Figure C-6. Standard values for the hydrodynamic pressure function $\bar{p}$ for full reservoir; i.e., H/H_s = 1, α = 0.75 and 0.50

C-10. Generalized Mass, $\tilde{M}_1$

$$\tilde{M}_1 = (R_r)^2 M_1$$

$$M_1 = (1/g) \int_0^{H_s} w_s \phi^2 dy = (1/32.2)\ (1{,}054.1)$$

$$= 32.74 \text{ k-sec}^2/\text{ft}$$

	POOL ELEVATION	
	NORMAL	LOW
R_r	1.110	1.000
M_1	40.34	32.74

C-11. Generalized Earthquake Force Coefficient, $\tilde{L}_1$

$$\tilde{L}_1 = L_1 + (1/g)\ F_{st}\ (H/H_s)^2 A_p$$

$$L_1 = (1/g) \int_0^{H_s} w_s \phi dy = (1/32.2)\ (3{,}324.3)$$

$$= 103.2 \text{ k-sec}^2/\text{ft}$$

$$F_{st} = wH^2/2 = (0.0624/2)\ H^2 = 0.0312H^2$$

$$A_p = \frac{2}{H} \int_0^{H} \frac{g\bar{p}}{wH}\, dy$$

	POOL ELEVATION	
	NORMAL	LOW
H	495	270
F_{st}	7,645	2,274
$\int_0^H \frac{g\bar{p}}{wH}$	78.29	27.82
A_p	0.316	0.206
$\tilde{L}_1$	154.26	106.15

C-12. Response Spectrum Acceleration, $\tilde{S}_a$

a. As discussed in Appendix B, the conditions for this example problem require site specific design response spectra. However, since this is only for the purpose of demonstrating Chopra's simpified method, the standard design response spectra shown in Figure 5-2 and Table 5-1 will be assumed to be the site-specific design response spectra.

b. For both the earthquake load cases, the fundamental period T_1 is greater than 0.4 sec; therefore:

$$S_a = K_2 S_{a(5\%)}$$

where

K_2 = $1.466 - 0.2895\ln(\beta)$

$S_{a(5\%)}$ = value at period $\tilde{T}_1$ obtained by interpolating Table 6-1 between the appropriate values of T.

The spectral ordinates S_a are for the design response spectrum normalized to a PGA = 1 g. These values must be scaled by the PGA factor shown in Table 5-2 for an MCE occurring in seismic Zone 3. The scaling factor is 0.550 g; therefore:

$$\tilde{S}_a = 0.550 \times K_2 S_{a(5\%)} \times 32.2 \text{ ft/sec}^2$$

	POOL ELEVATION	
	NORMAL	LOW
T_1	0.585 sec	0.527 sec
β	12.33%	11.16%
K_2	0.7388	0.7676
$S_{a(5\%)}$	1.7094 g	1.8975 g
$\tilde{S}_a$	22.37 ft/sec2	25.80 ft/sec2

C-13. Equivalent Lateral Earthquake Force for Fundamental Mode, f_1

$$f_1 = \frac{\tilde{L}_1 \tilde{S}_a}{\tilde{M}_1 g} (w_s\phi + gp) = \text{constant} \times (w_s\phi + gp)$$

	POOL ELEVATION	
	NORMAL	LOW
$\tilde{L}_1$	154.26	106.15
$\tilde{M}_1$	40.34	32.74
$\tilde{S}_a$	22.37 ft/sec^2	25.80 ft/sec^2
constant	2.657	2.598

for a section y-distance above the foundation, values of f_1 in (k/ft) are as follows:

		gp		f_1	
y	$ws\phi$	NORMAL	LOW	NORMAL	LOW
600	3.10			8.24	8.05
570	2.56			6.80	6.65
533	5.65			15.01	14.68
495	7.56	0		20.09	19.64
460	8.56	2.10		28.32	22.24
420	8.97	3.30		31.88	23.30
345	8.80	3.64		33.05	22.86
270	7.37	3.78	0	29.63	19.15
180	4.60	3.72	0.48	22.11	13.20
90	2.06	3.55	0.40	14.91	6.39
0	0	3.41	0.34	9.06	0.88

C-14. Equivalent Lateral Earthquake Force for the Higher Modes, f_{sc}

$$f_{sc} = \frac{1}{g}\left[w_s\left(1 - \frac{L_1}{M_1}\phi\right) + \left(gp_0 - \frac{B_1}{M_1}w_s\phi\right)\right]a_g$$

a_g/g = PGA = 0.550 g

$$f_{sc} = 0.550 \times \left[w_s\left(1 - \frac{L_1}{M_1}\phi\right) + \left(gp_0 - \frac{B_1}{M_1}w_s\phi\right)\right]$$

$$gp_0 = \left(\frac{g\bar{p}_0}{wH}\right) \times wH\left(\frac{H}{H_s}\right)^2 \qquad B_1 = 0.2\,\frac{F_{st}}{g}\left(\frac{H}{H_s}\right)^2$$

$\left(\frac{g\bar{p}_0}{wH}\right)$ = value from Figure C-7 (for values of y/H)

	POOL ELEVATION	
	NORMAL	LOW
L_1	103.2	103.2
M_1	32.74	32.74
$\left(\frac{H}{H_s}\right)^2$	0.681	0.202
$wH\left(\frac{H}{H_s}\right)^2$	21.03	3.40
F_{st}	7,645	2,274
B_1	32.34	2.85

NORMAL POOL

y	W_S	ϕ	$W_S(1 - \frac{L_1}{M_1}\phi)$	y/H	$\frac{g\bar{P}_o}{wH}$	gp_o	$W_S\phi$	$(gp_o - \frac{B_1}{M_1}W_S\phi)$	f_{sc}
600	3.10	1.000	-6.67				3.10	-3.06	-5.35
570	3.10	0.829	-5.00				2.56	-2.53	-4.14
533	8.34	0.678	-9.48				5.65	-5.58	-8.28
495	13.70	0.552	-10.14	1.000	0.000	0.00	7.56	-7.47	-9.69
460	18.66	0.459	-8.34	0.929	0.187	3.93	8.56	-4.53	-7.08
420	24.30	0.369	-3.96	0.848	0.312	6.56	8.97	-2.30	-3.44
345	34.92	0.252	7.18	0.697	0.473	9.95	8.80	1.26	4.64
270	45.52	0.162	22.28	0.545	0.587	12.34	7.37	5.06	15.04
180	58.25	0.079	43.74	0.364	0.677	14.24	4.60	9.70	29.39
90	70.97	0.029	64.48	0.182	0.727	15.29	2.06	13.26	42.76
0	83.70	0.000	83.70	0.000	0.746	15.69	0.00	15.69	54.66

LOW POOL

y	W_S	ϕ	$W_S(1 - \frac{L_1}{M_1}\phi)$	y/H	$\frac{g\bar{P}_o}{wH}$	gp_o	$W_S\phi$	$(gp_o - \frac{B_1}{M_1}W_S\phi)$	f_{sc}
600	3.10	1.000	-6.67				3.10	-0.27	-3.82
570	3.10	0.829	-5.00				2.56	-0.22	-2.87
533	8.34	0.678	-9.48				5.65	-0.49	-5.48
495	13.70	0.552	-10.14				7.56	-0.66	-5.94
460	18.66	0.459	-8.34				8.56	-0.75	-5.00
420	24.30	0.369	-3.96				8.97	-0.78	-2.61
345	34.92	0.252	7.18				8.80	-0.77	3.52
270	45.52	0.162	22.28	1.000	0.000	0.00	7.37	-0.64	11.90
180	58.25	0.079	43.74	0.667	0.500	1.70	4.60	1.30	23.34
90	70.97	0.029	64.48	0.333	0.693	2.36	2.06	2.18	24.77
0	83.70	0.000	83.70	0.000	0.746	2.54	0.00	2.54	47.43

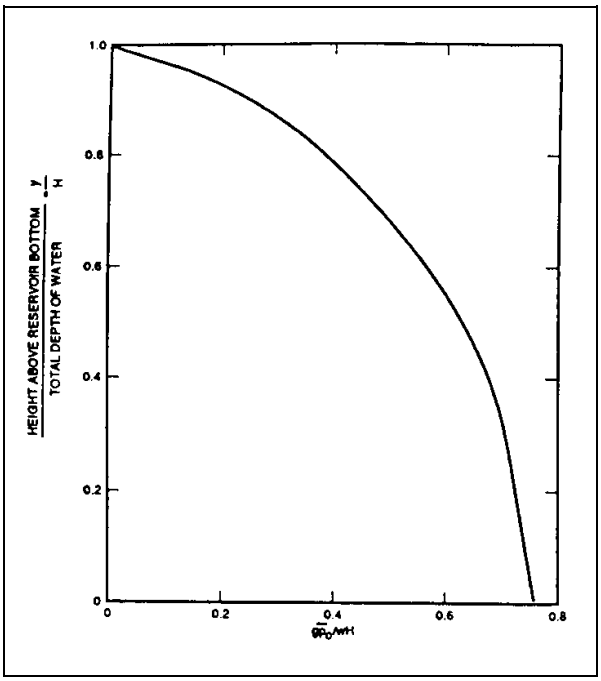

Figure C-7. Standard mode shape and fundamental period for the dam on a rigid foundation and empty reservoir. Chopra (1978)

C-15. Allowable Tensile Stress

Appendix B established the direct tensile strength of the basic RCC mix to be:

f'_t = 290 psi (for the parent concrete)

f'_t = 205 psi (for the lift joints)

Because of the high strain rates associated with a seismic event, the dynamic tensile strength is greater than the direct tensile strength obtained from the lab tests:

DTS = 1.5 f'_t = 1.5 × 290 = 435 psi (for the parent concrete)

DTS = 1.5 f'_t = 1.5 × 205 = 307 psi (for the lift joints)

In accordance with paragraph 4-3*c*, the allowable tensile stress for a new RCC dam in seismic Zone 3 for the MCE load condition is:

$f_{t(allowable)}$ = 1.33 × 435 = 579 psi (for the parent concrete)

$f_{t(allowable)}$ = 1.33 × 307 = 408 psi (for the lift joints)

C-16. Determining Stresses for the Earthquake Load Cases

a. The response of the dam to the design earthquake ground motion is obtained by applying the equivalent lateral forces f_1 and f_{sc} to the dam as static loads, and performing a static analysis to determine the tensile tresses. The lateral forces f_1 and f_{sc} are distributed forces in kips/ft. They are treated as individual loading cases in the static analysis. As discussed in paragraph 7-7, the stresses produced by these forces represent maximum modal responses. Thus, they must be combined by a statistical method. The square root of the sum of the squares (SRSS) method is used, and the maximum tensile stresses are as follows:

$$f_t = \sqrt{\sigma_1^2 + \sigma_{sc}^2}$$

where

f_t = maximum tensile stress due only to design earthquake loading in a direction normal to the lift joints (does not include hydrostatic or dead load)

σ_1 = tensile stress contribution of the fundamental mode as produced by the statically applied load f_1

σ_{sc} = tensile stress contribution of the higher modes as produced by the statically applied load f_{sc}

b. Two static analysis options are available for determining the tensile stresses σ_1 and σ_{sc}. The first option is to consider the dam as a simple vertical cantilever fixed at the foundation and loaded laterally by the loads f_1 and f_{sc}. The stresses σ_1 and σ_{sc} are simple bending stresses that can be hand calculated by the beam bending formula Mc/I. The maximum principal tensile stresses occurring at the downstream face are then approximated by the following:

$$f_{t(\max)} = \sqrt{\sigma_1^2 + \sigma_{sc}^2}\ \sec^2\Theta + \sigma_{st}\sec^2\Theta$$

where

$f_{t(max)}$ = the maximum principal tensile stress

Θ = the angle of the downstream face measured from vertical

σ_{st} = stress normal to the lift joints caused by static loads (hydrostatic, dead load of dam, etc.)

The second option is to apply the lateral loads f_1 and f_{sc} to a finite element model of the dam, fixed at the dam base, and perform a static analysis to obtain the tensile stresses normal to the lift joints σ_1 and σ_{sc}, and also the corresponding maximum principal tensile stresses $\sigma_{1(max)}$ and $\sigma_{sc(max)}$. The maximum tensile stress normal to the lift joints is calculated by the formula for f_1 described above, and the maximum principal tensile stress, $f_{t(max)}$, is calculated as follows:

$$f_{t(\max)} = \sqrt{\sigma^2_{1(\max)} + \sigma^2_{sc(\max)}}$$

c. The second option will be used for this example problem. The same finite element model of the dam will be used as formulated in Appendix D to analyze the example problem by the composite finite element-equivalent mass system method. This will allow a good comparison of the two different methods. Node points at the dam base, nodes 56 through 62, will be fully fixed for this analysis since Chopra's simplified method does not include modeling of the dam foundation. To load the finite element model, the distributed lateral forces f_1 and f_{sc} were converted to concentrated lateral joint loads applied to the appropriate upstream face node points. Note that y = the distance above the foundation in feet coincides with the node point locations of the finite element model shown in Figures D-1 and D-2 of Appendix D.

d. The static loads accompanying the earthquake ground motion loading consist of the hydrostatic load of the forebay on the upstream face and the dead load weight of the dam. These loads are identical to those calculated in Table D-2 and discussed in paragraph D-12 of Appendix D for the composite finite element analysis. However, since Chopra's simplified method does not account for deformations in the foundation, the static stresses σ_{st} and $\sigma_{st(max)}$ for Chopra's method are different than those derived by the composite finite element analysis.

e. The tabulations on the following pages show the critical tensile stresses for the MCE load cases.

MCE Normal Pool Load Case:
Critical Tensile Stresses Normal to the Lift Joints at the Upstream Face

	Stress Normal to the Lift Joint (ksf, tension is +)					
y	σ_1	σ_{sc}	Dynamic Response f_1	Static Stress σ_{st}	Critical Tensile Stress (psi)	Percent Overstressed
590	24.96	-16.16	29.73	-1.55	196	----
570	35.99	-23.49	42.98	-5.32	262	----
533	34.04	-20.77	39.88	-11.39	198	----
495	37.21	-21.16	42.81	-15.94	187	----
460	44.47	-25.23	51.13	-21.63	205	----
420	50.97	-25.38	56.94	-27.61	204	----
345	60.14	-25.69	65.40	-35.89	205	----
270	72.93	-26.86	77.72	-45.49	224	----
180	90.22	-26.54	94.04	-53.62	281	----
90	122.20	-5.22	122.31	-51.20	494	21
0	49.19	7.57	49.76	-14.20	247	----

MCE Low Pool Load Case:
Critical Tensile Stresses Normal to the Lift Joints at the Upstream Face

	Stress Normal to the Lift Joint (ksf, tension is +)					
y	σ_1	σ_{sc}	Dynamic Response f_1	Static Stress σ_{st}	Critical Tensile Stress (psi)	Percent Overstressed
590	24.39	-11.51	26.97	-1.55	176	----
570	35.20	-16.78	38.99	-5.31	234	----
533	32.93	-14.61	36.03	-11.54	170	----
495	35.46	-14.81	38.43	-16.47	152	----
460	43.95	-16.85	47.07	-22.23	172	----
420	49.12	-16.60	51.85	-28.80	160	----
345	54.77	-17.22	57.41	-37.81	136	----
270	63.01	-18.85	65.77	-49.40	114	----
180	73.96	-18.21	76.17	-63.43	88	----
90	94.48	-0.38	94.48	-75.90	129	----
0	36.71	6.17	37.22	-26.95	71	----

MCE Normal Pool Load Case:
Critical Tensile Stresses Normal to the Lift Joints at the Downstream Face

	Stress Normal to the Lift Joint (ksf, tension is +)					
y	σ_1	σ_{sc}	Dynamic Response f_1	Static Stress σ_{st}	Critical Tensile Stress (psi)	Percent Overstressed
590	-12.57	8.22	15.02	-1.53	94	----
570	-66.14	42.51	78.62	-2.77	527	----
533	-28.88	18.29	34.18	0.20	239	----
495	-37.32	22.07	43.36	0.55	305	----
460	-48.38	24.90	54.41	-0.12	377	----
420	-58.90	22.75	63.14	-3.02	418	2
345	-67.59	15.47	69.34	-7.89	427	5
270	-69.36	5.99	69.62	-12.26	398	----
180	-58.51	-2.58	58.57	-14.43	307	----
90	-39.08	-5.49	39.46	-12.46	188	----
62	-12.65	-1.76	12.77	-6.37	44	----

MCE Low Pool Load Case:
Critical Tensile Stresses Normal to the Lift Joints at the Downstream Face

	Stress Normal to the Lift Joint (ksf, tension is +)					
y	σ_1	σ_{sc}	Dynamic Response f_1	Static Stress σ_{st}	Critical Tensile Stress (psi)	Percent Overstressed
590	-12.29	5.88	13.62	-1.53	84	----
570	-64.53	30.26	71.27	-2.72	476	17
533	-28.87	12.50	31.46	-0.19	217	----
495	-36.55	14.91	39.47	0.07	275	----
460	-45.13	16.86	48.18	0.36	337	----
420	-51.52	15.28	53.74	0.57	377	----
345	-55.61	9.96	56.49	0.49	396	----
270	-54.69	3.17	54.78	0.03	381	----
180	-44.66	-2.71	44.74	-1.38	301	----
90	-29.18	-4.43	29.51	-2.48	187	----
0	-9.45	-1.43	9.56	-3.14	45	----

MCE Normal Pool Load Case:
Critical Principal Tensile Stresses at the Downstream Face

	Principal Tensile Stress (ksf, tension is +)					
y	$\sigma_{1(max)}$	$\sigma_{sc(max)}$	Dynamic Response $f_{1(max)}$	Static Stress $\sigma_{st(max)}$	Critical Tensile Stress (psi)	Percent Overstressed
590	13.09	8.56	15.64	-1.53	98	----
570	76.19	48.90	90.53	-3.15	607	5
533	49.78	31.11	58.70	-1.73	396	----
495	63.24	36.74	73.14	-2.14	493	----
460	79.09	39.67	88.48	-3.16	593	2
420	94.33	35.75	100.88	-6.48	656	13
345	111.10	25.71	114.04	-13.16	701	21
270	112.70	9.90	113.13	-20.42	643	11
180	95.51	7.40	95.80	-24.02	498	----
90	64.46	9.96	65.22	-21.27	305	----
0	16.50	2.91	16.75	-7.06	67	----

MCE Low Pool Load Case:
Critical Principal Tensile Stresses at the Downstream Face

	Principal Tensile Stress (ksf, tension is +)					
y	$\sigma_{1(max)}$	$\sigma_{sc(max)}$	Dynamic Response $f_{1(max)}$	Static Stress $\sigma_{st(max)}$	Critical Tensile Stress (psi)	Percent Overstressed
590	-12.80	6.12	14.19	-1.53	88	----
570	-74.33	34.80	82.07	-3.11	548	----
533	-49.43	21.34	53.84	-1.82	361	----
495	-61.73	24.79	66.52	-1.74	450	----
460	-73.50	26.79	78.23	-1.55	533	----
420	-82.26	24.03	85.70	-2.04	581	1
345	-91.19	16.71	92.71	-3.45	620	7
270	-88.52	5.70	88.70	-4.45	585	1
180	-72.64	-6.29	72.91	-6.12	464	----
90	-48.07	-7.89	48.71	-6.63	292	----
0	-12.24	-2.28	12.45	-3.15	65	----

C-17. Conclusions

The Chopra simplified method is used only for preliminary design of new dams. Preliminary design progresses to the point where it becomes apparent that, with limited refinement, the final design will be satisfactory. Refer to Figure C-8 which shows zones where the basic RCC mix is overstressed. It appears that use of superior mixes in these areas will lead to a satisfactory final design. Final design uses a more refined method such as the composite finite element method demonstrated in Appendix D for this example problem. The more refined methods allow for modeling and verifying the zones of superior concrete, where this is not possible with the simplified method.

C-18. Comparison of Results

Paragraph D-16 compares the results of this analysis using Chopra's simplified method with the results of the same example problem analyzed by the composite finite element method.

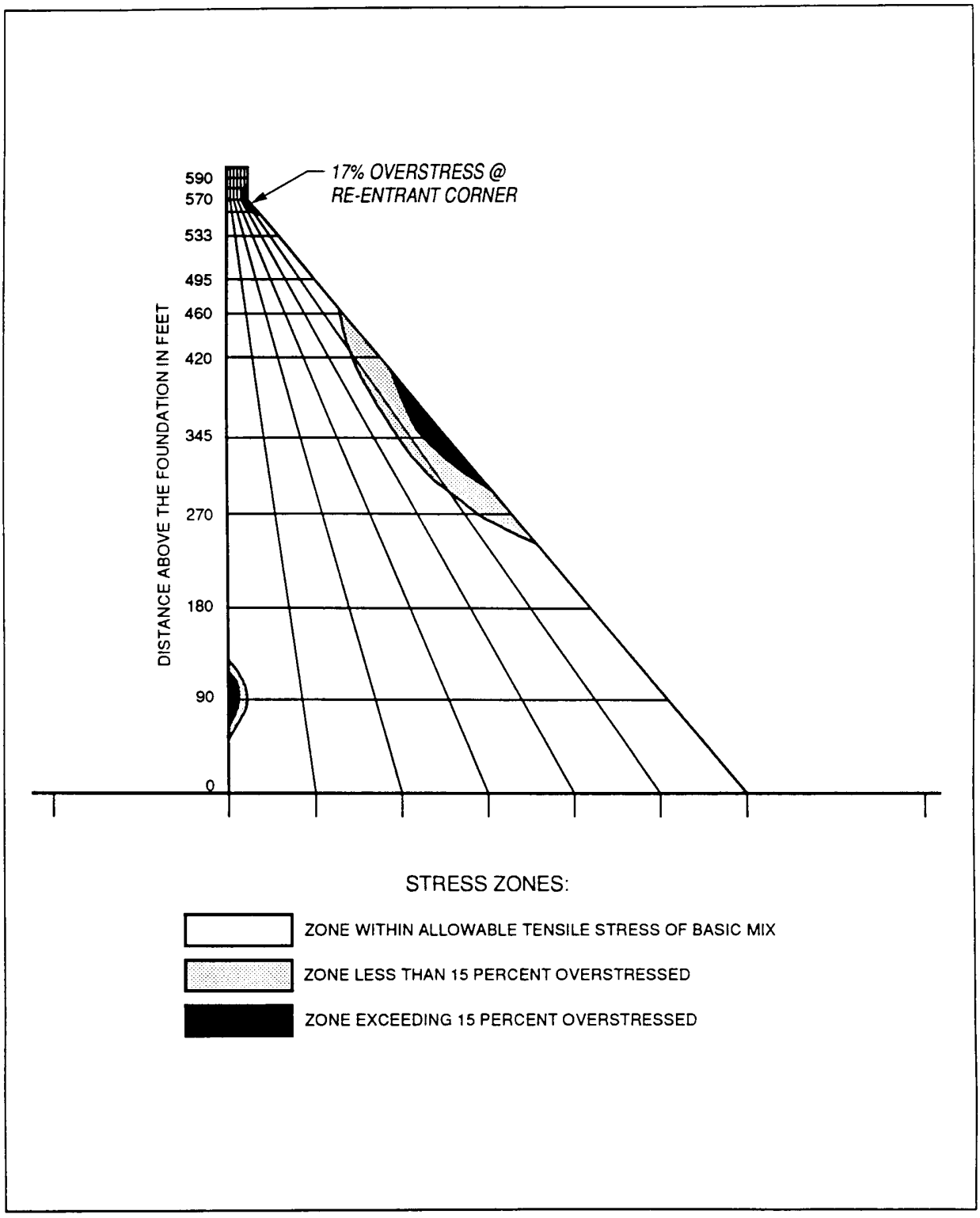

Figure C-8. Zones exceeding the allowable tensile stress for the basic RCC mix

Appendix D
Design Example-Finite Element Method

D-1. General

a. The design example problem described in Appendix B was analyzed using the composite finite element-equivalent mass system method. The analysis was performed on a PC using the computer program ALGOR-Finite Element Analysis System.

b. Definitions of symbols and notations used in this appendix can be found in the Glossary. Refer to Appendix B where the values of several parameters used as input to the finite element program were developed.

D-2. Computer Model

The computer model is shown in Figures D-1 and D-2. The general characteristics are as follows:

a. The dam/foundation is a 2-D representation using the critical transverse cross section of the dam. The geometry of the finite element mesh is established by 156 node points.

b. The foundation effects are modeled using a block of foundation with the width of the block equal to 3 times the width of the dam base, and the height of the block equal to 1.5 times the height of the dam.

c. The boundary conditions along the bottom and both sides of the foundation block consist of roller restraints of the node points establishing these boundary lines.

d. Both the dam and the foundation block are modeled with 2-D solid, isotropic, quadrilateral, plane strain elements. The dam consists of 78 elements, and the foundation block consists of 48 elements. The nodes establishing the corners of the elements have 2 degrees-of-freedom (Y and Z translations).

e. The material properties for the dam RCC and the foundation block are given in Appendix B. The density of the foundation block is set to zero so the ground motion is transmitted to the dam-foundation interface without modification.

f. The reservoir effects are modeled by developing an equivalent mass system which consists of adding lumped masses to the nodal points at the upstream face of the dam as shown in Figure D-1. Procedure for determining the magnitude of the added masses is given below.

D-3. Equivalent Mass System Representation of Reservoir Effects

a. This system models the hydrodynamic effects by adding mass to the finite element model. It is founded on the equations and techniques used by Chopra in developing his simplified analysis method. It is based on the fundamental mode, but since this usually contributes 85 to 90 percent of the response, it produces good results. The method accounts for the compressibility of water and the interaction of the water with the elastic structure and foundation. The equations used in deriving the equivalent mass system for finite element analysis are:

$$f_1 = \frac{\tilde{L}_1}{\tilde{M}_1} \frac{S_A}{g} (g\bar{m}) (\psi_1) \qquad \text{(D-1)}$$

where

f_1 = total lateral force per unit height acting at a certain elevation *including* the hydrodynamic contribution

$\bar{m}$ = equivalent mass system which consists of

$$\bar{m} = m_S + m_{HD} \qquad \text{(D-2)}$$

where

m_S = mass per unit height of concrete

m_{HD} = mass per unit height which must be added to account for the hydrodynamic effects

Ψ_1 = fundamental mode shape normalized so the crest of the dam has a unit deflection

$$m_{HD} = \frac{p}{\Psi_1} \qquad \text{(D-3)}$$

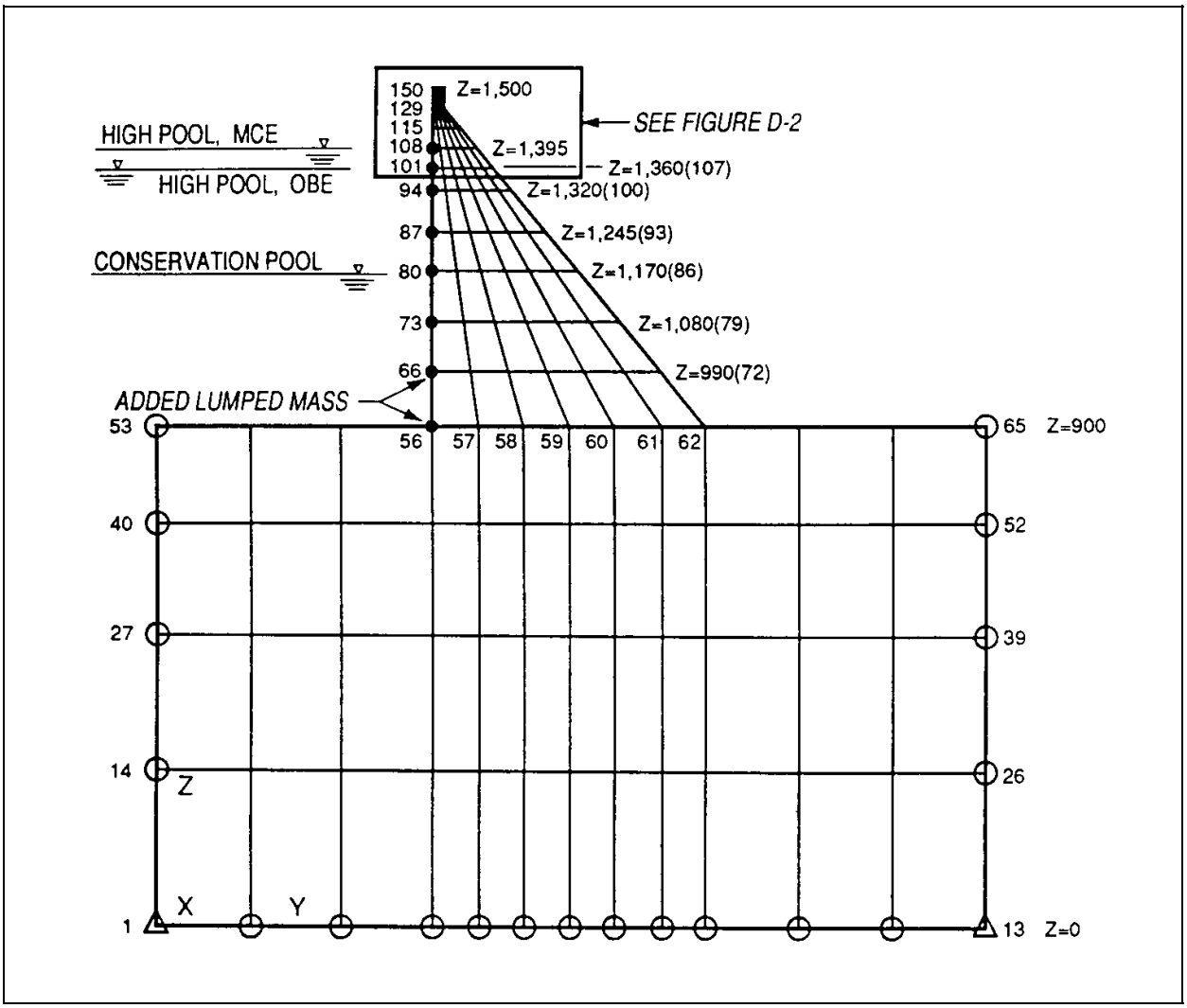

Figure D-1. Composite finite element-equivalent mass system model

where

p = the hydrodynamic pressure function determined by using Chopra's standardized curves of $\left(\frac{g\bar{p}}{wH}\right)$. This is discussed in detail later.

$$w_S = g(m_S) \qquad \text{(D-4)}$$

where

w_S = weight per unit height of concrete

b. It is now possible to substitute Equations D-2 through D-4 into Equation D-1 which gives the basic equation used in Chopra's simplified method:

$$f_1 = \frac{\tilde{L}_1}{\tilde{M}_1} \frac{S_A}{g} (w_S \Psi_1 + gp)$$

c. The above derivation shows that Chopra's simplified method is based on an "equivalent mass system." The added mass that accounts for the hydrodynamic effects is represented by m_{HD} in Equation D-3 above. This same added mass can be included in a finite element model, and it will cause the model to respond with a very good approximation of the interaction of the compressible water on the flexible structure/foundation system.

d. Chopra provides standardized curves of the hydrodynamic pressure function $\left(\frac{g\bar{p}}{wH}\right)$. It should be

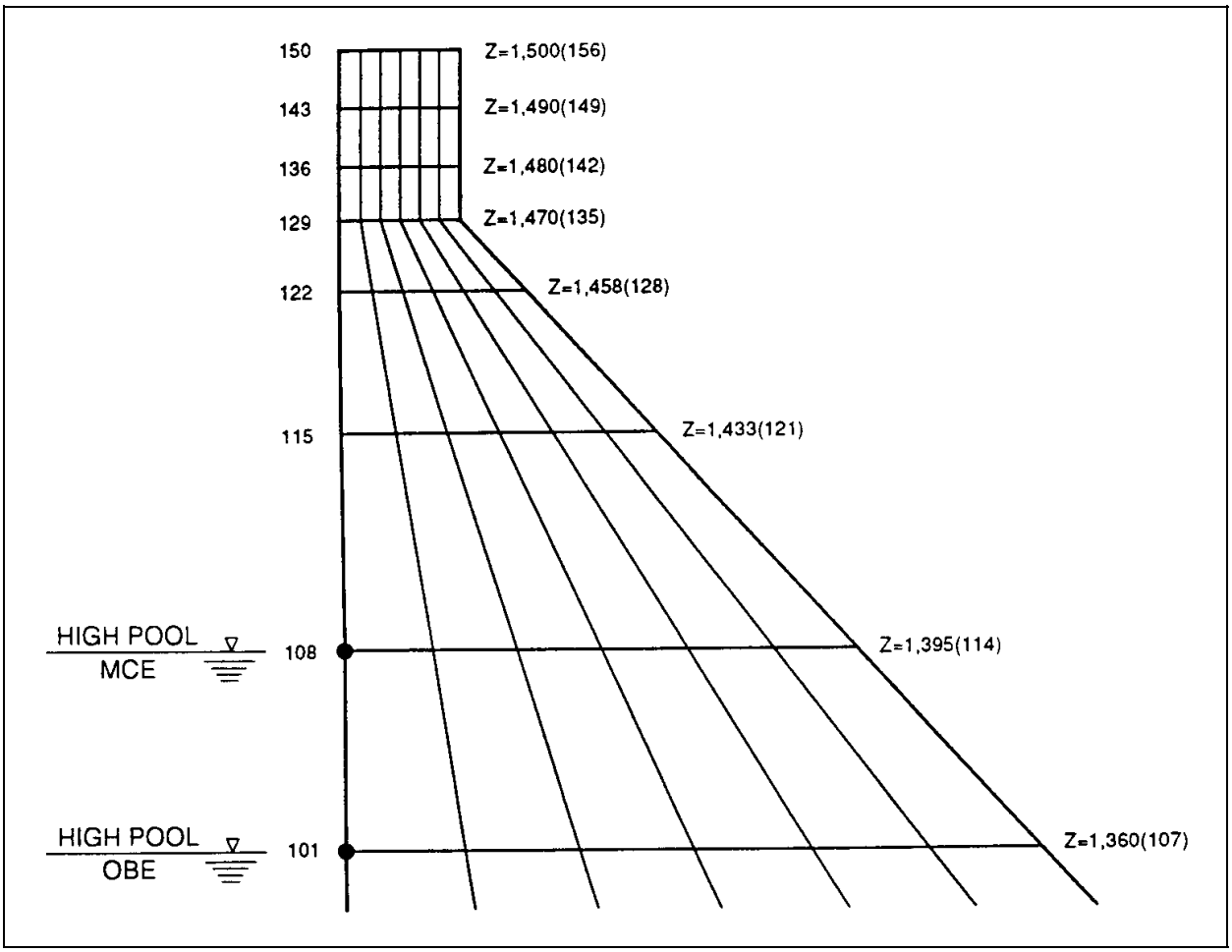

Figure D-2. Zoom-in of finite element mesh at top of dam

noted that these curves are based on the full reservoir condition where $H/H_s = 1$. To correct the values taken from the curves for other reservoir depths it is necessary to multiply these values by the following factor:

$$p = \left[\left(\frac{wH}{g} \right) \left(\frac{H}{H_S} \right)^2 \right] \left(\frac{g\bar{p}}{wH} \right)$$

where

p = hydrodynamic pressure function for a reservoir of depth H above the foundation

Then the added mass is calculated to be:

$$m_{HD} = \frac{p}{\psi_1} = \frac{1}{\psi_1} \left[\left(\frac{wH}{g} \right) \left(\frac{H}{H_S} \right)^2 \right] \left(\frac{g\bar{p}}{wH} \right) \qquad \text{(D-5)}$$

The finite element model requires the distributed mass m to be converted to lumped masses applied at appropriate nodes on the upstream face of the model as expressed by

$$M_n = C_{tr}\, m_{HD}$$

where

M_n = added lumped mass at a particular node

C_{tr} = the tributary area associated with a particular node

m_{HD} = the value of the distributed mass (mass per unit height) at a particular node location

Equation D-5 is then rewriten as:

$$M_n = \left[\left(\frac{wH}{g} \right) \left(\frac{H}{H_S} \right)^2 \right] \left(\frac{C_{tr}}{\psi_1} \right) \left(\frac{g\bar{p}}{wH} \right) \quad \text{(D-6)}$$

e. The Chopra curves for standardized pressure function are based on the ratio R_w which is defined by the following equation:

$$R_w = \frac{T_1^r}{\tilde{T}_r} \quad \text{(D-7)}$$

where

$$T_1^r = \frac{4H}{C} \quad \text{(D-8)}$$

Equations for T_r will now be derived which are based on terms that are determined by performing modal analyses using the computer model described in paragraph D-2 to extract the fundamental resonant period for the first mode and the characteristic shape of the first mode.

$$\tilde{T}_r = R_r T_1 \quad \text{(D-9)}$$

$$\tilde{T}_f = R_f T_1 \quad \text{(D-10)}$$

$$\tilde{T}_1 = R_r R_f T_1 \quad \text{(D-11)}$$

By rearranging terms of Equations D-9 and D-10, substituting into Equation D-11, and finally solving for T_r results in the following:

$$T_r = \frac{\tilde{T}_1}{\tilde{T}_f} T_1 \quad \text{(D-12)}$$

Use of these equations is further discussed in the procedure described below.

D-4. Procedure to Determine Added Lumped Masses

The following is a step-by-step procedure to determine the lumped masses to be added at the upstream node points to model the hydrodynamic effects:

Step 1. Perform the modal extraction phase of the dynamic analysis to determine the fundamental resonant period T_1 of the dam on a rigid foundation with an empty reservoir. This requires modifying the computer model described in paragraph D-2 by temporarily fixing the nodes at the dam-foundation interface to create the rigid foundation condition required for this step only. This step is referred to as *computer run #1*, and requires extracting only the first mode.

Step 2. Calculate H/H_s for the pool elevation of interest, and use Figure D-3 to determine a value of R_r. Then calculate $\tilde{T}_r$ using Equation D-9, and then calculate R_w using Equation D-7.

Step 3. With this value of R_w, use Figure D-4 to obtain values of the standard hydrodynamic pressure function ($g\bar{p}/wH$) at the locations of y/H that correspond to the upstream node point elevations. Use the R_w curve that is nearest the calculated value of R_w, but on the conservative side. Note that the appropriate value of α, the wave reflection coefficient, was calculated for the example problem in Appendix B. To determine the correct values of ($g\bar{p}/wH$) for this value of α, it will be necessary to interpolate between the appropriate pair of graphs. These values of ($g\bar{p}/wH$) are used to develop the initial added mass model (see Table D-1 for an example).

Step 4. Remove the temporary node point fixities at the dam-foundation interface leaving the computer model with the boundary conditions described in paragraph D-2, and perform the modal extraction phase of the dynamic analysis to determine the fundamental resonant period of the dam on its elastic foundation with an empty reservoir, $\tilde{T}_f$, and the corresponding characteristic mode shape for the first mode. This step is referred to as *computer run #2*, and requires extracting only the first mode.

Step 5. Normalize the first mode shape from *computer run #2* to a unit translation at the top of the dam by dividing the appropriate node point translation values by the translation value of the node at the top upstream corner of the dam. These are the values of ψ_1 for use in developing the initial added mass model.

Step 6. Using these values of ψ_1 and ($g\bar{p}/wH$), calculate the values of M_n using Equation D-6. Add

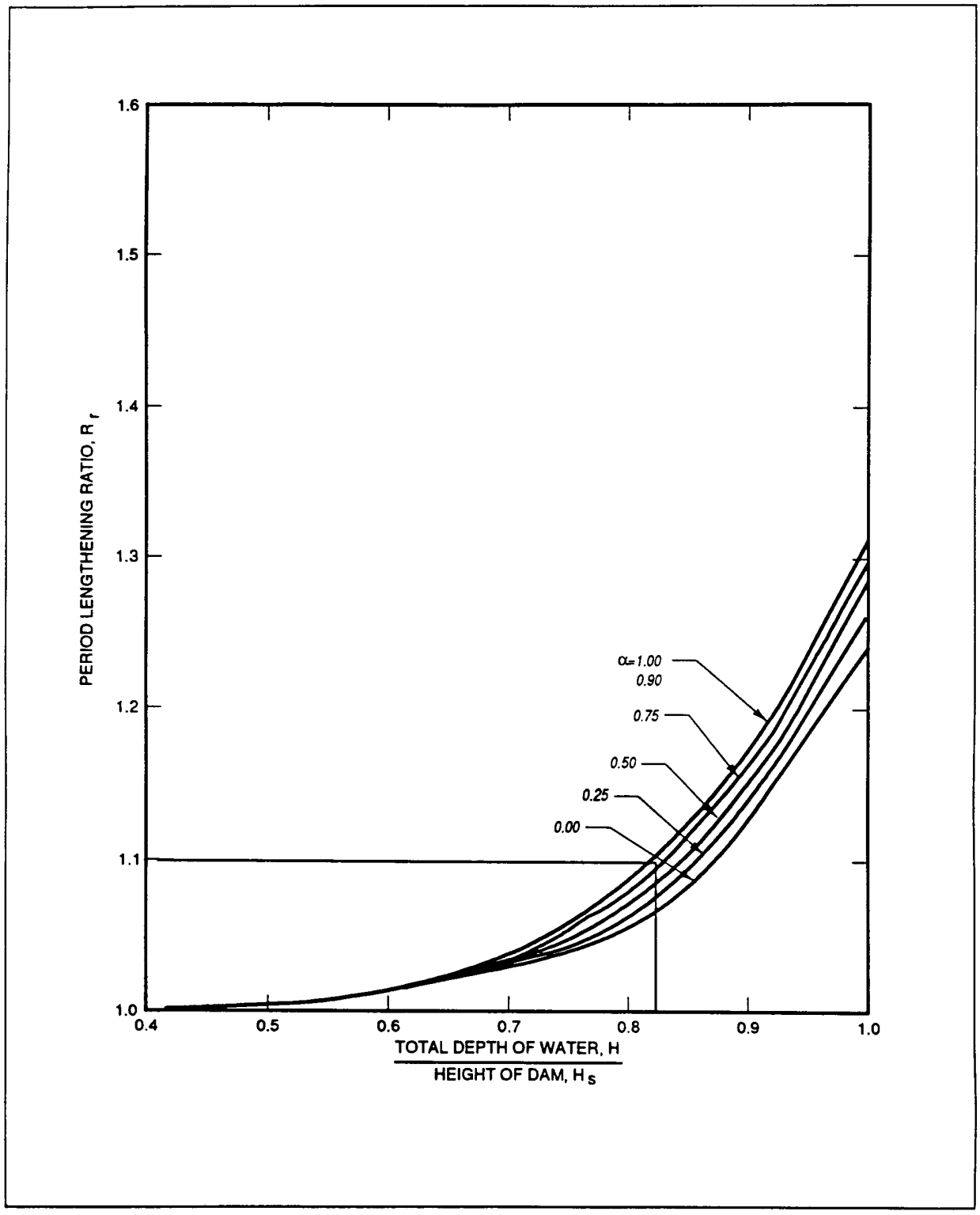

Figure D-3. Initial values of R_r, the period lengthening ratio due to hydrodynamic effects

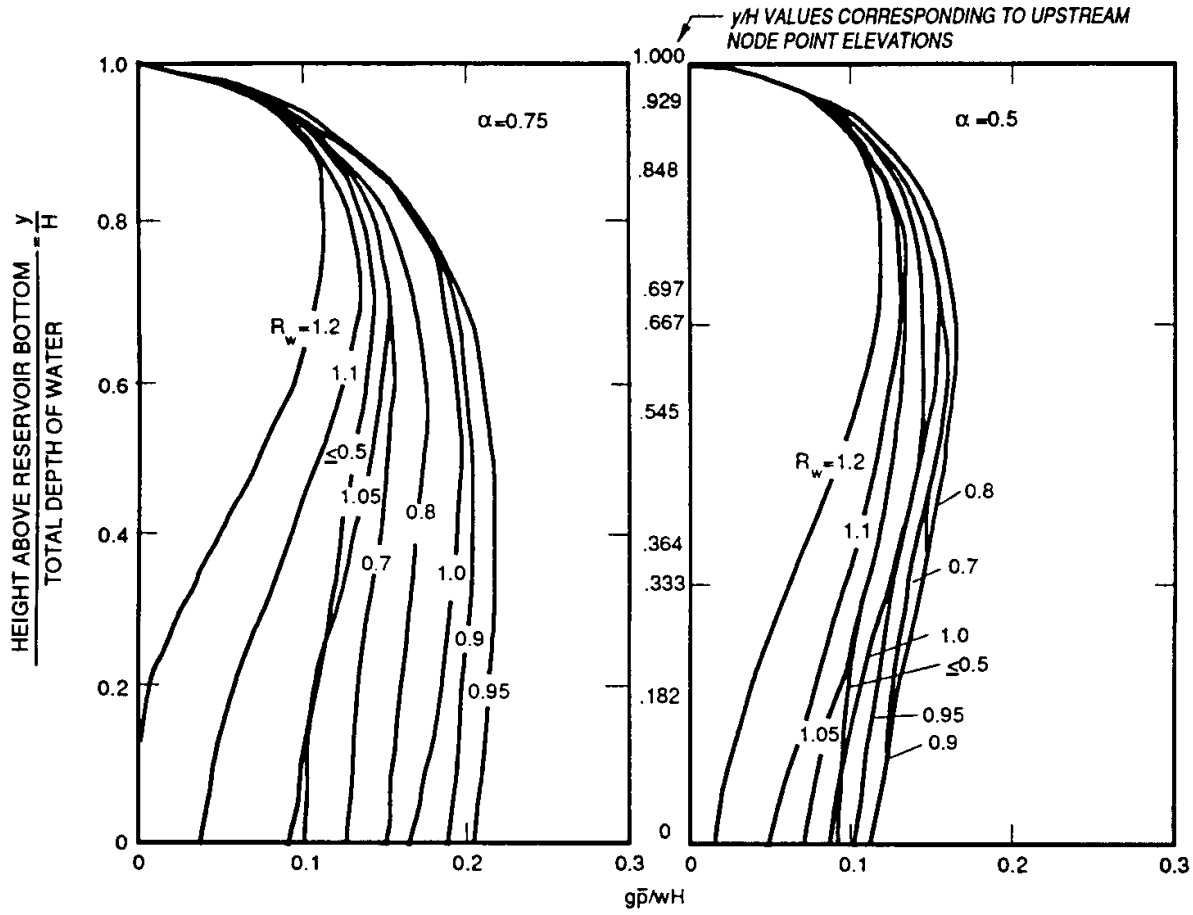

NOTE: PLOTS OF THE STANDARD VALUES FOR THE HYDRODYNAMIC PRESSURE FUNCTION $\bar{p}$; OTHER VALUES OF α ARE CONTAINED IN REPORT NO. UCB/EERC-85/10, JUNE 1986, EARTHQUAKE ENGINEERING RESEARCH CENTER, UNIVERSITY OF CALIFORNIA, BERKELEY, CALIF.

Figure D-4. Standard values for the hydrodynamic pressure function $\bar{p}$ for full reservoir, i.e. *H*/*Hs* = 1; α = 0.75 and 0.50

these lumped masses to the computer model at the appropriate upstream node points. This now becomes the initial added mass model.

Step 7. Using the initial added mass model, perform the modal extraction phase of the dynamic analysis to determine the fundamental resonant period of the dam, $\tilde{T}_1$, on its elastic foundation with reservoir of depth H, and the corresponding characteristic mode shape for the first mode. This step is referred to as *computer run #3*, and requires extracting only the first mode.

Step 8. Normalize the first mode shape from *computer run #3* to a unit translation at the top of the dam by dividing the appropriate node point translation values by the translation value of the node at the top upstream corner of the dam. These are the values of ψ_1 for use in developing the final added mass model.

Step 9. Using the values of T_1 from *computer run #1*, $\tilde{T}_f$ from *computer run #2*, and $\tilde{T}_1$ from *computer run #3*, calculate $\tilde{T}_r$ using Equation D-12. With this value of $\tilde{T}_r$, calculate R_w using Equation D-7.

Step 10. With the new value of R_w, use Figure D-4 to obtain values of the standard hydrodynamic pressure function ($g\bar{p}/wH$) at the locations of y/H that correspond to the upstream node point elevations. Use the R_w curve that is nearest the calculated value of R_w, but on the conservative side. The value of α is the same as used in step 3. To determine the correct values of ($g\bar{p}/wH$) for this value of α, it will be necessary to interpolate between the appropriate pair of graphs. These values of ($g\bar{p}/wH$) are used to develop the final added mass model (see Table D-1 for an example).

Step 11. Using the values of ψ_1 from step 8, and the values of ($g\bar{p}/wH$) from step 10, calculate the values of M_n using Equation D-6. Add these lumped masses to the computer model at the appropriate upstream node points. This completes the final equivalent mass system representation of the reservoir effects for the reservoir of depth H.

D-5. Applying Added Lumped Mass Procedure to the Example Problem

The added lumped mass procedure described in paragraphs D-3 and D-4 will be applied to the example problem. The normal pool condition associated with the MCE will be used to demonstrate the procedure. Determining the added lumped masses for the normal pool condition associated with the OBE and for low pool conditions is similar. The computer model as described in paragraph D-2 is used in the modal analyses mentioned below.

a. Initial added mass model.

H = 2445 - 1950 = 495 ft

T_1^r = 4H/C = 4(495)/4720 = 0.4195 sec (D-8)

H_s = 2550 - 1950 = 600 ft

H/H_s = 495/600 = 0.825

T_1 = 0.3882 sec from *computer run #1* where the nodes at the dam base-foundation interface (nodes 56 through 62) of the composite dam/foundation model are fixed to create the condition of a dam on a rigid foundation.

ψ_1 = the eigenvector (mode shape) for mode 1 from *computer run #2* which uses the composite dam/foundation model with empty reservoir. The lateral mode shape translations (y-direction) are taken from the mode shape computer analysis output at the upstream face node points shown in Figures D-1 and D-2, and are normalized to a unit translation at the top of the dam (by dividing each translation value by the translation output value for the node at the top upstream corner). The normalized values are entered in the appropriate column of Table D-1 for the initial added mass model.

R_r = 1.10 from Figure D-3 (for H/H_s = 0.825), which now allows the following to be calculated:

$$\tilde{T}_r = R_r T_1 = 1.10\ (0.3882) = 0.4270 \text{ sec} \quad \text{(D-9)}$$

$$R_w = T_1^r / \tilde{T}_r = 0.4195/0.4270 = 0.982 \quad \text{(D-10)}$$

($g\bar{p}/wH$) values are obtained from Figure D-4 for the values of y/H that correspond to the upstream node point elevations shown in Figure D-1. The curve lines for R_w = 0.95 are used since they are nearest

Table D-1
Computation Sheet to Determine the Added Lumped Masses to Model the Hydrodynamic Effects of the Reservoir for the Example Problem

Node No.	Normal Pool MCE H = 495 ft: Vertical Coordinate of Node	y	Element Height	C_w	$\frac{y}{H}$	Initial Added Mass Model (R_w = 0.982): Ψ_1	$\left(\frac{g\bar{p}}{wH}\right)$	M_n	Final Added Mass Model (R_w = 0.994): Ψ_1	$\left(\frac{g\bar{p}}{wH}\right)$	M_n
150	1500	Top of dam				1.000			1.000		
108	1395	495	▽	17.50	1.000	0.743	0	0	0.759	0	0
101	1360	460	35	37.50	0.929	0.671	0.105	3.83	0.691	0.104	3.68
94	1320	420	40	57.50	0.848	0.595	0.153	9.66	0.618	0.148	8.99
87	1245	345	75	75.00	0.697	0.468	0.191	19.99	0.493	0.179	17.78
80	1170	270	75	82.50	0.545	0.358	0.203	30.55	0.383	0.183	25.74
73	1080	180	90	90.00	0.364	0.246	0.199	47.54	0.268	0.175	38.38
66	990	90	90	90.00	0.182	0.151	0.190	73.95	0.169	0.161	55.99
56	900	0	90	45.00	0	0.064	0.182	83.56	0.074	0.148	58.77
$M_n = 0.653\left(\frac{C_w}{\Psi_1}\right)\left(\frac{g\bar{p}}{wH}\right)$						ΣM_n = 269.08			ΣM_n = 209.33		
Node No.	Conservation Pool H = 270 ft: Vertical Coordinate of Node	y	Element Height	C_w	$\frac{y}{H}$	Initial Added Mass Model (R_w = 0.909): Ψ_1	$\left(\frac{g\bar{p}}{wH}\right)$	M_n	Final Added Mass Model (R_w = 0.930): Ψ_1	$\left(\frac{g\bar{p}}{wH}\right)$	M_n
150	1500	Top of dam									
80	1170	270	▽	45.00	1.000	0.358	0	0	0.360	0	0
73	1080	180	90	90.00	0.667	0.246	0.193	7.48	0.248	0.193	7.39
66	990	90	90	90.00	0.333	0.151	0.196	12.38	0.153	0.196	12.22
56	900	0	90	45.00	0	0.064	0.182	13.56	0.066	0.182	13.15
$M_n = 0.106\left(\frac{C_w}{\Psi_1}\right)\left(\frac{g\bar{p}}{wH}\right)$						ΣM_n = 33.42			ΣM_n = 32.76		

the calculated value of R_w = 0.982 (on the conservative side), and the plots for α = 0.5 and 0.75 are interpolated to give the values of ($g\bar{p}/wH$) for the calculated value of α = 0.69. Values of ($g\bar{p}/wH$) are entered in Table D-1 for the initial added mass model.

M_n = the lumped masses to be added to the upstream node points which are calculated using the following:

$$M_n = [(wH/g)\ (H/Hs)^2]\ (C_{tr}/\psi_1)\ (g\bar{p}/wH) \qquad \text{(D-6)}$$

where

$$(wH/g)\ (H/Hs)^2 = (0.0624 \times 495 / 32.2)\ (0.825)^2 = 0.653$$

and

$$M_n = 0.653\ (C_{tr}/\psi_1)\ (g\bar{p}/wH)$$

b. Final added mass model.

$\tilde{T}_f$ = 0.5188 sec from *computer run #2* which uses the composite dam/foundation model with empty reservoir.

$\tilde{T}_1$ = 0.5638 sec from *computer run #3* using the composite dam/foundation model with the added lumped masses at the upstream face which represent the hydrodynamic effects of the reservoir as calculated for the *Initial Added Mass Model.*

$$\tilde{T}_r = \tilde{T}_1 T_1 / \tilde{T}_f = 0.5638\ (0.3882)/0.5188 = 0.4219 \text{ sec} \qquad \text{(D-12)}$$

$$R_w = 0.4195/0.4219 = 0.994 \qquad \text{(D-7)}$$

ψ_1 = the eigenvector (mode shape) for mode-1 from *computer run #3* which uses the composite dam/foundation model with lumped masses from the initial added mass model to represent the hydrodynamic effects of the reservoir. The lateral mode shape translations (*y*-direction) are taken from the mode shape computer analysis output at the upstream face node points, and are normalized to a unit translation at the top of the dam (by dividing each translation value by the translation output value for the node at the top upstream corner).

($g\bar{p}/wH$) values are obtained from Figure D-4 for the values of y/H that correspond to the upstream node point elevations shown in Figure D-1. The curve lines for R_w = 1.0 are used since they are so close to the calculated value of R_w = 0.994, and the plots for α = 0.5 and 0.75 are interpolated to give the values of ($g\bar{p}/wH$) for the calculated value of α = 0.69.

M_n = the lumped masses to be added to the upstream node points and are calculated using the following:

$$M_n = [\ (wH/g)\ (H/Hs)^2\ ]\ (C_{tr}/\psi_1)\ (g\bar{p}/wH) \qquad \text{(D-6)}$$

where

$(wH/g)\ (H/Hs)^2 = (0.0624 \times 495/32.2)\ (0.825)^2 = 0.653$

and

$M_n = 0.653\ (C_{tr}/\psi_1)\ (g\bar{p}/wH)$

The initial lumped mass model is then modified by replacing the lumped masses that were added to the upstream nodes with these new lumped mass values thus creating the final added mass model for the MCE high pool condition.

D-6. Effective Damping Factor

Since the dam, foundation, and reservoir respond together as a system to ground motion, the damping contribution of each component must be considered when developing the effective damping factor. As with the equivalent mass system, Chopra's equations and curves for his simplified analysis method may be utilized in the finite element approach. The equation for the effective damping factor is

$$\tilde{\varepsilon}_1 = \frac{1}{R_r}\ \frac{1}{(R_f)^3}\ \varepsilon_1 + \varepsilon_r + \varepsilon_f \qquad \text{(D-13)}$$

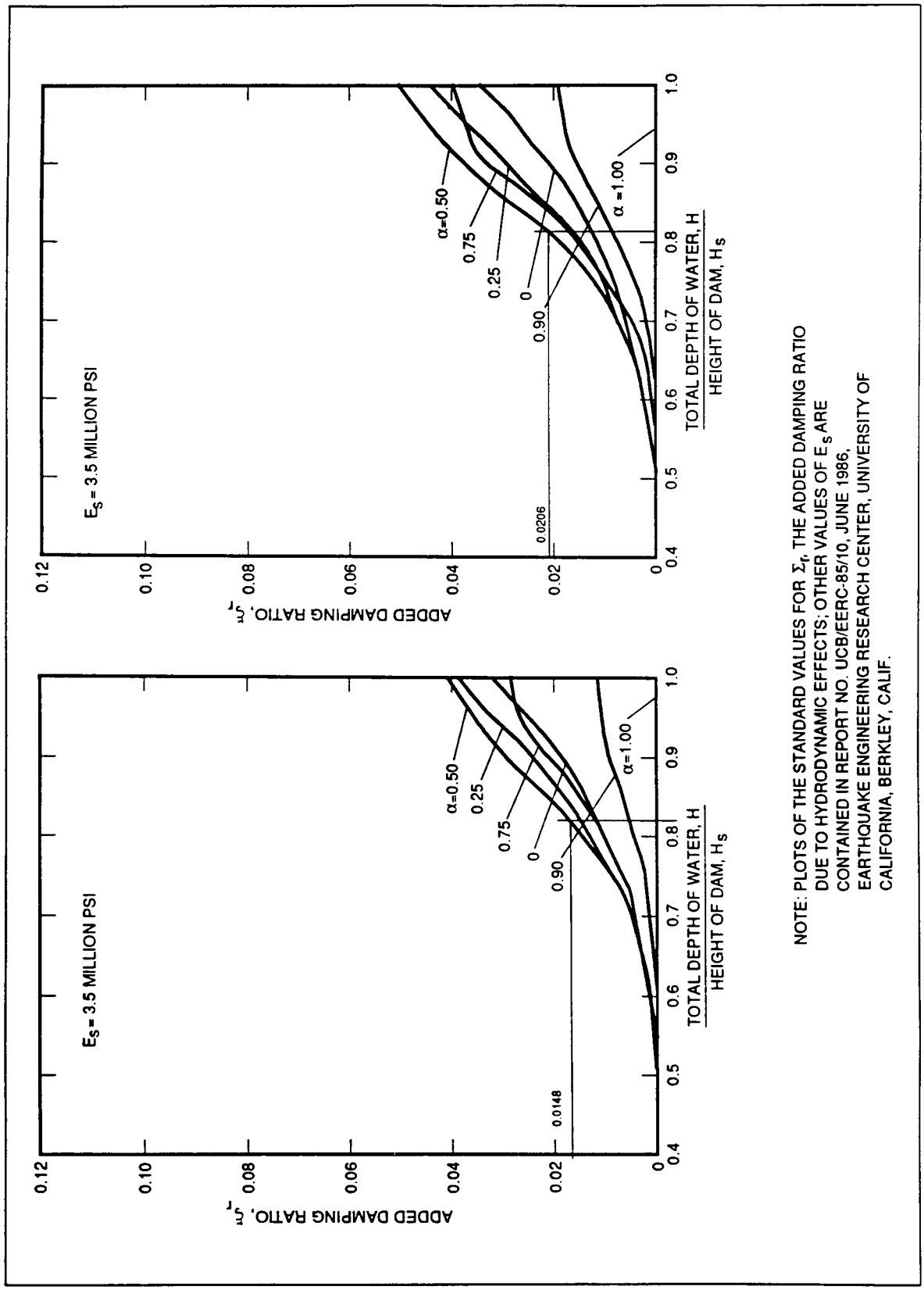

Figure D-5. Values for ε_r, the added damping ratio due to hydrodynamic effects; E_s = 3.5 and 4.0 million psi

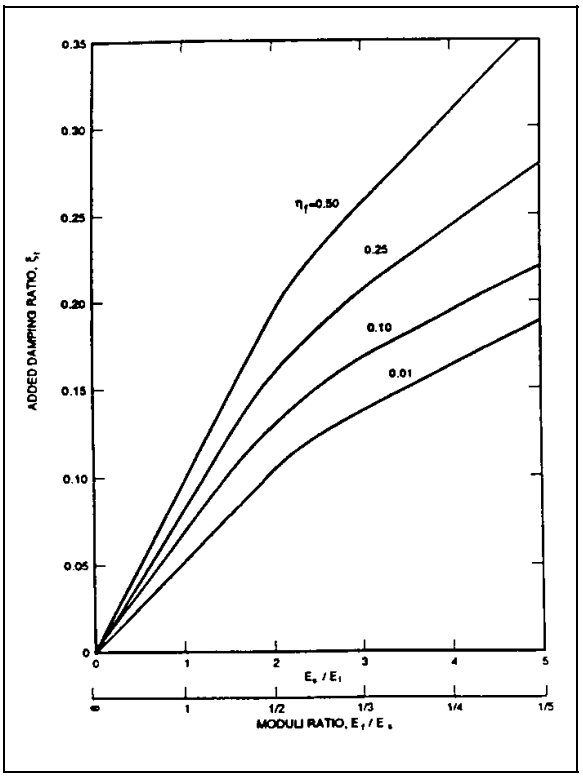

Figure D-6. Values for ε_f , the added damping ratio due to dam-foundation rock interaction

where

$\tilde{\varepsilon}_1$ = the effective damping factor

ε_1 = 5.0% for the OBE

ε_1 = 7.0% for the MCE

ε_r is taken from Figure D-5

ε_f is taken from Figure D-6

and

$$R_f = \tilde{T}_f / T_1 \qquad \text{(D-14)}$$

$$R_r = \tilde{T}_1 / T_f \qquad \text{(D-15)}$$

D-7. Procedure to Determine the Effective Damping Factor

a. Using the final added mass model, perform the modal extraction phase of the dynamic analysis to determine the fundamental resonant period of the dam, $\tilde{T}_1$, on its elastic foundation with reservoir of depth *H*. This is *computer run #4*.

b. Using the value of T_1 from *computer run #1*, $\tilde{T}_f$ from *computer run #2*, and $\tilde{T}_1$ from *computer* run #4, calculate R_f using Equation D-14, and R_r using Equation D-15.

c. Determine the value of ε_r from Figure D-5 interpolating between the appropriate curve lines for the required value of α, and between the appropriate pair of graphs for the required value of E_s. Note that the appropriate value of α, the wave reflection coefficient, and E_s, the seismic modulus of elasticity, were calculated for the example problem in Appendix B.

d. Determine the value of ε_f from Figure D-6. If the constant hysteretic damping factor for the foundation is not known, assume $n_f = 0.10$.

e. Calculate the effective damping factor using Equation D-13.

D-8. Applying Damping Factor Procedure to the Example Problem

The procedure for determining the effective damping factor will be applied to the example problem. The high pool condition associated with the MCE, and the conservation pool (low pool) condition for the MCE will be used to demonstrate the procedure.

T_1 = 0.3882 sec from *computer run #1*

$\tilde{T}_f$ = 0.5188 sec from *computer run #2*

$\tilde{T}_1$ = 0.5575 sec (normal pool for MCE) from *computer run #4*

$\tilde{T}_1$ = 0.5208 sec (low pool for MCE) from *computer run #4*

R_f = $\tilde{T}_f / T_1$ = 0.5188/0.3882 = 1.3364 (Equation D-14)

R_r = $\tilde{T}_1 / T_f$ = 0.5575/0.5188 = 1.075 (normal pool for MCE, Equation D-15)

R_r = $\tilde{T}_1 / T_f$ = 0.5208/0.5188 = 1.003 (low pool for MCE, Equation D-15)

H = 2550 - 1950 = 600 ft

H_s = 2445 - 1950 = 495 ft (normal pool for MCE), and H/H_s = 0.825

H_s = 2220 - 1950 = 270 ft (low pool for MCE), and H/H_s = 0.450

α = 0.69, E_s = 3590 ksi, and E_f = 3500 ksi as calculated in Appendix B

ε_r = 0.0158 (normal pool for MCE) from Figure D-5 for H/H_s = 0.825, interpolating between the α = 0.50 and 0.75 curve lines for the required value of α = 0.69, and also interpolating between the graphs of E_s = 3.5 million psi and 4 million psi for the required value of E_s = 3590 ksi

ε_r = 0.0 (low pool for MCE). When $H/H_s < 0.5$, ε_r = 0.0

ε_f = 0.0703 from Figure D-6 for E_s/E_f = 3590/3500 = 1.025, and an assumed value of n_f = 0.10

ε_1 = 7.0 percent

$\tilde{\varepsilon}_1$ = $(1/1.075)(1/(1.3364)^3)(7.0) + 100(0.0158) + 100(0.0703)$ = 11.34 percent (normal pool for MCE, using Equation D-13)

$\tilde{\varepsilon}_1$ = $(1/1.003)(1/(1.3364)^3)(7.0) + 100(0.0) + 100(0.0703)$ = 9.95 percent (low pool for MCE, using Equation D-13)

D-9. Design Response Spectra

As discussed in Appendix B, the conditions for this example problem require a site-specific design response spectra. However, since this is only for the purpose of demonstrating the finite element method, the standard design response spectra shown in Figure 5-1 and Table 5-1 will be assumed to be the site-specific design response spectra.

a. Normalized design response spectra. The design response spectra normalized to a PGA = 1.0 g is calculated as follows:

$\tilde{T}_1$ = 0.5575 sec for the MCE normal pool

$\tilde{T}_1$ = 0.5208 sec for the MCE low pool

The design response spectra needs to be defined only for values of the period T up to the above values of $\tilde{T}_1$.

β = $\tilde{\varepsilon}_1$ = 11.34% normal pool for MCE

β = $\tilde{\varepsilon}_1$ = 9.95% low pool for MCE

K_2 = 1.466 - 0.2895ln(11.34) = 0.76300 normal pool for MCE

K_2 = 1.466 - 0.2895**ln**(9.95) = 0.80085 low pool for MCE

K_3 = log(2.5 × 0.76300) = 0.28046 normal pool for MCE

K_3 = log(2.5 × 0.80085) = 0.30149 low pool for MCE

S_a = spectral acceleration for period = T

S_a = $10.0^{K_1 K_3}$ for $T < 0.400$

S_a = $K_2 S_{a(5\%)}$ for $T > 0.400$

b. Scaling factors-horizontal component of ground motion. The above normalized design spectra are scaled according to the scaling factors in Table 5-2. The site is located in seismic Zone 3; therefore, the scaling factors for the horizontal component of ground motion = PGA = the following:

OBE: 0.210 g

MCE: 0.550 g

c. Design response spectra for the vertical component of ground motion. In accordance with the requirements of paragraph 5-6, independent vertical component site-specific design response spectra are required for the example problem. However, for demonstration purposes, the standard design response spectra normalized to a PGA = 1.0 g as described above will be assumed to also be the vertical component site-specific design response spectra. The scaling factors for the vertical component of ground motion will be based on Figure 5-3 as follows:

T = period (sec)	$S_{a(5\%)}$ (g's)	K_1	S_a MCE Normal Pool (g's)	S_a MCE Low Pool (g's)
0.002	1.0000	0.00000	1.0000	1.0000
0.010	1.0000	0.00000	1.0000	1.0000
0.020	1.2643	0.25596	1.1797	1.1945
0.040	1.5985	0.51192	1.3918	1.4267
0.060	1.8335	0.66164	1.5331	1.5830
0.080	2.0210	0.76787	1.6419	1.7041
0.100	2.1795	0.85028	1.7317	1.8045
0.120	2.3182	0.97160	1.8728	1.9630
0.150	2.5000	1.00000	1.9075	2.0021
0.400	2.5000	1.00000	1.9075	2.0021
0.450	2.2222		1.6955	1.7796
0.500	2.0000		1.5260	1.6017
0.550	1.8182		1.3873	1.4561
0.600	1.6667		1.2717	1.3348

R = source to site distance = 35 km (see Appendix B)

$\tilde{T}_1$ = 0.5577 sec for the MCE normal pool

$\tilde{T}_1$ = 0.5208 sec for the MCE low pool

Based on these data, the ratio of (PGA of vertical component)/(PGA of horizontal component) = 0.5. Therefore, the scaling factors for the vertical component of ground motion are

OBE = 0.5 × 0.210 = 0.105 g

MCE = 0.5 × 0.550 = 0.275 g

D-10. Response to Ground Motion

The procedure has now progressed to the point where it is possible to determine the dynamic response to the ground motion associated with the design earthquakes (the OBE and the MCE). For demonstration purposes the example problem is considering only the MCE; however, determining the response for the OBE would follow the same procedure. A summary of the work steps completed thus far is as follows:

Step 1. The computer model of the dam/foundation system has been formulated.

Step 2. Two critical earthquake load cases for the MCE have been identified, one combining the design earthquake with the normal pool condition which is considered reasonable at the time of the MCE event, and the second load case combining the design earthquake with the lowest possible pool at the time of the MCE event (the conservation pool).

Step 3. The hydrodynamic effects of these two pool elevations have been determined in terms of added lumped mass attached to the upstream face at appropriate node points. Thus the single computer model of step 1 becomes two added mass computer models, one for the normal pool load case and one for the low pool case.

Step 4. The effective damping factors for the combined dam/foundation/reservoir system have been determined for both the normal pool and low pool load cases.

Step 5. The design response spectra have been developed for the two effective damping factors.

a. Modal analysis.

(1) The next step in the procedure is to perform the final, complete modal analysis. This computer run will extract all the modes which will make a

significant contribution to the response. This requires some judgment, but 10 modes normally suffice for the typical gravity dam cross section like that of the example problem. Therefore, the first 10 modes will be extracted and the modal participation factors for these 10 modes will be examined to ensure adequate precision in the response spectrum analysis to follow.

(2) The modal participation factors are a function of the mode shape and the mass distribution. They are not influenced at all by ground motion as expressed by the response spectrum. They only give an indication of the energy absorbing capability of a particular mode. Along with the participation factors, the response spectrum also has an obvious effect on the response (deflection, stress .... etc.). Thus, the contribution for a given mode is not directly proportional to the participation factor. However, the participation factor can be used for the purpose of judging a reasonable cutoff point where higher modes would not contribute significantly to the total response based on a reasonable precision for the analysis.

(3) The modal participation factors for the first 10 modes produced by both the added mass computer models are given in the accompanying tabulation.

(4) The tabulations of modal participation factors indicate that the fundamental mode for the horizontal (*y*-direction) component of ground motion is mode 1. It is also apparent that for the horizontal component of ground motion, mode 7 through mode 10 have participation factors no greater than 1/14th of the participation factor for mode 1. Therefore, it is judged that modes 1 through 6 would have been adequate for the analysis for the horizontal component of ground motion. The fundamental mode for the vertical (*z*-direction) component of ground motion is mode 2. For this component, mode 6 through mode 10 have participation factors no greater than 1/16th of the participation factor for mode 2. Therefore, it is judged that modes 1 through 5 would have been adequate to determine the response for the vertical component of ground motion. On this basis, it is concluded that for the example problem, the

MCE Normal Pool Load Case
1** Modal Participation Factors**

Mode	X-Direction	Y-Direction	Z-Direction	period (sec)
1	0.0000E+00	2.4886E+01	4.7916E+00	5.5753E-01
2	0.0000E+00	1.1126E+01	-2.4501E+01	2.8220E-01
3	0.0000E+00	-1.2864E+01	-1.0706E+01	2.4083E-01
4	0.0000E+00	-6.8721E+00	-2.0829E+00	1.4334E-01
5	0.0000E+00	8.3296E-01	4.3875E+00	1.0627E-01
6	0.0000E+00	3.2880E+00	-3.8116E-01	9.7209E-02
7	0.0000E+00	-1.5844E+00	1.4926E+00	8.9524E-02
8	0.0000E+00	-1.3661E+00	9.1764E-02	8.0562E-02
9	0.0000E+00	1.7230E+00	-2.4378E-02	7.6114E-02
10	0.0000E+00	-9.1725E-01	1.1421E-01	7.0581E-02

MCE Low Pool Load Case
1** Modal Participation Factors**

Mode	X-Direction	Y-Direction	Z-Direction	period (sec)
1	0.0000E+00	2.2133E+01	5.4826E+00	5.2080E-01
2	0.0000E+00	9.0977E+00	-2.5568E+01	2.7845E-01
3	0.0000E+00	1.3024E+00	7.4132E+00	2.2800E-01
4	0.0000E+00	-6.4719E+00	-2.5863E+00	1.3591E-01
5	0.0000E+00	2.8372E-01	-4.3314E+00	1.0239E-01
6	0.0000E+00	3.3446E+00	-5.1985E-01	9.1338E-02
7	0.0000E+00	-5.1590E-02	-4.2117E-01	7.9362E-02
8	0.0000E+00	-7.3791E-01	-1.9763E-01	7.1327E-02
9	0.0000E+00	-1.5412E+00	-9.8779E-01	6.4530E-02
10	0.0000E+00	9.7924E-01	-1.3636E+00	6.2772E-02

response spectrum analysis using the first 10 modes of vibration for both load cases will produce the dynamic response well within the required precision.

(5) Figure D-7 shows the results of the modal analysis in the form of the mode shapes for the first six modes which were extracted from the equivalent mass system model for the normal pool. The low pool mode shapes are similar to these.

b. Response spectrum analysis.

(1) With the significant mode shapes and frequencies extracted, the design response spectrum developed in paragraph D-9 is introduced into the dynamic analysis. For each significant mode, the modal analysis produced the normalized mode shape, the natural period or frequency, and the participation factor for each ground motion component direction. The spectral ordinate corresponding to the period or frequency of each mode is the only additional parameter required to determine the maximum response for each mode for each ground motion component direction. The procedure is simple. A mode coefficient is calculated as a function of the participation factor and the spectral ordinate, and the maximum modal response, in terms of the deflected shape, is simply the mode coefficient times the normalized mode shape. The maximum modal stresses are then computed once the displaced shape is known.

(2) For each mode and for each ground motion component direction, there is a complete set of stresses. Therefore, the example problem has 20 complete sets of maximum modal stresses for each earthquake load case. The final phase of the dynamic analysis is to combine these 20 sets of stresses into a single set of stresses representing the maximum dynamic response to the design earthquake for that earthquake load case. This phase of analysis can be subdivided into two steps as follows:

Step 1. Combine each set of 10 maximum modal stresses to produce the maximum component response for each of the two ground motion component directions.

Step 2. Combine the two maximum component responses for each of the two ground motion component directions to give the final maximum dynamic response.

(3) For the example problem, paragraph 7-7*e* requires that the maximum modal stresses (step 1 above) be combined using the complete quadratic combination (CQC) method. Unfortunately, the ALGOR Finite Element program does not provide the CQC option; however, it does provide the ten percent method (TPM) discussed in paragraph 7-7*d*. Similar to the CQC, the TPM will give additional accounting to modes with nearly the same frequencies. It is noted from the above tables, the first 5 or 6 modal frequencies are well separated, so it is unlikely that there would be significant difference in the results produced by CQC or TPM for this example problem. Therefore, each set of 10 maximum modal stresses will be combined by the TPM to produce the maximum component response for the Y-direction ground motion component and the Z-direction ground motion component.

(4) Referring to paragraph 7-8*e*, the maximum component responses are to be combined by the square root of the sum of the squares method (SRSS) to produce the final maximum dynamic response.

D-11. Results of the Response Spectra Dynamic Analyses

a. As discussed in Chapters 4 and 5 of this EP, an acceptable response to the design earthquakes is based on satisfying allowable tensile stress criteria to prevent or control the extent of concrete cracking. Two different allowable tensile stresses were established, one for the parent RCC, and a lesser allowable for the lift joints. It is also noted that there are two allowables for the OBE, and two greater allowables for the MCE.

b. Based on the acceptance criteria stated above, it is necessary to determine the maximum principal tensile stress at critical node points of the computer model to determine if the design satisfies the allowable tensile stress for the parent RCC. It should be noted that the response spectrum analysis first produces the maximum modal stresses that occur at the node points, and these stresses are broken down into their component stresses in the global coordinate system. The ALGOR computer program uses these component stresses for each mode to calculate the principal tensile stress for that mode (at each node

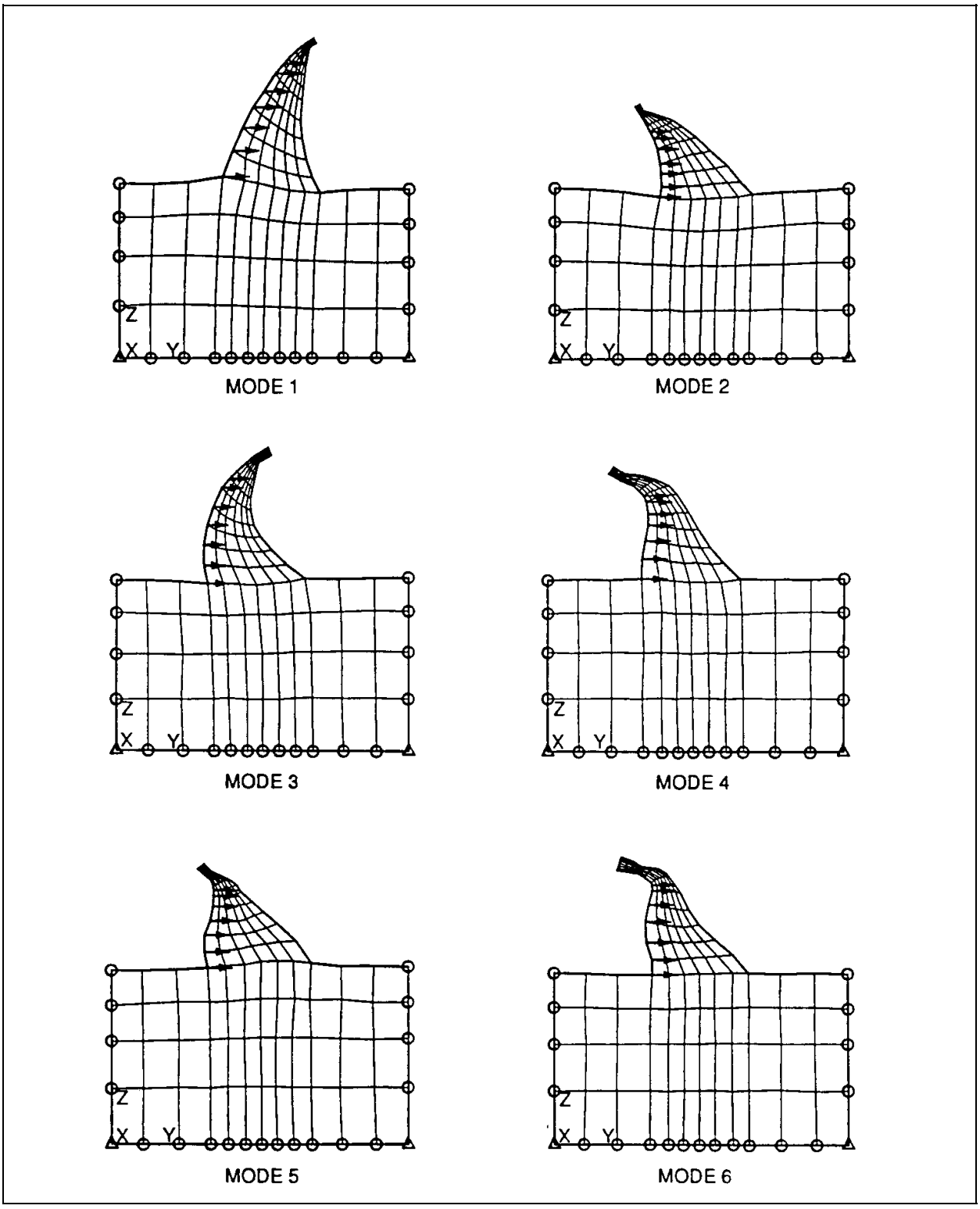

Figure D-7. Results of modal analysis-mode shapes 1 through 6 from composite finite element-equivalent mass system model for the MCE normal pool load case

point), and it then combines these individual mode principal tensile stresses by the requested modal combination method (the 10 percent method was used for the example problem) to produce the maximum principal tensile stress at each node. However, the orientation (or direction) of the principal stress vector is different for each mode, so the combined maximum principal tensile stress is not theoretically correct, but in most instances it can be considered to be a reasonably conservative estimate. In contrast to this method, other computer programs will first combine the component stresses for each mode using the requested modal combination method, and then calculate the principal tensile stress from the combined component stresses. The problem with this method is that the signs of the component stresses are lost in the combination process because all of the combination methods involve taking square roots of the sums of the squares. Again, the maximum principal tensile stress calculated from the combined (and always nonnegative) component stresses is not theoretically correct, but in most instances it produces a reasonably conservative estimate.

c. Based on the acceptance criteria stated earlier, it is also necessary to determine the maximum tensile stress normal to the plane of the horizontal lift joints to determine if the design satisfies the allowable tensile stress for the lift joints. For the computer models used in the dynamic analyses, this represents the component stress vector in the global-Z direction. It is noted that the problems associated with the principal tensile stress calculation are not inherent in combining the Z-direction component stress vectors for each of the modes using the required modal combination method. Thus, the combined Z-direction component stress vector at each node point correctly represents the maximum tensile stress normal to the lift joint at that node.

d. The maximum principal tensile stresses occur near the upstream and downstream faces of the dam in much the same manner as the maximum stresses in a beam in flexure occur at the extreme fibers of the cross section. It is also noted that the direction of the maximum principal tensile stresses near the upstream and downstream faces, for a typical dam cross section, is approximately parallel to the upstream and downstream faces, respectively. Therefore, the difference between the maximum principal tensile stress at the typically near vertical upstream face and the maximum tensile stress normal to the lift joints at the upstream face is small. Thus, the stresses normal to the lift joints will govern along the upstream face since the allowable tensile stress normal to the lift joints is considerably less than the allowable tensile stress for the parent concrete. Figure D-8 presents graphically the stress contours of the maximum tensile stresses normal to the lift joints for both MCE load cases. It is noted that these results represent only the dynamic response to the ground motion shaking. Static stresses such as the dead load weight of the dam or the hydrostatic load acting against the upstream face are not included in these results.

e. Since the direction of the maximum principal tensile stresses near the sloping downstream face is approximately parallel to the face, it is more difficult to predict whether the tensile stresses normal to the lift joints or the principal tensile stresses in the parent concrete will be critical. Therefore, both sets of stresses must be determined along the downstream face. Figure D-9 shows graphically the stress contours of the maximum principal tensile stresses that will occur near the downstream face of the dam for both MCE load cases. Note that these maximum principal tensile stresses occur during that part of the oscillation cycle when the top of the dam is translating upstream. It is noted that these results represent only the dynamic response to the ground motion shaking. Static stresses such as the dead load weight of the dam or the hydrostatic load acting against the upstream face are not included in these results.

D-12. Static Analyses

a. To complete the dynamic analyses for each earthquake load case, it is necessary to determine the static state condition of the RCC dam at the time of the design earthquake event. For the design example the static loads acting on the dam at the time of the earthquake are:

(1) Dead load weight of the RCC.

(2) Hydrostatic pressure of the reservoir against the upstream face of the dam.

b. By activating the minus Z-direction gravitational element load option in the ALGOR computer program, the dead weight of the elements is internally computed and distributed to the element corner node points. The hydrostatic loading was calculated as concentrated Y-direction forces acting on the

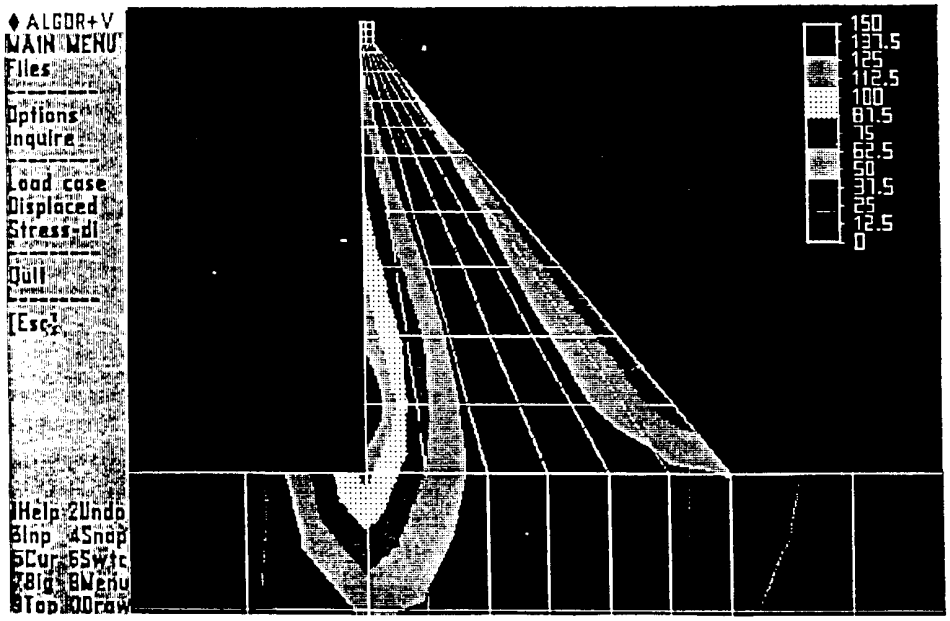

Maximum Tensile Stress Normal to Lift Joints (KSF) - MCE Normal Pool Load Case - for Full Oscillation Cycle

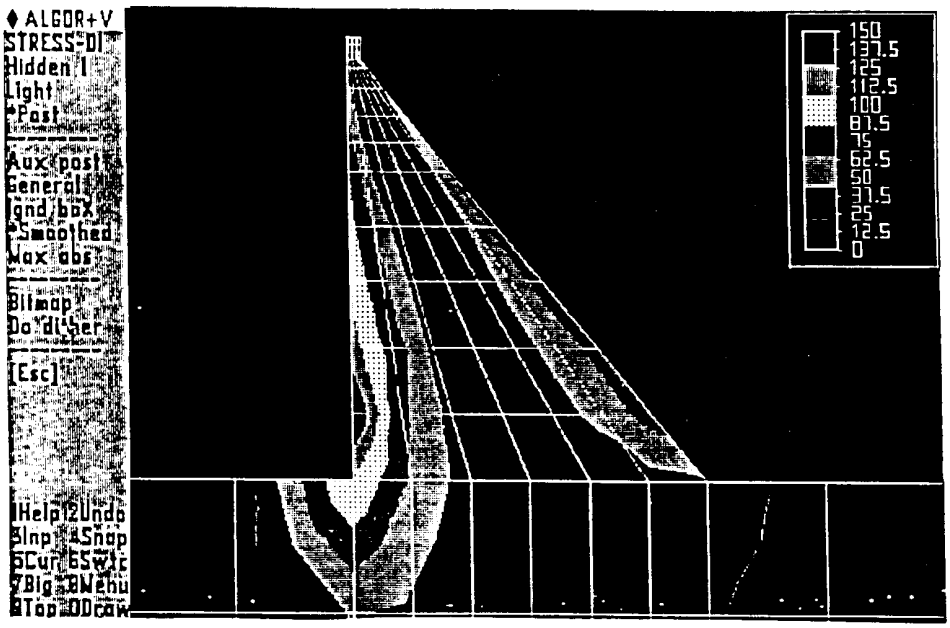

Maximum Tensile Stress Normal to Lift Joints (KSF) - MCE Low Pool Load Case - for Full Oscillation Cycle

Figure D-8. Results of response spectrum analysis-dynamic response to combined horizontal and vertical components of ground motion for MCE load cases--expressed as maximum tensile stresses normal to the lift joints

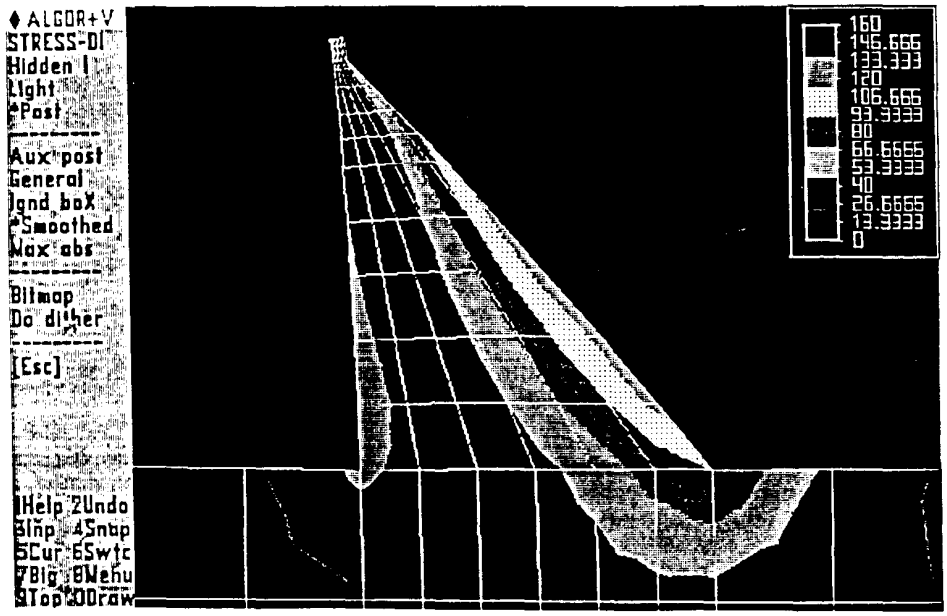

Maximum Principal Tensile Stress (KSF) - MCE Normal Pool Load Case for Upstream Translation Part of Oscillation Cycle Only

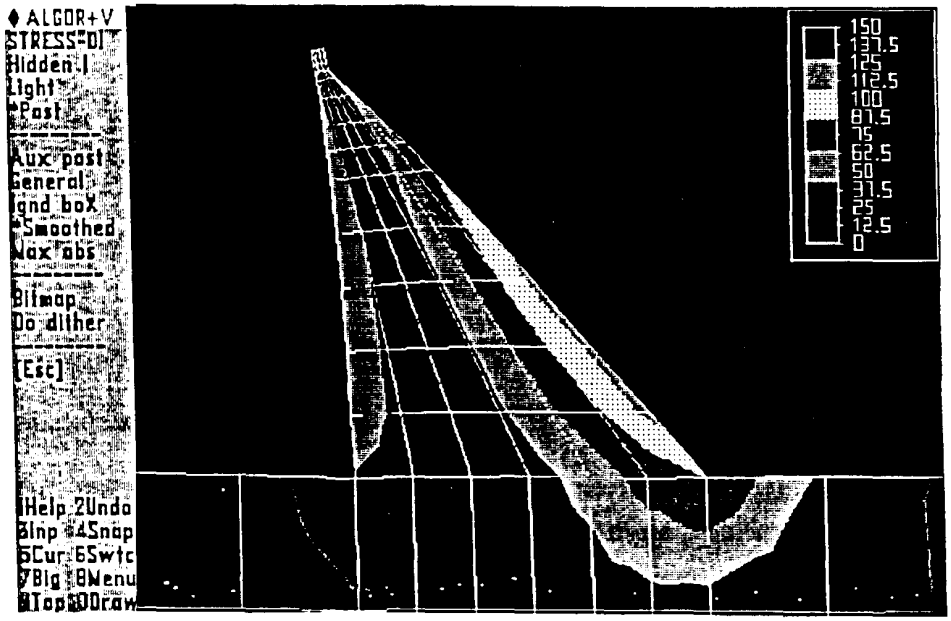

Maximum Principal Tensile Stress (KSF) - MCE Low Pool Load Case for Upstream Translation Part of Oscillation Cycle Only

Figure D-9. Results of response spectrum analysis-dynamic response to combined horizontal and vertical components of ground motion for MCE load cases--expressed as maximum principal tensile stresses.

appropriate upstream face node points. Figure D-10 shows the calculations for the hydrostatic load.

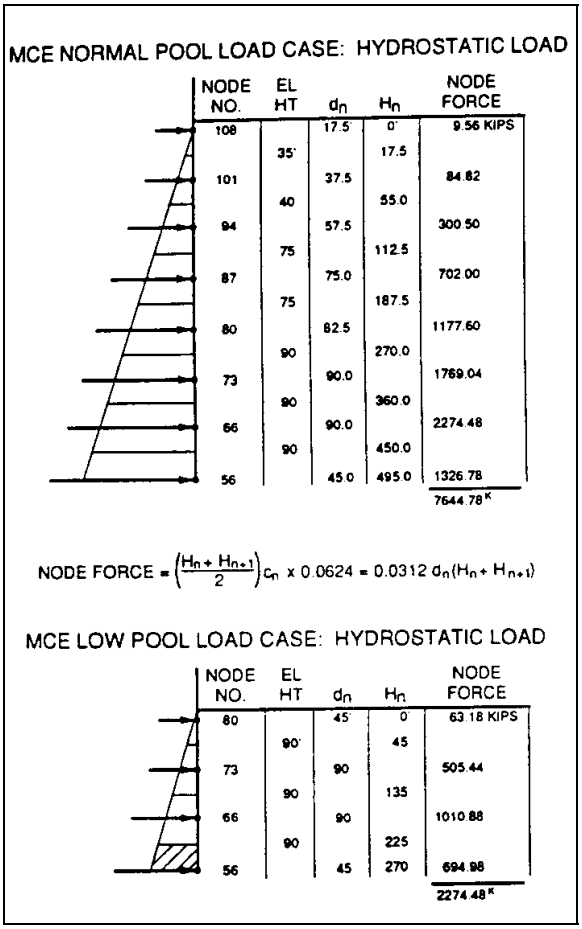

Figure D-10. Computation sheet to determine the forces to apply to the upstream node points to represent the hydrostatic pressure of the pool

c. With these loads applied to the computer model, a static finite element analysis was executed to determine the static stresses. The static stresses normal to the lift joints for both the high pool and low pool conditions are shown graphically in Figure D-11, and the principal static stresses are shown in Figure D-12.

D-13. Allowable Tensile Stress

Appendix B established the direct tensile strength of the basic RCC mix to be:

f'_t = 290 psi (for the parent concrete)

f'_t = 205 psi (for the lift joints)

Because of the high strain rates associated with a seismic event, the dynamic tensile strength is greater than the direct tensile strength obtained from the lab tests:

DTS = 1.5 f'_t = 1.5 x 290 = 435 psi (for the parent concrete)

DTS = 1.5 f'_t = 1.5 x 205 = 307 psi (for the lift joints)

In accordance with paragraph 4-2*c*, the allowable tensile stress for a new RCC dam in seismic zone 3 for the OBE load condition is:

$f_{t(allowable)}$ = 0.90 × 435 = 392 psi (for the parent concrete)

$f_{t(allowable)}$ = 0.90 × 307 = 276 psi (for the lift joints)

and in accordance wih paragraph 4-3*c*, the allowable tensile stress for the MCE load condition is:

$f_{t(allowable)}$ = 1.33 × 435 = 579 psi (for the parent concrete)

$f_{t(allowable)}$ = 1.33 × 307 = 408 psi (for the lift joints)

D-14. Critical Tensile Stresses for the Earthquake Load Cases

a. The critical tensile stresses are obtained by adding the dynamic response tensile stresses with the static stresses at the node points along the upstream and downstream faces of the dam. These tensile stresses are then compared to the allowable tensile stresses to determine the acceptability of the design.

b. The following tabulations show the critical tensile stresses for the MCE. Also shown in bold print are the locations where the critical tensile stress exceeds the allowable tensile stress along with the percent overstress for these locations.

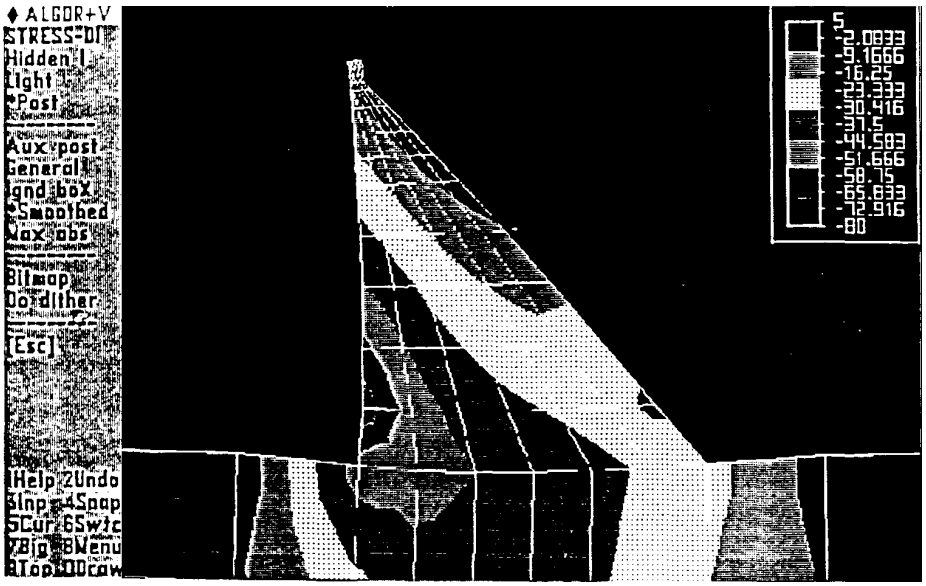

Static Stresses Normal to the Lift Joints (KSF, tension is +) - MCE Normal Pool Load Case

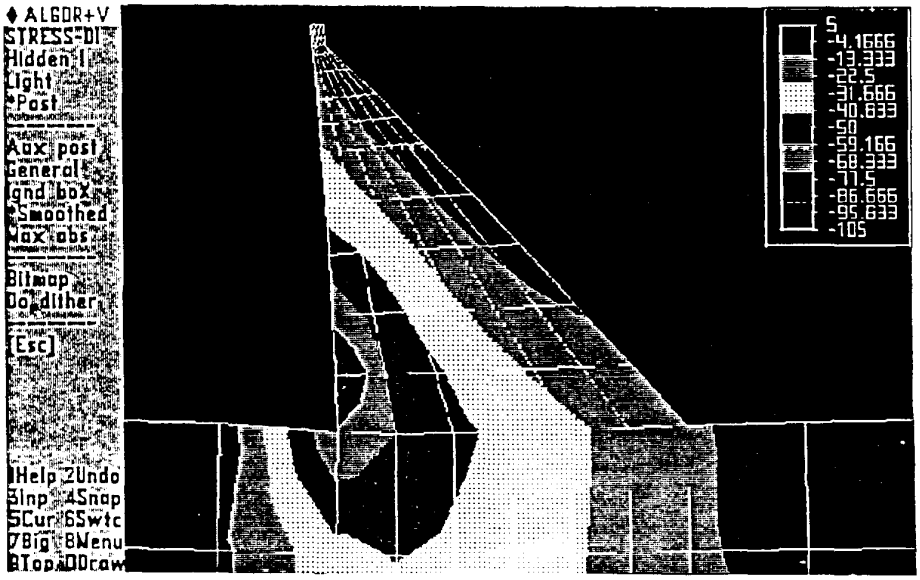

Static Stresses Normal to the Lift Joints (KSF, tension is +), - MCE Low Pool Load Case

Figure D-11. Static stresses normal to the lift joints - MCE load cases

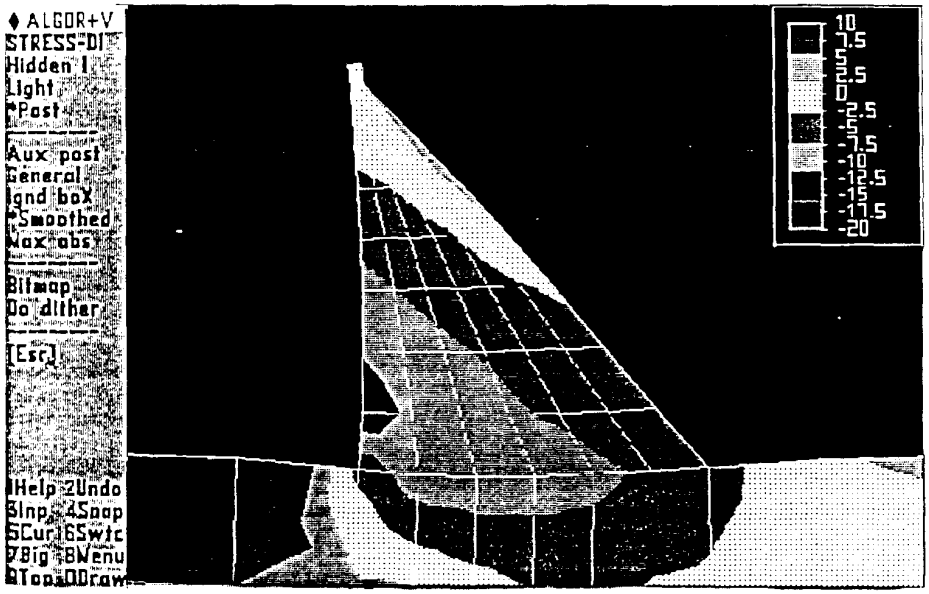

Principal Static Stresses (KSF, tension is +) - MCE Normal Pool Load Case

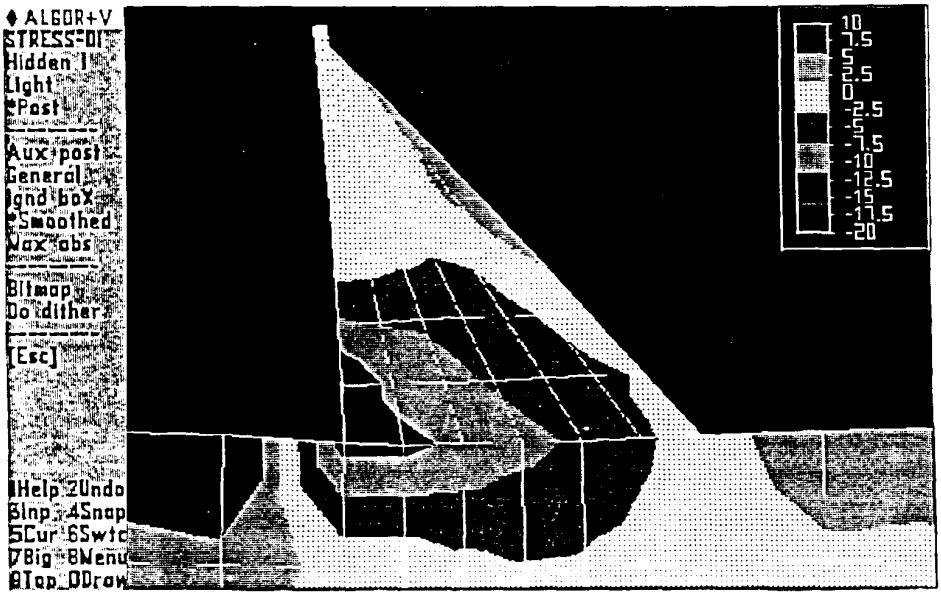

Principal Static Stresses (KSF, tension is +) - MCE Low Pool Load Case

Figure D-12. Principal static stresses - MCE load cases

MCE Normal Pool Load Case:
Critical Tensile Stresses Normal to the Lift Joints at the Upstream Face

Node No.	Stress Normal to the Lift Joint (ksf, tension is +)		Critical Tensile Stress (psi)	Percent Overstressed
	Dynamic Response	Static Stress		
143	12.52	-1.55	76	-----
129	53.23	-5.32	333	-----
115	57.06	-11.40	317	-----
108	65.15	-15.97	342	-----
101	76.27	-21.66	379	-----
94	84.29	-27.39	395	-----
87	95.30	-35.14	**418**	**2**
80	108.1	-45.25	**436**	**7**
73	122.2	-59.42	**436**	**7**
66	161.9	-78.37	**580**	**42**
56	113.8	-49.16	**449**	**10**

MCE Low Pool Load Case:
Critical Tensile Stresses Normal to the Lift Joints at the Upstream Face

Node No.	Stress Normal to the Lift Joint (ksf, tension is +)		Critical Tensile Stress (psi)	Percent Overstressed
	Dynamic Response	Static Stress		
143	13.35	-1.55	82	-----
129	56.84	-5.31	358	-----
115	59.98	-11.55	336	-----
108	68.03	-16.50	358	-----
101	80.83	-22.25	407	-----
94	88.26	-28.60	**414**	**1**
87	96.68	-37.15	**413**	**1**
80	106.8	-49.09	401	-----
73	118.3	-68.30	347	-----
66	154.8	-101.3	372	-----
56	108.3	-71.84	253	-----

MCE Normal Pool Load Case:
Critical Tensile Stresses Normal to the Lift Joints at the Downstream Face

Node No.	Stress Normal to the Lift Joint (ksf, tension is +)		Critical Tensile Stress (psi)	Percent Over-stressed
	Dynamic Response	Static Stress		
149	7.82	-1.53	44	-----
135	76.70	-2.77	**513**	**26**
121	39.77	0.16	277	-----
114	49.12	0.54	345	-----
107	59.55	0.19	**415**	**2**
100	67.83	-2.28	**455**	**12**
93	75.12	-8.04	**466**	**14**
86	79.57	-16.28	**440**	**8**
79	77.45	-25.06	364	-----
72	79.95	-33.68	321	-----
62	43.39	-24.10	134	-----

MCE Low Pool Load Case:
Critical Tensile Stresses Normal to the Lift Joints at the Downstream Face

Node No.	Stress Normal to the Lift Joint (ksf, tension is +)		Critical Tensile Stress (psi)	Percent Over-stressed
	Dynamic Response	Static Stress		
149	8.56	-1.53	49	-----
135	82.49	-2.72	**554**	**26**
121	42.66	-0.02	296	-----
114	51.86	0.06	361	-----
107	61.14	0.64	**429**	**5**
100	67.41	1.21	**477**	**17**
93	72.58	0.28	**506**	**24**
86	75.68	-3.44	**502**	**23**
79	73.05	-9.58	**441**	**8**
72	74.98	-15.40	**414**	**1**
62	40.63	-13.79	186	-----

MCE Normal Pool Load Case:
Critical Principal Tensile Stresses at the Downstream Face

Node No.	Principal Tensile Stress (ksf, tension is +)		Critical Tensile Stress (psi)	Percent Over-stressed
	Dynamic Response	Static Stress		
149	7.82	-1.53	44	-----
135	76.70	-2.77	513	-----
121	60.24	-1.75	406	-----
114	74.68	-2.09	504	-----
107	89.66	-2.90	**602**	**4**
100	103.7	-6.19	**677**	**17**
93	120.8	-13.69	**744**	**28**
86	126.0	-26.38	**692**	**20**
79	121.4	-40.07	564	-----
72	121.7	-52.48	481	-----
62	91.63	-46.83	311	-----

MCE Low Pool Load Case:
Critical Principal Tensile Stresses at the Downstream Face

Node No.	Principal Tensile Stress (ksf, tension is +)		Critical Tensile Stress (psi)	Percent Over-stressed
	Dynamic Response	Static Stress		
149	8.56	-1.53	49	-----
135	82.49	-2.72	554	-----
121	48.86	-1.84	326	-----
114	60.06	-1.70	405	-----
107	71.20	-1.36	485	-----
100	84.48	-1.89	574	-----
93	103.4	-4.51	**687**	**19**
86	112.2	-8.29	**722**	**25**
79	111.8	-14.80	**674**	**16**
72	113.5	-23.74	**623**	**8**
62	85.91	-24.10	429	-----

D-15. Conclusions and Recommendations

a. The critical tensile stresses shown in paragraph D-14*b* indicate certain areas or zones where superior RCC mixes are required so the RCC dam can be made to satisfy the earthquake resistant design criteria for new dams as established by this EP. Figure D-13 shows the zones that require RCC mixes with higher tensile capacity than the basic RCC mix with f'_c of 3,000 psi.

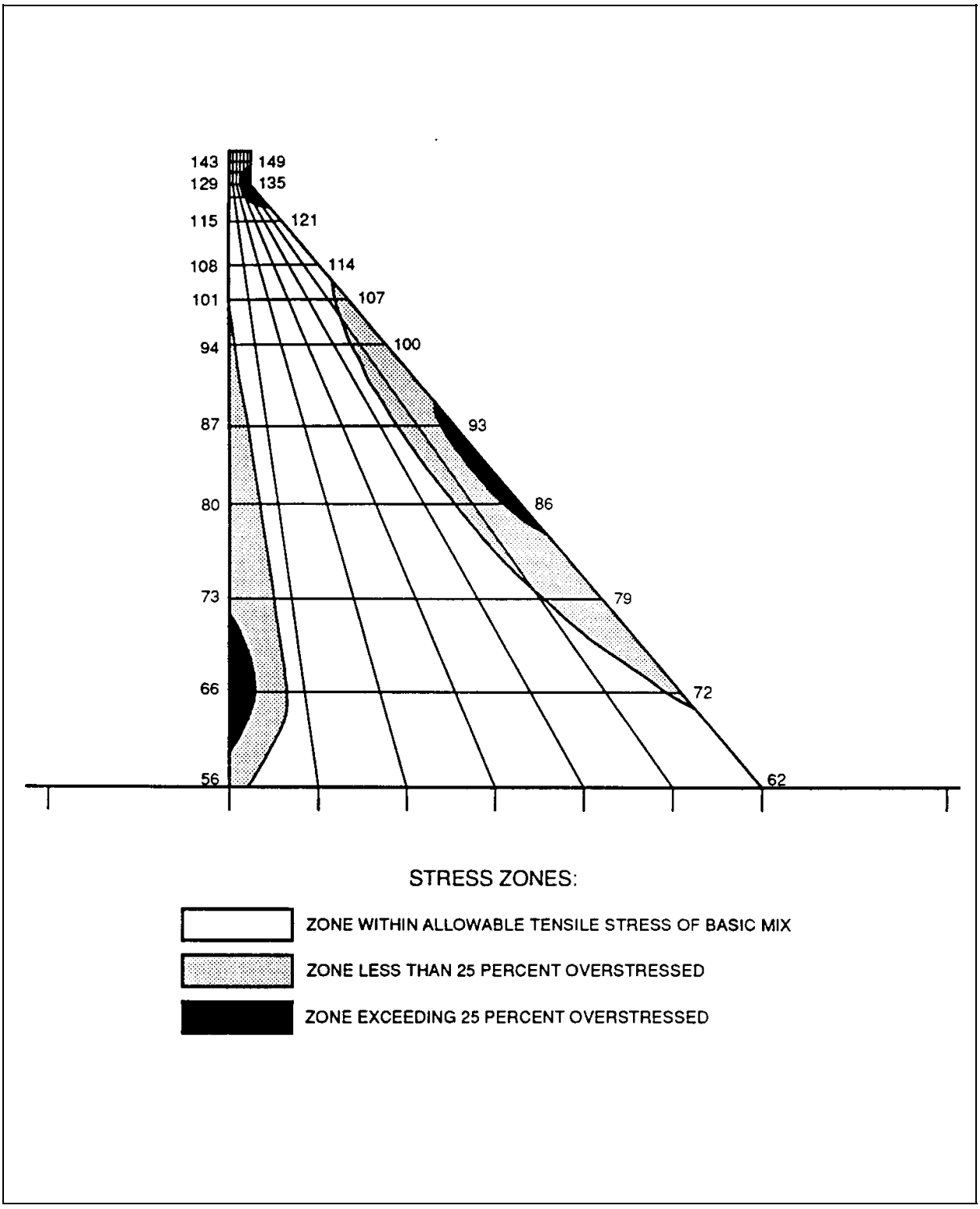

Figure D-13. Zones exceeding the allowable tensile stress for the basic RCC mix

b. The final step of the earthquake resistant design procedure would be to develop some higher strength RCC mix designs. Once the lab and field placement tests have been completed for these superior mixes, and their material properties established, the computer model shown in Figures D-1 and D-2 would be adjusted to reflect the zones of superior RCC. The dynamic analysis would be performed with the new computer model following the same procedure demonstrated above. If continued design upgrade attempts fail to meet the acceptability requirements, a more refined time-history analysis may be used to gain more insight regarding the dynamic response.

D-16. Comparing Response From Different Analysis Methods

a. Differences and similarities of attributes. In this appendix the design example problem was analyzed with the composite finite element-equivalent mass system method using a general purpose finite element program as discussed in paragraph 8-2*c*. In Appendix C, the same design example problem was analyzed using Chopra's simplified method as described in paragraph 8-2*a*. A comparison will now be made of the results produced by the two different methods of analysis. The earthquake loads for the normal reservoir condition will be used for the comparison. Referring to the attributes of dynamic analysis methods described in paragraph 8-1, the attribute differences and similarities for the two methods are:

(1) Material behavior - both methods used linear elastic material behavior. Material properties are identical for the two methods.

(2) Design earthquake definition - both methods used a design response spectrum to define the free field ground motion for the design earthquakes. Both methods anchored the design spectrum using the same PGA of 0.550 g.

(a) Differences in effective damping affect the response. The composite finite element method used a damping factor of 11.34 percent, and Chopra's method used a damping factor of 12.33 percent. Since damping in the response spectrum analysis is reflected in the spectral shape, the slightly higher damping in the Chopra analysis results in a slightly smaller response compared to the response produced by the composite finite element method.

(b) Another parameter associated with defining the design earthquake is whether both horizontal and vertical components of ground motion are specified or if only the horizontal component is specified. The composite finite element method used both horizontal and vertical components of ground motion. Chopra's simplified method is capable of only analyzing for the horizontal component of ground motion. As discussed in paragraph 7-8, the vertical component of ground motion can have significant effect on the response.

(3) Dimensional representation of project conditions - both methods used 2-D representation. The same 2-D cross section of the critical element of the dam was used in both analyses.

(4) Model configuration - the composite finite element method uses discrete finite elements to model the dam and a block of the foundation, and added mass to represent the hydrodynamic effects. Dynamic response is obtained by eigen solution of the stiffness and mass matrices. This type of equivalent mass system model is discussed in paragraph 8-1*d*(3). Chopra's simplified method uses a "standardized model" as discussed in paragraph 8-1*d*(1). With a "standardized model," dynamic loads are characterized by equivalent static load so that the stresses can be determined by either simple beam bending theory or by applying the equivalent static load to a finite element model of the dam fixed at the base. Appendix C utilized the latter method to determine the stresses because it provides a more realistic distribution of stress.

(a) Although the "standardized model" accounts for the foundation effects by increasing the fundamental period and the damping factor, its use of a simplified standard mode shape, based solely on horizontal translations relative to the fixed base, only approximates the 2-D deformations within the dam in response to the inertial effects of the ground motion. For example, the rigid body translation and rotational effect of the dam on its flexible foundation are not incorporated in the simplified approach. Therefore, the stress pattern produced by the two different analysis methods can be quite different at some locations in the dam.

(b) Another difference that can be considered as a part of the model configuration is the method used to combine the modal responses. In the composite finite element method the maximum modal responses

were combined by the Ten Percent Method (TPM) discussed in paragraph 7-7, where the modal responses for Chopra's simplified method were combined by square root of the sum of the squares method (SRSS). The TPM gives some additional accounting for modes of nearly the same frequency, and thus produces greater combined response.

b. Comparing common parameters. The following table compares the values of the parameters common to both methods of analysis:

Table of Common Parameters - MCE Normal Pool Load Case

Parameter	Chopra's Simplified Method	Composite Finite Element Method
T_1	0.443 sec	0.388 sec
R_r	1.100	1.075
R_w	0.85	1.00
R_f	1.190	1.336
$\tilde{T}_1$	0.585 sec	0.558 sec
β	12.33%	11.34%
$\tilde{S}_a$	22.37 ft/sec^2	22.26 ft/sec^2

c. Method for comparing results. To gain an understanding of the causes of the difference in the dynamic stress response as produced by the two analysis methods, several parameters will be adjusted to determine to what extent they contribute to the difference in stress response.

(1) The composite finite element analysis represents the more refined of the two analysis methods since its attributes and their associated parameters more closely represent the design conditions of the example problem. To determine how refinement of these parameters contributed to the difference in response, they will be set to the same value as was used in the simplified analysis. Adjustment of parameters is easy because of the flexible attribute capabilities of the composite finite element method as discussed in paragraph 8-2*c*(1).

(2) It is more difficult to adjust parameters in Chopra's simplified method because this method has primarily fixed attributes. However, one adjustment that is possible consists of placing the equivalent lateral static load on the same composite dam-foundation finite element model as was used in the more refined composite finite element analysis method. This will produce a more realistic stress pattern, particularly near the dam foundation interface because it allows for deformation of the foundation and associated redistribution of stresses from that of the fixed condition of the dam base as described in Appendix C.

(3) To help evaluate the difference in response of the two methods, a single parameter will be adjusted and an analysis made to determine it's effect on the stresses. A description of the adjustment of parameters follows. Note that Analysis #1 is the most refined analysis progressing sequentially to Analysis #6 which is the least refined analysis.

ANALYSIS #1: The composite finite element-equivalent mass system analysis as presented in this appendix with no modifications.

ANALYSIS #2: Analysis #1 modified by deleting the vertical component of ground motion.

ANALYSIS #3: Analysis #2 modified by using SRSS to combine the maximum modal responses.

ANALYSIS #4: Analysis #3 modified by using a 12.33 percent effective damping factor.

ANALYSIS #5: Chopra's simplified method as presented in Appendix C, but the stresses are determined by applying the equivalent static load on a composite finite element model of the dam-foundation as discussed above in paragraph D-16*c*(2).

ANALYSIS #6: Chopra's simplified method as presented in Appendix C with no modifications.

MCE Normal Pool Load Case:
Critical Tensile Stresses Normal to the Lift Joints at the Upstream Face

	Critical Tensile Stress (psi)					
	Composite Finite Element Method				Chopra's Method	
Node No.	Analysis #1	Analysis #2	Analysis #3	Analysis #4	Analysis #5	Analysis #6
143	76	72	71	68	196	196
129	333	315	313	302	262	262
115	317	293	291	279	198	198
108	342	312	310	297	186	187
101	379	343	341	326	205	205
94	395	354	353	336	206	204
87	**418**	371	370	351	210	205
80	**436**	385	385	363	218	224
73	**436**	385	385	360	219	281
66	**580**	**535**	**534**	**500**	316	**494**
56	**449**	**428**	**428**	404	285	247

MCE Normal Pool Load Case:
Critical Tensile Stresses Normal to the Lift Joints at the Downstream Face

	Critical Tensile Stress (psi)					
	Composite Finite Element Method				Chopra's Method	
Node No.	Analysis #1	Analysis #2	Analysis #3	Analysis #4	Analysis #5	Analysis #6
149	44	42	41	40	94	94
135	**513**	**493**	**490**	**474**	**527**	**527**
121	277	265	264	255	239	239
114	345	330	329	319	305	305
107	**415**	398	398	385	378	377
100	**455**	**440**	**439**	**425**	**422**	**418**
93	**466**	**453**	**453**	**437**	**430**	**427**
86	**440**	**431**	**431**	**414**	395	398
79	364	357	357	340	310	307
72	321	311	311	294	253	188
62	134	125	125	115	93	44

MCE Normal Pool Load Case:
Critical Principal Tensile Stresses at the Downstream Face

	Critical Tensile Stress (psi)					
	Composite Finite Element Method				Chopra's Method	
Node No.	Analysis #1	Analysis #2	Analysis #3	Analysis #4	Analysis #5	Analysis #6
149	44	42	41	40	98	98
135	**513**	**493**	**490**	**474**	**607**	**607**
121	406	455	453	374	395	396
114	504	482	482	466	493	493
107	**602**	579	579	560	**593**	**593**
100	**677**	**655**	**655**	**633**	**657**	**656**
93	**744**	**725**	**724**	**699**	**702**	**701**
86	**692**	**679**	**679**	**652**	**637**	**643**
79	564	554	554	527	493	498
72	481	463	463	437	385	305
62	311	290	290	270	234	67

Appendix E
Tensile Strength of Roller Compacted Concrete[1]

The tensile strength of roller compacted concrete (RCC) differs from conventional concrete by the extent of material differences in the makeup of mixture proportions and the differences in the measures of control exercised in the production, methods of placement, and curing of the concrete. Any discussion of the tensile properties of RCC must also discuss the tensile properties of conventional concrete as well as other differences.

E-1. Tensile Properties of Conventional Concrete

a. Introduction. Raphael {1} discusses the tensile strength of concrete, the various test methods used for measurement, and the differences in test measurements. He also makes recommendations for relating tensile and compressive strengths in the design of concrete dams. While he discusses the importance of the tensile strength of concrete during earthquakes, he fails to consider any affects of the size of aggregate on tensile properties of massive dam concrete or to discuss the influence of factors other than surface drying on the tensile strength of cores. It is clear from the size of test specimens reported by Raphael that the vast majority of the 12,000 test specimens consisted of maximum aggregate sizes less than 2 in. The exception would be the 500 6-in. cores taken from the 14 concrete dams. No mention is made of size of aggregate or the possible influence of large aggregate, within the 6-in. core specimens, on test results.

b. Effects of mixture proportions and aggregate size on tensile strength. The tensile strength of concrete is dependent on the tensile properties of paste and aggregate, the bond of paste to aggregate, and the presence of any air voids and/or microcracking within the matrix. With normal weight aggregates, the bond of paste to aggregate generally controls the tensile strength of the concrete. Thomas and Slate {2} found the paste-aggregate tensile bond strength to vary from 41 to 91 percent of the tensile strength of paste depending on the rock type, the surface roughness of aggregate, and the w/c ratio. (Lowest values are sandstone aggregates and highest values are limestone aggregates.) They also found the mortar-aggregate tensile bond strength to vary from 33 to 67% of the tensile strength of mortar. Bond is enhanced by roughness of crushed aggregate surfaces and will improve with age of chemically reactive aggregates such as limestone. Bond may also be influenced by differences in thermal properties of aggregate and paste as a result of microcrack formation during cooling of the concrete from peak hydration temperatures. Such cracks, within the paste matrix, may be expected to heal with time; however, healing may not occur in bond to the aggregate.

(1) It is common practice in proportioning concrete mixtures for dams to utilize large aggregates in order to decrease cementitious material requirements and lower costs and heat generation. To effectively reduce the volume of paste required to coat all the aggregate particles and provide the workability required for placement, the total surface area of aggregate must be reduced by increasing the proportions of larger aggregate sizes. The effect of increased proportions of large aggregate on the tensile strength of concrete is to require a larger proportion of the tensile load to be transmitted through aggregate bond. The compressive strength of concrete is less dependent on aggregate bond than tensile strength. Thus, it is apparent that the relationship between the tensile strength of concrete and compressive strength of concrete not only varies with the method of test, as indicated by Raphael, but also varies with the type and maximum size of aggregate.

(2) Test data on the tensile properties of conventional mixtures containing aggregate larger than 1-1/2 in. is limited. Walker and Bloem {3} tested aggregates from 3/8 to 2-1/2 in. in 6- by 12-in. cylinders but found little effect of aggregate size on splitting tensile strength with the natural gravel tested. Tynes {4} compared the splitting tensile strength of 6-in. limestone aggregate mixtures in 20- by 40-in. cylinders with wet-screened 6- by 12-in. cylinders. The effect of excluding aggregates larger than 1-1/2 in. from the test specimens is indicated by the variation in tensile strength ratio of small to large specimens from 1.25 to 1.36. By comparison, the variation in compressive strength ratio of small to large specimens was from 0.99 to 1.15.

[1] Robert W. Cannon, Consulting Engineer.

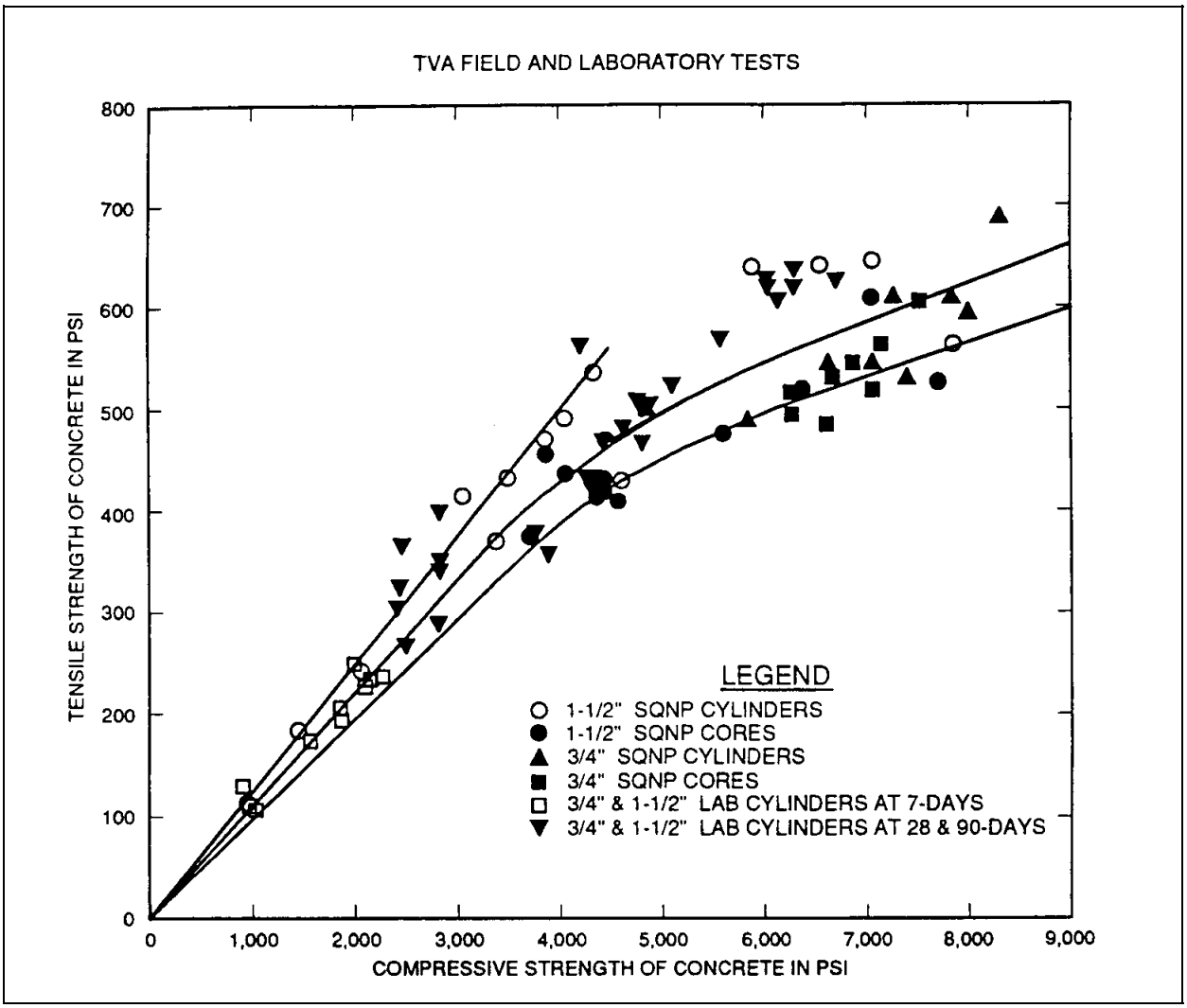

Figure E-1. Tensile strength versus compressive strength for conventional concrete

(3) Figure E-1, is a plot of data taken from studies performed at TVA's Singleton Laboratory and TVA's Sequoyah Nuclear Plant on comparison of splitting tensile and compressive strengths with limestone aggregates having a maximum size of 3/4 and 1-1/2 in. in mixtures containing fly ash and for strengths at ages varying from 7 days to 2 years. Compressive strengths varied from 900 psi to 9,000 psi. Laboratory specimens were standard-cured to the time of test. Field cylinders were standard-cured for 28 days, then sealed in plastic bags and stored at standard temperatures until tested. The cores were drilled from five 6-ft-high by 6-ft-wide by 2-ft-thick blocks at 90 days age, then sealed in plastic bags and stored at laboratory temperatures until tested.

(4) In comparing the ratios of individual tensile strength tests with compressive strength, or with compressive strength raised to the powers of 1/2 or 2/3, it is obvious that the data do not fit any single equation. The only obvious trend is the changing of ratios with strength. Figure E-2 is a plot of the data from reference {3} which shows the same basic trends.

(5) Prediction equations, based on variation with compressive strength raised to the powers of 1/2 or 2/3, are reasonably accurate in predicting tensile strengths of structural concrete in excess of 3,500 psi but overpredict tensile strengths with lower strength concretes. For compressive strengths less than

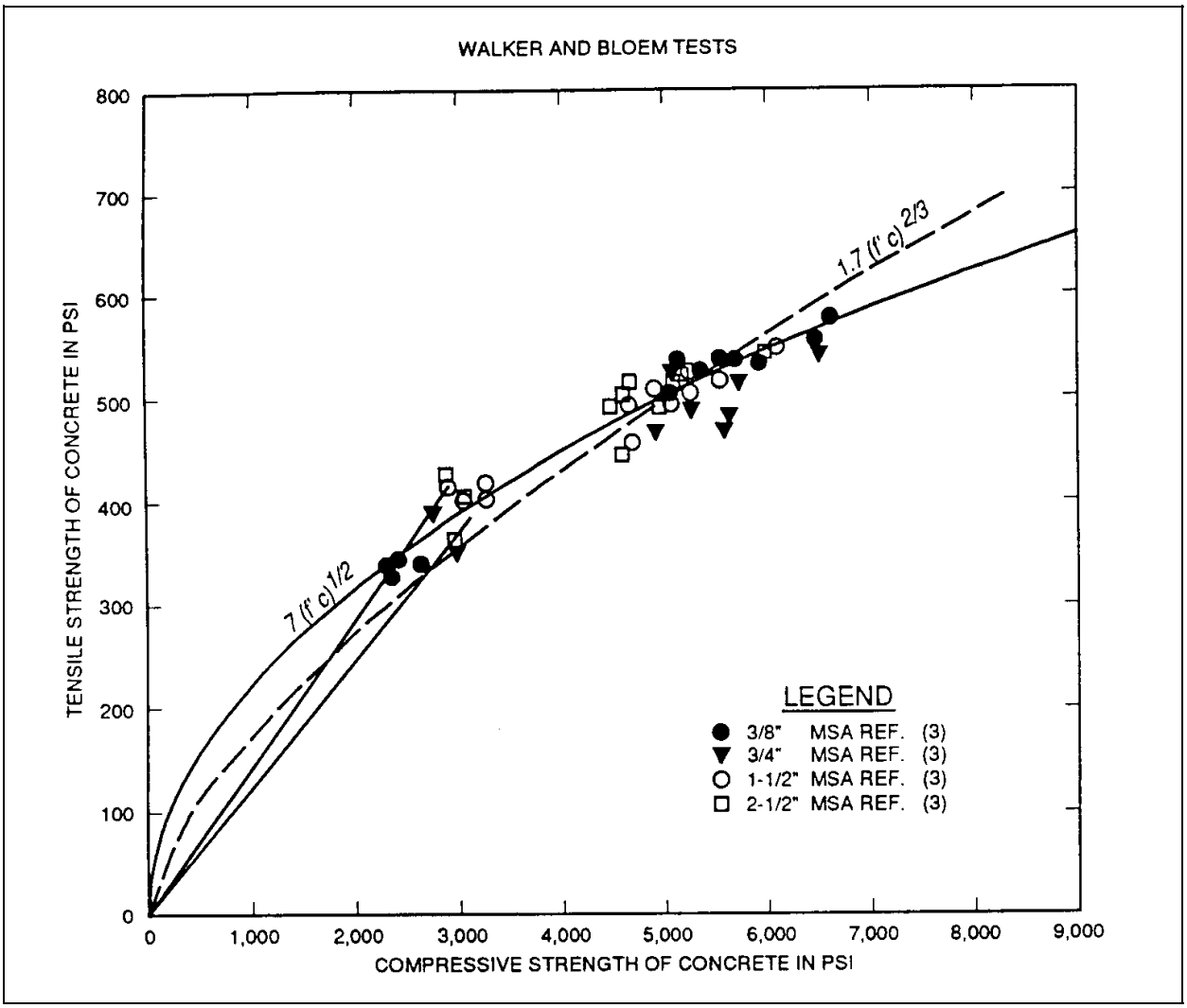

Figure E-2. Tensile strength versus compressive strength for conventional concrete

3,500 psi, tensile strengths vary in direct proportion to compressive strengths.

(6) Figure E-3 from reference {2} shows that the tensile bond strength of mortar to aggregate is relatively unaffected by changes in w/c ratio from 0.36 to 0.75 whereas the tensile strength of the mortar is significantly affected. It also shows that increasing the sand fraction by increasing the cement/sand ratios of the mortar from 1:2 to 1:3 lowers bond strength more than increasing the w/c ratios. From this it would appear that the proportion of tensile strength transmitted through bond is higher for lower strength concretes and lower for higher strength concretes. This would explain the changing relationship of tensile properties with strength.

c. Splitting tensile versus direct tension tests.

(1) Splitting tensile tests are simple to perform and generally have reasonably low within-test-variations similar to that of compression tests. On the other hand, load transfer has always been a problem in direct tension tests. Epoxied end plates have been used to transfer direct tensile loads but clean-up of plates after testing is a major problem. In some cases strengths are also limited by bond of the epoxy to the specimen. Epoxy bond failure was experienced

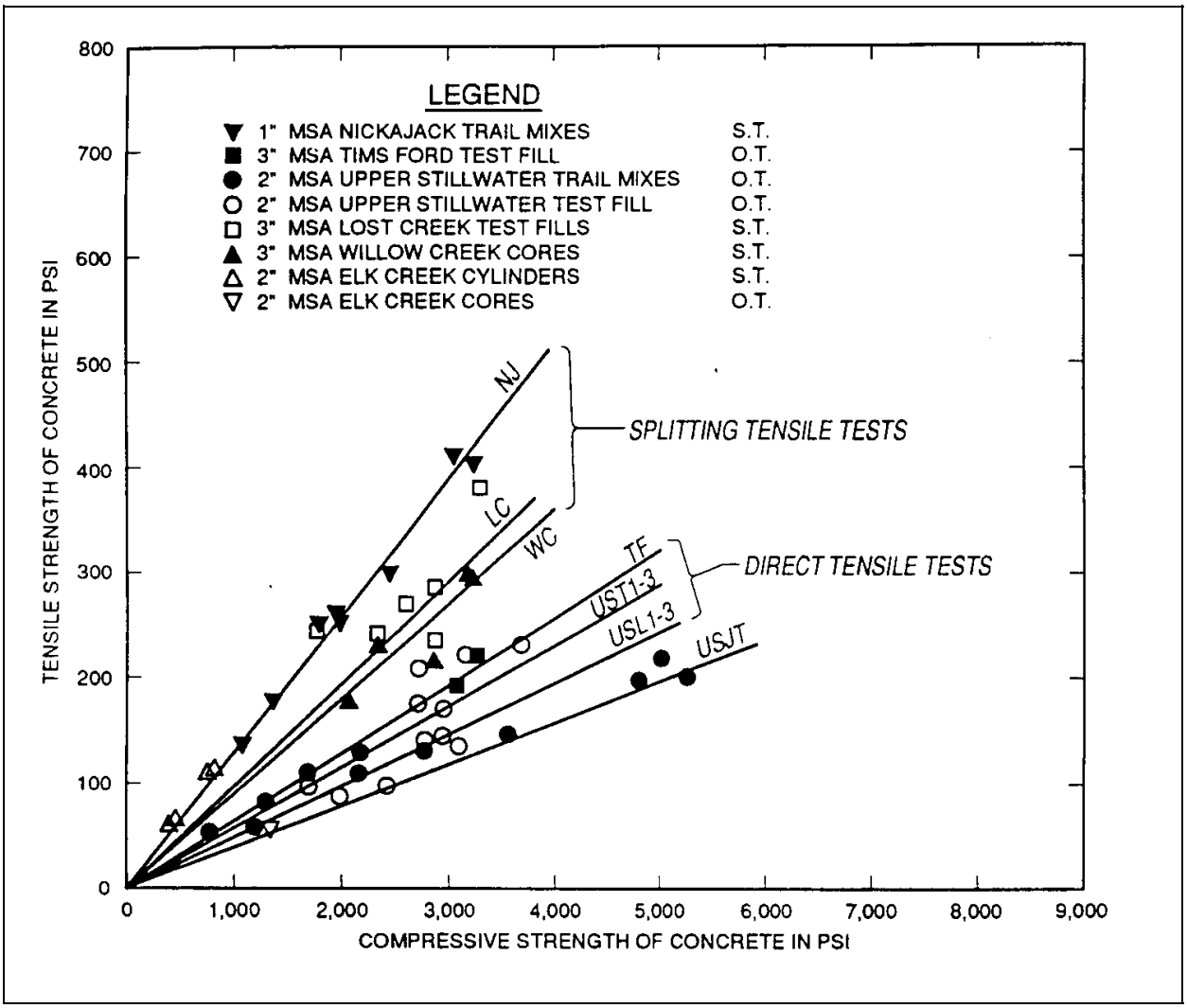

Figure E-3. Tensile strength versus compressive strength for roller compacted concrete

at approximately 280 psi tension in reference {7} tests. A simple means of performing the direct tensile tests is shown in Figure E-4 using standard capping compound and 2-in. deep socket end plates for applying load. These were developed for use at Tims Ford {16}. They have been used for maximum tensile strengths as high as 345 psi without failure of the connection.

(2) Direct tension test results are lower and somewhat more variable than splitting tensile tests. Because of the problems involved with the direct tension test, most investigators accept the splitting tensile test as being representative of concrete tensile strengths. However, there are some distinct differences in the two tests which account for the differences in results and should be considered in evaluating tensile strengths.

(3) Dunstan {9} discussed the anisotropic nature of concrete and the effects on strength of the orientation of testing with respect to the orientation of casting. Most of his discussed research involved casting and testing the compressive strength of cubes and prisms in the horizontal and vertical positions. Cubes tested with the axis of casting vertical are reported {10, 11} to be stronger in compression by about 12% to 15% than those tested with the axis of casting

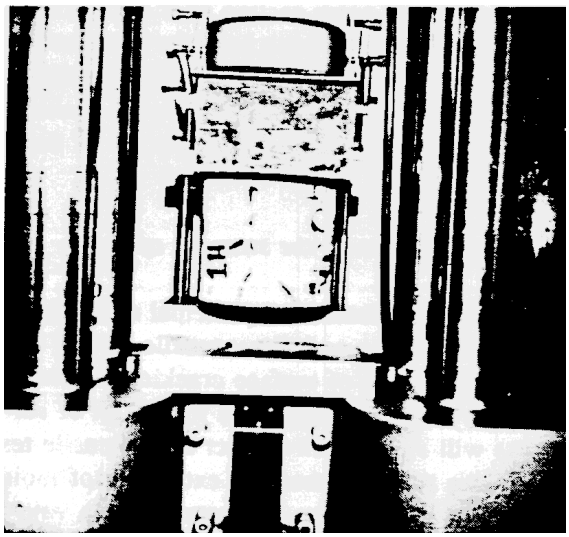

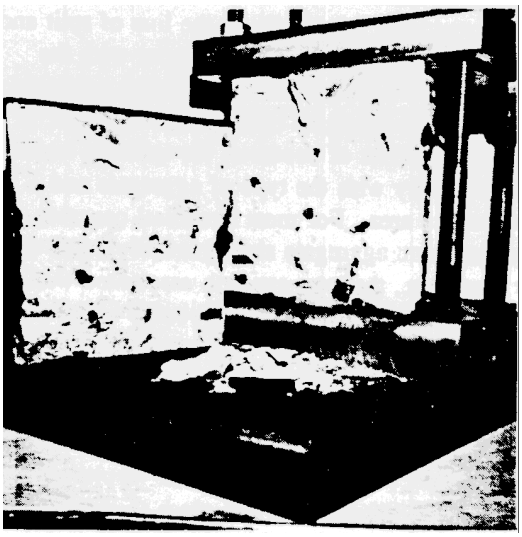

a. Push-off test for shear strength

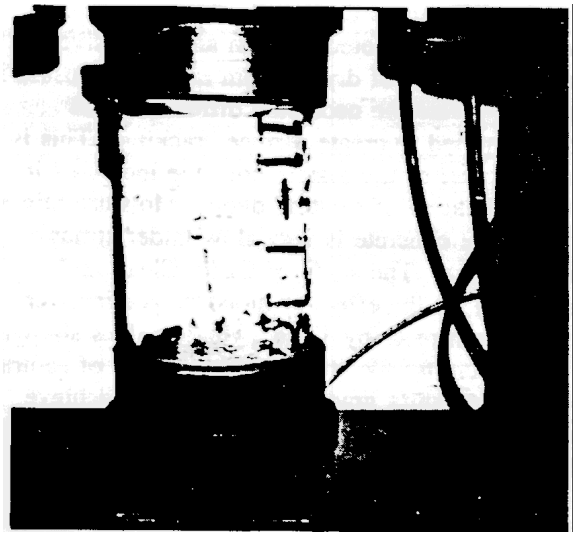

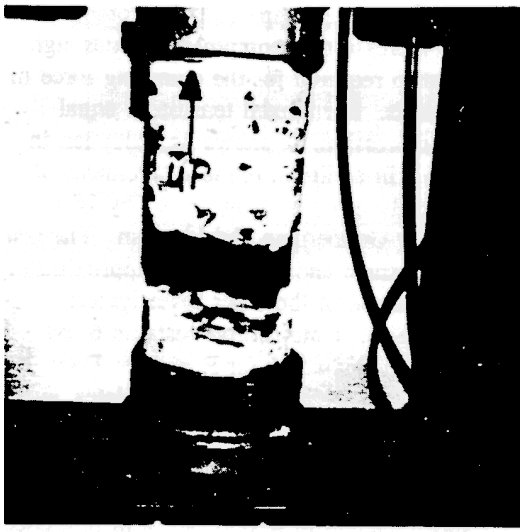

b. Tensile strength test

Figure E-4. Strength tests

horizontal. Similarly, prisms were reported {11, 12} to be 8% and 18% stronger cast and tested vertically while a value of 12% was reported {13} for cores. The behavior of concrete in tension is less documented; however, one report {12} found the strength of specimens tested with the axis of casting vertical to be 8% weaker than that of samples tested with the axis of casting horizontal. Bleed water accumulation at the underside of aggregate particles was the reason given {14, 15} for this anisotropic behavior in conventional concrete. In the case of cubes and prisms there is also a difference in efficiency of tamping specimens in the vertical and horizontal directions which contributes to the differences in test results since all testing was done in the vertical plane. In the Tims Ford test fill {16}, the compressive strength of horizontal cores was 27% higher than that of vertical cores which is exactly opposite to the findings in reference {13}.

(4) In the splitting tensile test the plane of failure is normally in line with the direction of casting. Failure is restricted principally to the line of split and goes through aggregate as well as mortar with the amount of failed aggregate increasing with compressive strength. If aggregate bond is the weak link in the tensile properties of concrete, the splitting tensile strength will vary with the type of aggregate and bonded surface area. For most structural concrete having maximum aggregate sizes generally equal to or less than 1 in., the over-strength associated with the controlled plane of failure is probably in the order of 10% to 15% depending on aggregate shape and w/c ratio. With larger size aggregate, the difference may be substantially more.

(5) Raphael plots the direct tensile results of Gonnerman and Shuman {5} but gives them no further consideration because of the friction grips at the ends of the 6- by 18-in. test specimens. He quotes Rusch {6} as the basis for lower tensile strengths. Rusch does show reduced capacities for combined tension and compression at compression loads significantly higher than required for the clamping force in direct tension tests. For biaxial tension or equal tension and compression, he shows no reduction in tensile capacity. In addition, the test specimens of Rusch are radically different from the 6- by 18-in. cylinders used by Gonnerman and Shuman. The test results for Gonnerman and Shuman are approximately 20% lower than those of the other investigators reported by Raphael. Comparative tests on 6- by 12-in. wet screened cylinders for Portugues Dam {7}, for direct tension tests with epoxied end plates, averaged 0.8 of the corresponding splitting tensile tests with comparisons ranging from 0.7 to 0.92. The average ratio of direct to split tensile strength for 6-in. aggregate concrete in Report No. 4 of reference {24} was 0.77. It thus appears that a 20% reduction may well represent the difference between splitting tensile and direct tensile tests for the aggregate sizes investigated by Raphael.

(6) If the concrete within a direct tension test specimen is uniform throughout, failure will occur in the central portions of test specimens having length-to-diameter ratios equal to or greater than two. If the compression of friction clamps at the specimen ends affects a reduced tensile capacity as Raphael indicates, failure would occur at the ends and not in the interior of the test specimen. Friction grips are not as previously discussed. Direct tension test failures typically fail bond around the aggregate and always occur at the weakest cross section of the specimen. Thus failure is associated with both the weakest axis and the weakest plane in the axis. Therefore the average of direct tensile test results may be assumed to represent the minimum tensile properties of the concrete.

d. Factors affecting the strength of cores.

(1) Raphael attributed the principal differences in splitting tensile testing and direct tensile testing of cores to the formation of surface cracking due to differential drying shrinking. The formation of surface cracks will significantly affect direct tensile test strengths. It is apparent that any extraction of moisture from the surface of the concrete leaves a void within the matrix which will affect strengths to some degree. Some investigations disagree with his assumptions concerning the magnitude of restraint created by differential drying. In the first place, cores are normally protected from any extensive drying and the rate of drying from normal exposure is too slow to create the necessary differentials in restraint required to create surface cracking. This is particularly true of the mature concrete indicated in the re-examination of existing dams. Moisture migration in mature concrete is very slow under atmospheric exposure. The study of Cady, Clear, and Marshall {8} on the effect of moisture gradients on tensile strength of 6- by 12-in. cylinders does show a loss of splitting tensile strength with degree of saturation due to moisture gradients. In order to achieve those gradients their tests were rapidly performed “in a vented, air-circulating oven at either 187 C or 110 C for sufficient lengths of time to produce different degrees of saturation.”

(2) In the TVA Sequoyah N. P. study, the curing for both cores and cylinders from 90 days to 2 years age was identical. In comparing the relationship of split tensile to compressive strengths at 90, 180, 365, and 730 days for the five different strength concretes, the variation of tensile strength to the square root of compressive strength was more uniform than either a direct comparison or comparison with compressive strength to the 2/3 power. The following tabulation summarizes the average of the tests at the indicated ages:

1-1/2-in. MSA				3/4-in. MSA			
Compressive Strength, psi		Tensile Strength, psi		Compressive Strength, psi		Tensile Strength, psi	
Cylinders	Cores	Cylinders	Cores	Cylinders	Cores	Cylinders	Cores
4,900	5,160	521	471	7,190	6,840	577	526

The data indicate 9% lower core strengths for the 3/4-in. and 10% lower core strengths for the 1-1/2-in. aggregate indicating a probable minimum effect of coring on split cylinder strengths.

(3) In the extraction of cores, the surface of the core is subjected to a variety of strains due to the effects of the differential hardness of paste and aggregates on the cutting action of the core bit, the expansion of the surface relative to the interior of the core due the sudden stress relief by the cutting action, and the torque imposed on the core by the rotating bit. The successful drilling of cores requires an experienced operator. It also requires a double-barrel core bit which has an inner barrel to clamp and hold the core to reduce the torque imposed on the core and to reduce breakage and loss of core at weak sections. Successful extraction also depends on the strength of concrete and is probably more dependent on tensile than compressive strengths. All of these factors contribute to surface defects which act as stress raiser or crack initiators from which a crack can propagate at a stress lower than the tensile strength of the material. Once a crack is initiated it will propagate under a lesser load than required to initiate the crack. The relative magnitude of propagating crack load has not been quantified; however, Raphael's 50% reduction for direct tensile strength of cores extracted from dams may be indicative of this effect with large size aggregate.

(4) In the splitting tensile test the orientation of surface cracks due to the coring operation is at right angles to the splitting failure plane and therefore relatively unaffected by the orientation of cracks compared with the in-line orientation in the direct tensile test. Past experience has shown that core extraction is sensitive to core diameter. It is not unusual to obtain complete core recovery with a larger core where problems of core recovery are encountered with a smaller one. It also appears reasonable to expect the ratio of aggregate size to core size to affect test results.

(5) Direct tensile testing of vertical cores should be used in determining the tensile properties of horizontal construction joints or of concrete in the vertical direction. Point load testing is a splitting test performed on the cross section of cores or cylinders and may also be used to determine the strength of horizontal construction joints from vertical cores. Split tensile testing of horizontal cores has been used to establish joint strength; however, identification and location of the joint in the central portion of the core, for correct performance of the test, is very difficult. Core recovery of weak joints is generally more successful if extracted at an angle rather than vertical; however, tests performed on cores extracted in any other plane may overestimate tensile strengths on the horizontal plane considering the anisotropic nature of concrete.

(6) In the above-mentioned TVA field tests with the 3/4- and 1-1/2-in. aggregates, curing was identical following the extraction of cores; therefore, the apparent 10% reduction in splitting tensile strength of cores over cylinders was not affected by differential drying. For direct tensile testing of cores, the minimum effect of vertical core extraction would be more than 10% and probably less than Raphael's 50%.

e. Tensile strength of conventional mass concrete.

(1) The minimum design tensile strength for static analysis should be based on the direct tensile strength of the concrete. The relationship between direct tensile strength and compressive strength may be determined from known splitting tensile strengths by the following:

(2) For compressive strengths less than 3,000 psi:

The tensile splitting strength of 6- by 12-in. wet-screened cylinders containing 1-1/2-in. and smaller

size aggregates may be expected to vary from 0.10 f'_c to 0.15 f'_c depending on type of aggregate.

(3) For compressive strengths equal to or greater than 3,000 psi:

For tensile splitting strength of 1-1/2-in. and smaller size aggregate use one of the following formulas with an expected range of plus or minus 15% depending on aggregate type:

$f'_{st} = 1.7 (f'_c)^{2/3}$ Raphael's formula

$f'_{st} = 7 (f'_c)^{1/2}$

(4) For aggregates larger than 1-1/2 in., reduce strengths by 10%.

For direct tensile strengths, reduce strengths by an additional 20%.

E-2. Tensile Properties of Roller Compacted Concrete

a. Introduction. The definitions of terms "roller compaction" and "roller compacted concrete" in ACI 207.5R {17} are broad definitions which can be applied to almost any mixture of materials containing cement and having sufficient stiffness to support any type of roller during compaction. Thus RCC mixtures can vary anywhere between that of a dense, high quality concrete to that of a porous, low quality cemented conglomeration of aggregate particles. The tensile properties of RCC may therefore be expected to vary widely.

b. Establish basic mix. In establishing the basic mix for RCC, the needed stiffness for support of rollers during compaction is best accomplished by establishing the coarse aggregate fraction slightly higher than that of conventional concrete having the same maximum size aggregate. (See Table 2.2 of reference {17}.) The mortar fraction of the mixture should be proportioned to provide the strength requirements of the mixture and the workability needed for uniform compaction and consolidation during placement. Workability, as a measure of vibration time, is affected by the maximum size, quantity, and grading of coarse aggregate and the makeup of the mortar fraction. The utilization of any specification requirement which increases the water requirements, of the mortar fraction, is detrimental to proportioning efficiency. The practice of increasing the fines content of the fine aggregate may be beneficial in the compaction of unworkable mixtures, but simply requires an increase in paste to maintain workability at a given level for workable mixtures. For a given makeup of mortar, the optimum coarse aggregate fraction is the maximum providing the desired level of workability.

c. Consistency and workability.

(1) The Elk Creek test fills {18} clearly demonstrated that lean 3-in. MSA mass RCC concrete should have a minimum workability in the range of 10 to 20 seconds vibration time when measured by the modified vebe test method using a 27.5-pound surcharge. As a result of that experience, mixtures with vibration times in excess of 30 seconds are not recommended. It has been this author's experience that a 20- to 30-second time frame is optimum for 1-1/2-in. and smaller MSA mixtures without a surcharge using the TVA test procedure {19} of a loosely filled unit weight container filled to the top.

(2) Dunstan {20} found that the TVA procedure and the standard vebe had essentially the same vibration times for 1-1/2-in. MSA mixes with vibration times equal to or less than 30 seconds. In the Lost Creek RCC investigations {21}, laboratory studies indicated that the standard vebe required approximately twice the vibration time (35 sec) compared with that of using a 27.5-pound surcharge (17 sec) for a 3-in. MSA mix with 160 pounds of water. In the Upper Stillwater laboratory investigations {21}, a 50-pound surcharge was used to modify the vebe. For the wetter mixes the modified vebe required vibration times of 25 to 35 seconds compared to vibration times of 35 to 45 seconds without the surcharge. By either of the above criteria, the Upper Stillwater laboratory mixes appear to be in a questionable range of workability. This is verified by the adjustments to the RCC mix at Upper Stillwater from an average vebe time of 30 seconds to about 17 seconds following the 1986 coring program {27}. USBR personnel indicate that future RCC designs will have a still lower target vibration time.

(3) It should be apparent from the above discussion that the trends of all agencies concerned with the quality of concrete placement are toward increased workability and shorter vibration times. It is also apparent that a range of plus or minus 5 seconds is needed for reasonable control of consistency. The

surcharge weights of 27.5 and 50 pounds by the Corps and Bureau were established on the basis of substantially less workable mixes. The use of the surcharge may be an unnecessary hindrance to the performance of the test if the workability of the concrete can be controlled within a 10-second time frame without the surcharge.

d. Effect of consolidation and compaction on tensile properties.

(1) Conventional concrete is deposited in piles or within forms in a loose configuration which is then broken down and consolidated by internal vibration. If the mixture is properly proportioned there will be little if any separation or segregation of the coarse aggregate particles from the matrix of mortar during the consolidation process with the larger aggregate particles remaining suspended within the matrix of the mortar. Thus the particles of coarse aggregate remain in a generally random orientation irrespective of their particle shape.

(2) RCC is deposited in piles and spread in a loose configuration with a dozer or similar piece of equipment. During the spreading operation, the coarse aggregate particles are not suspended within the matrix of the mortar and temporary separation of aggregate and mortar occurs. During this temporary separation, flatter particles tend to align their flatter sides with the horizontal {9}. If the mortar matrix has poor workability or is insensitive to vibration no lateral movement of coarse aggregate particles will occur during compaction. If the mortar matrix is workable and sensitive to vibration, lateral displacement and consolidation of the coarse aggregate particles will occur resulting in a more random orientation of the coarse aggregate particles. The extent of this occurrence and its effect on tensile properties of the concrete is dependent on the particle shape of the aggregate.

e. Anisotropic nature of RCC.

(1) The water content of RCC is generally assumed to be less than that of conventional concrete because of its no-slump consistency. This may, or may not, be true dependent on the aggregates and the proportioning of the mortar matrix for which the comparison is made. Thus RCC may be as susceptible to the accumulation of water under the aggregate particles as conventional concrete. The anisotropic nature of the tensile strength of RCC may equal or exceed that of conventional concrete dependent on the shape and gradation of the aggregates, their affect on water contents, and the extent to which the flatter particles increase the surface area of the aggregates on the horizontal plane. Thus the magnitude of differences in the tensile strength of RCC, on horizontal planes compared with vertical or other planes within the concrete, will vary with mixture proportions, type, size, and shape of the coarse aggregate.

f. Data on RCC tensile strengths.

(1) Figure E-3 is a plot of split cylinder and direct tensile tests for RCC. Only a limited amount of both split cylinder and direct tensile tests were performed on the same concrete in these plots; however, the difference in test methods is apparent. Additional data were obtained from ASCE special publication “Roller Compacted Concrete II” {27, 28, 29, 30}.

(2) At Galesville {27}, the ratio (ST/C) of split tensile strength to compressive strength was 0.134 and the ratio of direct tensile to split tensile (DT/ST) of untreated construction joints was 0.24. Where bedding concrete was used the ratio was 0.5.

(3) At Upper Stillwater {21}, the average (DT/C) ratio of cylinders for Mixes L-1 through L-3 was 0.050 whereas the average (DT/C) ratio of parent core material from test fill mixes T-1 through T-3 was 0.058. Apparently the coring of the relatively soft sandstone aggregate concrete had little, if any, affect on strengths. In the 1986-87 coring program for the dam {27}, the (ST/C) ratio of cores from the dam was 0.076 and the (DT/ST) ratio of intact construction joints was 0.5. While there was substantial increase in tensile strengths from one to two years age, there was very little, if any, change in the (DT/C) ratios.

(4) The average (ST/C) ratio for concrete from reference 30 for six different mixes having relatively high water contents (220 lb to 260 lb) was 0.167.

(5) For the same size and type of aggregate, the direct tensile strengths of RCC appear to be 25 to 30 percent lower than splitting tensile strengths. This compares with a 20% reduction for conventional concrete. While the data are limited, the range of splitting tensile strengths of RCC appears to correspond to that of conventional concrete.

(6) The data on tensile strength from Elk Creek Dam are limited and difficult to interpret. In the test fills of 1982 and 1985, the principal interest was the shear strength of joints from sawed blocks out of the test fills and cores were not extracted. The results of split cylinder tests at 28 and 90 days age are shown in Figure E-3 and indicate a (ST/C) strength ratio of approximately 0.15. The average (ST/C) ratio of cores extracted from the dam was 0.17. In contrast to this, the results of direct tensile tests on cores, extracted from the dam concrete, indicate a (DT/C) ratio of approximately 0.04. This difference is unrealistic in comparison with other test data and must be attributed to the effects of coring the relative low (1,300 psi) strength concrete. (Observation of the cores indicates substantially higher breakage than should have occurred in a quality coring operation. Apparently a double barrel core bit was not used and the contractor was more interested in production than quality.) As a minimum, the direct tensile strength of the parent concrete should not have been less than 1/2 of the splitting tensile strength.

g. Lift joints.

(1) The critical tensile properties of concrete for seismic resistance to earthquakes are the lift joints. It is not reasonable to expect the bonding of cold joints, under varying conditions of exposure, to be equivalent to that of the parent material. From 1959 through 1973 the U.S. Army Engineer Waterways Experiment Station (WES) {24} investigated methods of treating horizontal construction joints for conventional mass concrete. All joints were standard cured. From Report No. 1, uncleaned joints averaged approximately 2/3 of cleaned joint strengths. After completion of all tests, Report No. 4 concluded the method of treatment (wet, dry, mortar, no mortar) was judged to have no significant bearing on strength.

(2) WES {25} also performed laboratory tests on the bonding of workable 1-1/2-in. MSA RCC using a relatively small roller and 6-in. lifts. In one investigation the untreated, moist-cured joints exposed for 1 hour and 24 hours had joint tensile strengths of 87 and 53% respectively, of parent concrete. (Note: This comparison is intended to show the relative effects of joint age on strengths. It does not suggest equivalent compaction of the small roller, nor equivalent strengths, to normal RCC placement.) In another investigation the relative joint strengths of lean and rich RCC mixtures along with conventional concrete indicated joint strengths of 27, 44, and 74%, respectively, of parent concrete for 1-day-old untreated joints. (Please note the similar results of conventional concrete with the earlier investigations.) In these tests it is important to note that only 7 of 12 joints of the lean mixture bonded compared with 11 of 12 for the richer mix and 100% for the conventional mix.

(3) The condition of the joint surface is critical to the development of bond regardless of the covering mixture. Plastic concrete is particularly vulnerable to drying during the hardening process when subjected to low humidity, warm weather, and/or windy conditions. There is sufficient moisture within the concrete itself for continued hydration if the moisture is not removed by drying. If the rate of drying is slow, the migration of moisture to the surface from below is sufficient for continued hydration and strength development of the concrete at the surface. If rapid drying occurs, the hydration process at the surface will stop along with any development of strength. It is thus critical, for bond development, to protect the plastic concrete from rapid drying during setting of the concrete. Under conditions of rapid surface drying, it may be necessary to cover the RCC for the first two to three hours after placement until the concrete reaches initial set. After initial set, water from a mist spray should not be expected to affect the w/c ratio of the surface concrete {26}.

(4) Surface conditions are also affected by the size of aggregate and the workability of the concrete. If the concrete is workable, paste and mortar will rise to the surface under the vibrating action of the roller and the finished surface of the concrete will be relatively smooth if not over-rolled. (Over-rolling is evident when paste accumulates on the roller and mortar is picked up from the surface.) If the concrete is unworkable, there will be little if any lateral displacement of the concrete during compaction and paste and mortar will not rise to the surface. The surface will generally be rough and granular in texture as mortar and aggregate are simply forced into a closer relationship of their spread condition by the compactive effort.

(5) A principal difference between workable and unworkable concrete, with respect to bond, concerns the compactive density of the concrete with respect to the hardened concrete surface. With workable concrete, the density of the covering mixture increases with depth becoming a maximum at the

hardened surface {16}. With unworkable concrete the reverse occurs.

(6) Bond is dependent upon the intimate relationship of the covering mixture to the hardened surface. Maximum bond has always been achieved with sand blasting which removes a minimum of material and leaves the surface in a relatively smooth condition. Thus bonding improves with relative smooth hardened surfaces allowing lateral displacement of aggregates at the surface and densification of the workable concrete. It should therefore be apparent that the opposite effect can be expected with rough surfaces and unworkable concrete.

(7) Large aggregates decrease workability, increase surface roughness, and create voids at the surface due to bridging of large particles. All testing to date indicates that bond will decrease with increased size of aggregate. For bonding of maximum size aggregates larger than 1-1/2 in., it is essential that a bedding mix of mortar or slumpable concrete of 1 in. and smaller size aggregate be used {22}.

(8) Some idea of the relative bonding qualities of workable and unworkable concrete can be seen from examination of cores and data from Willow Creek and Elk Creek Dams {23}. At Willow Creek, consistency measurements of vibration time were considered unsuitable for controlling water contents. In the direct tensile testing of 9-in. cores at Willow Creek, the average strength of bonded joints was 46% of the parent concrete. (Limited data on 6-in. cores indicate joint strengths in excess of parent concrete which is unreasonable.) The percentage of bonded area, based on examination of cores, would indicate from 30 to 50% bonded. At Elk Creek, consistency measurements were used to control the workability of the concrete. The combined effectiveness of workable concrete and the use of mortar on cold joints is indicated by an apparent joint efficiency of 82%. While the data for both joint and parent concrete are below probable strengths, as previously discussed, their relative values should be indicative of actual conditions. A 70% intact joint recovery and only 15% smooth joint separations indicating a possible 85% bonded joints was reported at Elk Creek.

(9) In comparing the effects of cementitious quantities of mixtures using natural river gravel (supplemented by crushing) and requiring the same vebe time for compaction on bond strength, the bond strength of mixtures containing 150 pounds of cement is improved from 6.3 to 9.2% of their compressive strengths with joint treatment, whereas the bond strength of mixtures containing an additional 150 pounds of fly ash is improved from 6.8 to 7.4% with joint treatment {28}. From the same report, similar cementitious mixtures using limestone aggregates had direct tensile core strengths for the lean and richer mixes of 9.5 and 7.8% of their compressive strengths which were 840 and 1,920 psi, respectively.

h. Joint treatment and clean-up.

(1) One of the expressed advantages of RCC construction has been the elimination of the need for joint clean-up (if uncontaminated by foreign substances) because of the lack of laitance. The 82% bonded joint efficiency at Elk Creek compared with the 74% joint efficiency of conventional concrete on one-day-old joints in the WES {25} experiments may be considered an indication of the laitance effect. This advantage for RCC is dependent on strict adherence to specification requirements for curing and joint treatment, otherwise there is an increased probability of joint contamination and improper curing because of the increased number of cold joints in RCC construction.

(2) The relative strength of clean and treated joints for conventional mass concrete, in the WES {24} experiments, was approximately 70% of the parent concrete. At Elk Creek, joints were not cleaned unless contaminated or more than 72 hours old. The possible 85% bonded joints for Elk Creek represents a combined efficiency of bonded area and joint efficiency which is comparable to that of cleaned and treated joints for conventional construction.

(3) While the results of the lean and richer mixtures of workable RCC in the WES investigations may be lower than expectations due to differences in laboratory and field compaction, their differences are a clear indication of the effect of cementitious material contents on the bonding of cold joints. Thus where bedding mixes of either concrete or mortar are used to achieve or improve bond, they should be proportioned for higher strengths than the strength of the cold joint concrete.

(4) Extensive clean-up of cold joints is not required for development of bond with RCC as long as the joints are not contaminated by foreign

substance and are maintained in a relative moist condition throughout exposure. All loose particles of aggregate or mortar should be removed by washing with low pressure just prior to placement of covering concrete.

i. Tensile strength of RCC lift joints.

(1) For workable mixtures, the tensile bond strength of properly clean and cured joints covered with a suitable mortar or bedding mix may be assumed as 70% of the tensile strength of parent material which is equivalent to the joint strength of properly prepared conventional concrete.

(2) The tensile strength of parent material should be based on direct tensile test strengths or a maximum of 75% of splitting tensile strengths. If test strengths are based on wet-screening of aggregates larger than 1-1/2 in., reduce test values by 10%.

(3) When test data are not available, the following represents a range of acceptable design values for workable mixtures based on type of aggregate. Low values are based on natural aggregates and sandstone and the high values are based on all crushed aggregates such as limestone.

(a) For design compressive strengths less than 3,500 psi: The splitting tensile strength for RCC mixtures containing aggregates smaller than 2 in. may be expected to vary from 0.08 f'_c to 0.17 f'_c. For 1-1/2-in. and smaller MSA, the direct tensile strength of RCC lift joints may be assumed to range from 0.04 f'_c to 0.09 f'_c.

(b) For design compressive strengths equal to or greater than 3,500 psi: The splitting tensile strength for RCC mixtures containing aggregates smaller than 2 in. may be expected to vary from 5.5 to 8.5 times the square root of f'_c. For 1-1/2-in. and smaller MSA, the direct tensile strength of RCC lift joints may be expected to range from 3.0 to 4.5 times the square root of f'_c.

(c) For aggregates larger than 1-1/2 in., reduce these values by 10%.

(4) For unworkable mixtures which will not consolidate within 30 seconds vibration time:

(a) If mortar is used on all lift joints, use 2/3 of the design tensile strengths for workable concrete.

(b) If mortar is not used, use 1/3 of the design tensile strengths for workable concrete.

j. Design tensile strengths for dynamic and finite element analysis.

(1) Raphael {1} discusses the effects of dynamic loading on the tensile strength of concrete and the effects of nonlinear strain at failure on finite element analysis.

(2) For static finite element analysis, increase the above design tensile strengths of lift joints by a factor of 1.35.

(3) For seismic finite element analysis, increase the above design tensile strengths of lift joints by a factor of 2.

E-3. Tensile Strengths of Conventional and Roller Compacted Concrete.

Split and design tensile strengths of conventional mass concrete and roller compacted concrete are shown in Tables E-1 through E-3.

E-4. Conclusions and Recommendations

a. The design tensile strength of concrete should be based on the direct tensile strength of concrete in the direction of principal stress and should account for the relative strengths of construction joints and the effects of construction methods on the probability of attaining anticipated joint strengths.

b. The relationship between the direct tensile strength of RCC and conventional mass concrete varies with the workability of the RCC mixture and the quality of the concrete placement. The trends toward more workable RCC mixtures and improvements in production control are indicative of tensile strength attainment equivalent or superior to the conventional concrete.

c. The bond strength of horizontal construction joints depends on: (1) the soundness of the cold joint, (2) the paste content and strength of the covering mixture, and (3) the amount of reflective vibration and compaction at the joint.

Table E1
Conventional Mass Concrete

MSA in.	Max/Min	Split Tensile Strength[a] ≤ 3.0 ksi	Split Tensile Strength[a] > 3.0 ksi	Conv. Fctr.[b]	Design Tensile Strength[c] ≤ 3.0 ksi	Design Tensile Strength[c] > 3.0 ksi
≤ 1.5	Max	0.15 f'_c	8 $(f'_c)^{1/2}$	0.56	0.085 f'_c	4.5 $(f'_c)^{1/2}$
	Min	0.10 f'_c	6 $(f'_c)^{1/2}$	0.56	0.055 f'_c	3.4 $(f'_c)^{1/2}$
> 1.5	Max	0.15 f'_c	8 $(f'_c)^{1/2}$	0.50	0.075 f'_c	4.0 $(f'_c)^{1/2}$
	Min	0.10 f'_c	6 $(f'_c)^{1/2}$	0.50	0.050 f'_c	3.0 $(f'_c)^{1/2}$

[a] Splitting tensile strength of parent material.
[b] Includes conversion for direct tensile, joint strength, and probable percent of bonded joint.
[c] Direct tensile strength of construction joints.

Table E2
Roller Compacted Concrete, Consistency ≤ 30 Seconds Vibration

MSA in.	Mortar Yes	Mortar No	Max/Min	Split Tensile Strength[a] ≤ 3.5 ksi	Split Tensile Strength[a] > 3.5 ksi	Conv. Fctr.[b]	Design Tensile Strength[c] ≤ 3.5 ksi	Design Tensile Strength[c] > 3.5 ksi
≤ 1.5	-	-	Max	0.17 f'_c	8.5 $(f'_c)^{1/2}$	0.53	0.090 f'_c	4.5 $(f'_c)^{1/2}$
			Min	0.08 f'_c	5.5 $(f'_c)^{1/2}$	0.53	0.040 f'_c	2.9 $(f'_c)^{1/2}$
> 1.5	Y		Max	0.17 f'_c	8.5 $(f'_c)^{1/2}$	0.47	0.080 f'_c	4.0 $(f'_c)^{1/2}$
	Y		Min	0.08 f'_c	5.5 $(f'_c)^{1/2}$	0.47	0.040 f'_c	2.6 $(f'_c)^{1/2}$

[a] Splitting tensile strength of parent material.
[b] Includes conversion for direct tensile, joint strength, and probable percent of bonded joint.
[c] Direct tensile strength of construction joints.

Table E3
Roller Compacted Concrete, Consistency > 30 Seconds Vibration

MSA in.	Mortar Yes	Mortar No	Max/Min	Split Tensile Strength[a] ≤ 3.5 ksi	Split Tensile Strength[a] > 3.5 ksi	Conv. Fctr.[b]	Design Tensile Strength[c] ≤ 3.5 ksi	Design Tensile Strength[c] > 3.5 ksi
≤ 1.5	Y		Max	0.17 f'_c	8.5 $(f'_c)^{1/2}$	0.35	0.060 f'_c	3.0 $(f'_c)^{1/2}$
			Min	0.08 f'_c	5.5 $(f'_c)^{1/2}$	0.35	0.030 f'_c	1.9 $(f'_c)^{1/2}$
> 1.5	Y		Max	0.17 f'_c	8.5 $(f'_c)^{1/2}$	0.32	0.055 f'_c	2.7 $(f'_c)^{1/2}$
			Min	0.08 f'_c	5.5 $(f'_c)^{1/2}$	0.32	0.025 f'_c	1.7 $(f'_c)^{1/2}$
≤ 1.5		N	Max	0.17 f'_c	8.5 $(f'_c)^{1/2}$	0.18	0.030 f'_c	1.5 $(f'_c)^{1/2}$
			Min	0.08 f'_c	5.5 $(f'_c)^{1/2}$	0.18	0.015 f'_c	1.0 $(f'_c)^{1/2}$
> 1.5		N	Max	0.17 f'_c	8.5 $(f'_c)^{1/2}$	0.16	0.025 f'_c	1.4 $(f'_c)^{1/2}$
			Min	0.08 f'_c	5.5 $(f'_c)^{1/2}$	0.16	0.015 f'_c	0.9 $(f'_c)^{1/2}$

[a] Splitting tensile strength of parent material.
[b] Includes conversion for direct tensile, joint strength, and probable percent of bonded joint.

c Direct tensile strength of construction joints.

d. While tracked dozers impart some vibration and a significant amount of compaction to the concrete, the additional vibration needed for joint bond can be attained, without over-rolling the top lift, by the placement on one plastic lift upon another, and rolling between lifts. The thickness of rolled lifts should not be more than approximately one foot.

e. Lower heat generation and water requirements can be obtained with improved workability by utilizing fly ash in place of aggregate fines in the RCC mixes. This can be accomplished at cost savings despite higher cost of fly ash due to the water-reducing qualities and additional pozzolanic strength contribution of the ash.

f. For workable mixtures and construction procedures equivalent to Elk Creek, the above design recommendations assume direct tensile strength of RCC to range from 0.73 to 1.06 times that of conventional concrete.

E-5. References

{1} Raphael, Jerome M. Tensile Strength of Concrete, ACI Journal / March-April 1984, pp 158-165.

{2} Thomas, T. C. Hsu, and Slate, Floyd O. Tensile Bond Strength Between Aggregate and Cement, Paste or Mortar, ACE Journal Proceedings V. 60 No. 4, April 1963, pp 465-485.

{3} Walker, Stanton, and Bloem, Delmar L. Effects of Aggregate Size on Properties of Concrete, ACI Proceedings V. 57, April 1960, pp 283-298.

{4} Tynes, W. O. Correlation Between Tensile and Compressive Strengths for Lean Mass Concrete, Technical Report C-74-2, U.S. Army Engineer Waterways Experiment Station Concrete Laboratory, Vicksburg, MS.

{5} Gonnerman, H. F., and Shuman, E. C. Compression, Flexural, and Tension Tests of Plain Concrete, Proceedings, ASTM, F 28, Part II, 1928, pp 527-564.

{6} Kupfer, Helmut, Hilsdorf, Hubert K., and Rüsch, Hubert. Behavior of Concrete Under Biaxial Stresses, ACI Journal, Proceedings V. 66 No. 8, Aug 1969, pp 656-666.

{7} U.S. Army Corps of Engineers, Jacksonville District. Portugues and Bucana Rivers, Puerto Rico, Design Memorandum No. 21 (Structural Properties and Special Studies) Appendix B, Portugues Dam.

{8} Cady, P. D., Clear, K. C., and Marshall, L. G. Tensile Strength Reduction of Mortar and Concrete Due to Moisture Gradients, ACI Journal Proceedings V. 69 No. 11, November 1972, pp 700-705.

{9} Dunston, Malcom R. H. Rolled concrete for dams - construction trials using high fly ash content concrete, Technical Note No. 106, Construction Industry Research and Information Association, London, May 1981, pp 96.

{10} L'Hermite, R. Recent Research on Concrete, Cement and Concrete Association Library Translation Cj 24, London, 1951.

{11} Bloem, D. L. Study of horizontal mould for concrete cylinders, Series D-58, National Ready-mix Concrete Association, Washington, DC, Sept. 1958.

{12} Johnston, C. D. Anisotrophy of concrete and its practical application, Highway Research Board 423, 1973, pp 11-16.

{13} Petersons, N. Strength of concrete in finished structures, Transactions of the Royal Institute of Technology 232, Stockholm, Sweden, 1964.

{14} Hughes, B. P., and Ash, J. E. Water gain and its effect on concrete. Concrete, December 1969 3, pp 494-496.

{15} Gilkey, H. J. Water gain and allied phenomena in concrete work, Engineering News Record, February 1927, 98(no. 6), pp 242-247.

{16} Cannon, Robert W. Compaction of Mass Concrete with Vibratory Roller, ACI Journal / October 1974, pp 506-513.

{17} ACI 207.5R-89. Roller Compacted Mass Concrete, Manual of Concrete Practice, American Concrete Institute, 1989.

{18} Elk Creek Lake Rogue River Basin, Oregon, Concrete Investigations and RCC Construction Techniques for a Concrete Gravity Dam,

U.S. Army Corps of Engineers, Portland District, Design Memorandum 8, Final, 1987.

{19} General Construction Specification No. G-48 for Roller Compacted Concrete, Tennessee Valley Authority, Knoxville, Aug. 1975, Appendix A & B.

{20} Dunstan, Malcom R. H. Roller concrete for dams - a laboratory study of the properties of high fly ash content concrete, Construction Industry Research and Information Association Technical Note 105, May 1981, pp 96.

{21} Mix Design Investigation - Roller Compacted Concrete Construction, Upper Stillwater Dam, Utah, U.S. Department of Interior, Bureau of Reclamation, REC-ERC-84-15, June 1984, pp 72.

{22} Cannon, Robert W. Design Considerations for Roller Compacted Concrete and Rollcrete in Dams, ACI Concrete International / Dec. 1985, pp 50-58.

{23} Communication from Ralph Strom to Bob Cannon dated 14 March 1990. Data on tensile strengths from Willow Creek and Elk Creek.

{24} Investigation of Methods of Preparing Horizontal Construction Joints in Concrete, Technical Report No. 6-518, U.S. Army Engineer Waterways Experiment Station, Vicksburg, MS, July 1959; Testing of Joints in Large Blocks, Report No. 2, July 1963; Evaluation of High-Pressure Water Jet and Joint Preparation Procedures, Report No. 4, Aug. 1973.

{25} Saucier, K. L. Investigation of No-Slump Roller Compacted Concrete (RCC) for Use in Mass Concrete Construction, Roller Concrete for Dams, International CIRIA Conference Held on 9/10 June 1981, pp 9-1 through 9-14.

{26} Cannon, Robert W. Boney Falls Dam RCC Spillway, Evaluation of Cores. Communication transmitted to Barr Engineering of Minneapolis, 9 January 1990.

{27} Dolen, T. P., and Drahushak-Crow, R. Evaluation of Cores from Two RCC Gravity Dams, ASCE Special Publication, Roller Compacted Concrete II, pp 203-213.

{28} Dolen, T. P., and Tayabji, S. D. Bond Strength of Roller Compacted Concrete, ASCE Special Publication, Roller Compacted Concrete II, pp 170-186.

{29} McLean, F. G., and Pierce, J. S. Comparison of Joint Strengths for Conventional and Roller Compacted Concrete, ASCE Special Publication, Roller Compacted Concrete II, pp 151-169.

{30} Wong, Biscoff, and Johnson. Dam Strengthening and Raising, ASCE Special Publication, Roller Compacted Concrete II, pp ?

Appendix F
Glossary

The following symbols and notations are used throughout the EP.

a_g Maximum ground acceleration, ft/sec^2

C Velocity of pressure waves in water, 4,720 ft/sec

C_r Velocity of pressure waves in the foundation

CQC Complete quadratic combination method for combining the modal responses in a response spectrum analysis

DTS Dynamic tensile strength which accounts for an increase in strength due to the high strain rate loading associated with earthquake ground motion

E_f Young's modulus of elasticity of foundation rock

E_s Young's modulus of elasticity of dam concrete

f_1 Equivalent lateral force on the upstream face of the dam due to the fundamental vibration mode at a y-distance above the foundation

f_{sc} Equivalent lateral forces acting on dam due to higher vibration modes at a y-distance above the foundation

f_{r1} Fundamental resonant frequency of dam on flexible foundation rock with impounded water

f'_c Specified compressive strength of RCC, psi

f'_t Tensile strength of RCC based on direct tensile tests

f_t Tensile stress

$f_{t(allowable)}$ Allowable tensile stress defining an acceptable response

F_{st} Hydrostatic force of the forebay acting on the upstream face of the dam

g Acceleration due to gravity, 32.2 ft/sec^2

H Depth of forebay pool above the foundation

H_s Height of upstream face of dam

L_1 Generalized earthquake force coefficient for the empty reservoir condition

$\tilde{L}_1$ Generalized earthquake force coefficient for the loading condition with the reservoir at depth H

M_1 Generalized mass for the empty reservoir condition

$\tilde{M}_1$ Generalized mass for the loading condition with the reservoir at depth H

MCE Maximum credible earthquake which is the most severe earthquake believed possible at a site

OBE Operating basis earthquake which is the earthquake with a 50% chance of exceedence during the 100-year life of the dam

$\bar{p}$ Standard value of the hydrodynamic pressure function associated with the fundamental vibration mode for the full reservoir condition (H/H_s = 1), and at a y-distance above the foundation

p Hydrodynamic pressure function associated with the fundamental vibration mode for the load condition with the reservoir at depth H, and at a y-distance above the foundation

$\bar{p}_o$ Standard value of the hydrodynamic pressure function associated with the higher modes for the full reservoir condition (H/H_s = 1), and at a y-distance above the foundation

p_o Hydrodynamic pressure function associated with the higher modes for the loading condition with the reservoir at depth H, and at a y-distance above the foundation

PGA Peak Ground Acceleration for the OBE or MCE as appropriate

r_1 Maximum response (usually expressed as a stress at a y-distance above the foundation) due to the fundamental vibration mode

r_d Maximum dynamic response (usually expressed as a stress at a y-distance above the foundation)

r_{max} Maximum total response including both the maximum dynamic response and the summation of the responses due to initial static effects (ususally expressed as a stress at a y-distance above the foundation)

r_{sc} Maximum response due to the higher vibration modes (usually expressed as a stress at a y-distance above the foundation)

r_{st} Response due to an initial static effect such as the weight of the dam or the static water pressure which exists just before the earthquake event (usually expressed as a stress at a y-distance above the foundation)

RCC Roller compacted concrete

R_f Period lengthening ratio due to foundation-rock flexibility effects

R_r Period lenghtening ratio due to hydrodynamic effects

R_w Ratio of the fundamental vibration period of impounded water to the fundamental resonant period of the dam on a rigid foundation with impounded water

S_a Ordinate of acceleration from the design response spectrum normalized to a maximum ground acceleration of 1 g evaluated at period $\tilde{T}_1$ and damping ratio $\tilde{\varepsilon}_1$

$\tilde{S}_a$ The spectral acceleration obtained by scaling S_a by the peak gound acceleration (PGA) for either the OBE or MCE as appropriate

SRSS Square root of the sum of the squares method for combining the modal responses or out-of-phase components of the response in a response spectrum analysis

T_1 Fundamental vibration period of dam on rigid foundation rock with empty reservoir

$\tilde{T}_1$ Fundamental resonant period of dam on flexible foundation rock with impounded water

T_1^r Fundamental vibration period of impounded water (4H/C)

$\tilde{T}_r$ Fundamental resonant period of dam on rigid foundation rock with impounded water

$\tilde{T}_f$ Fundamental resonant period of dam on flexible foundation with empty reservoir

w Unit weight of water

w_c Unit weight of concrete (usually taken as 0.15 kips/ft^3)

w_s Weight of dam per unit height at a location y-distance above the foundation (base width x w_c)

y Coordinate along the height of the dam

α Wave reflection coefficient

β Percent of critical damping associated with a response spectrum

ε_1 Damping ratio of dam on rigid foundation rock with empty reservoir

$\tilde{\varepsilon}_1$ Effective damping factor for dam on flexible foundation rock with impounded water

ε_f Added damping ratio due to foundation-rock flexibility effects

ε_r Added damping ratio due to hydrodynamic effects

n_f Constant hysteretic damping factor for the foundation rock

ρ Mass density of water

ρ_r Mass density of the foundation rock

ϕ,Ψ Normalized fundamental vibration mode shape of dam at upstream face

ω_1 Fundamental frequency of the dam on rigid foundation rock with empty reservoir

ω_1^r Fundamental frequency of the impounded water idealized by a fluid domain of constant depth and infinite length

Ω Significance parameter for water compressibility